ANTIMICROBIAL POTENTIAL OF THE MARINE ACTINOMYCETE *SALINISPORA TROPICA* CNB-440 IN CO-CULTURE: A METABOLOMIC, PROTEOMIC AND GENOME ENGINEERING APPROACH.

by

Audam Chhun

A thesis submitted for the degree of Doctor of Philosophy

University of Warwick | School of Life Sciences

October 2020

TABLE OF CONTENTS

LIST OF ILLUSTRATIONS AND TABLES

ACKNOWLEDGMENTS

I would first like to express my deep gratitude to my thesis supervisors **Dr Joseph Christie-Oleza** and **Dr Christophe Corre**. They are both incredible scientists and mentors who always believed in me, even when I did not. I am grateful for the trust, the patience and the freedom they gave me in pursuing my project. Their always kind guidance and passion for science have made these challenging last three years not so difficult after all.

I thank the members of my advisory panel, **Dr Hendrik Schäfer** and **Prof Kevin Purdy**, for their help and kind encouragement throughout my project. I also thank my examiners **Prof Matt Hutchings** and **Dr Richard Puxty** for showing interest in my work and the time they dedicated to examining this thesis.

I am also grateful for the help I have been given by many scientists at the University of Warwick. Thank you to **Dr Lijiang Song** for his assistance with NMR and metabolomics; **Dr Emzo de Los Santos** for his patience explaining everything bioinformatics and **Dr Matt Jenner** for his help with detecting interesting things in my proteomic data.

A warm thank you to every member of the **Christie-Oleza group** and the **Corre group**. Special thanks to **Dr Despoina Sousoni**, for initiating this project and for her help in continuing it. I also thank the original plastic gang, **Dr Vinko Zadjelovic**, **Dr Gabriel Erni Cassola**, and **Dr Robyn Wright**, for welcoming me in the group so wholeheartedly, their support and the memorable times spent together. Thank you to **Dr Mar Aguiló Ferretjans**, an amazing friend with a beautiful soul, who continuously and selflessly supported me and believed in me throughout the Ph.D. I could not have gotten that far without her.

A special thought for **Nikita Sergejevs**, **Frances Plumley**, **Laurence Quenault** and **Matthew Corney**, brilliant undergraduate students who were kind enough to trust me to teach them science things. They have, in fact, taught me as much as I taught them, and I am very proud to have shared a part of their scientific journey with them.

I want to thank the people from our famous Cake Rota group, for the brilliant lunch breaks and delicious cakes that made each week sweet. A big thank you in particular to **Dr Fabrizio Alberti**, for helping me immensely in the laboratory but above all for being such an incredible friend. I am thankful for the precious time spent together sharing great food, personal stories and laughs. I thank my dear **Linda Westermann**, the best bench neighbour and an even better friend, with such a loving and caring heart. Her singing and her hugs never fail to cheer me up during the lows of my project. We did go the distance, together. I thank **Eleonora Silvano**, for her beautiful smile, for shining bright as a sun even in the bad British weather and for giving the best hugs. I also thank **Dr**

Sandra Bedarida, **Dr Chiara Borsetto**, **Betty Sands**, **Sireethorn Tungsirisurp**, **Letizia Pondini**, **Holly Shropshire**, **Alberto Torcello** and **Dr Alevtina Mikhaylina** for the moments spent together.

A very particular thanks to **Dr Séverine Rangama**, with who I kept joking that we were not friends and only flatmates, but truth be told, she has become more than just a friend to me. I will forever be grateful for the sense of family and home she brought to my heart during these past three years. Words fail to describe how thankful I am for her loving support and for the incredible light she has shined on every single day we have lived together.

A warm thank you to **Cécile Jacry, Dr Sophia Belkhelfa, Dr Tiffany Souterre** and **Dr Tristan Cerisy** for making my time at University so memorable. A special thanks to **Nora Benkraouda**, with whom I have lived an incredible year in Boston and shared unforgettable moments.

My gratitude goes to **Dr Jonathan Kotula**, **Dr David Riglar** and **Dr Andrew Tolonen**, amazing mentors who I met throughout my career. I am thankful for everything they taught me and for the way they paved for me to get where I am now.

A loving thought for my lifelong friends **Elsa Dorme**, **Jonas Joachim** and **Grégory Ludot**, without whom my life would not be as bright. The unwavering love and the memories I have been sharing with them for the past fifteen years and counting mean the world to me.

No existen palabras para describir lo agradecido que estoy por compartir mi vida con el **Dr. Ismael Torres Romero**. Su amor incondicional consigue siempre iluminar hasta el más oscuro de mis días, y a su lado cada día se convierte en una aventura digna de ser vivida.

Last but not least, je remercie les membres de ma famille pour le soutiens et l'amour qu'ils m'ont porté malgré la distance et les années passées au loin. En particulier, merci à mon frère **Vic**, mes sœurs **Damra** et **Vicheara**, que j'aime de tout cœur et qui me manque chaque jour.

Je dédie cette thèse à mes chers parents, **Ly Chhun** et **Morin Chhun**, pour qui j'éprouve une gratitude infinie et un amour démesuré. Merci pour la famille que vous avez construite, l'amour inconditionnel que vous lui portez, la vie que vous nous avez offerte et l'incroyable lumière dont vous la parez.

DECLARATION

This thesis is submitted to the University of Warwick in support of my application for the degree of Doctor of Philosophy. It was composed by me and has not been submitted in any previous application for any degree.

The work presented (including data generated and data analyses) was carried out myself except in the cases outlined below:

- **Chapter 2:**
  - Flow cytometry data shown in Figure 9, B were collected by Laurence Quenault, an undergraduate student under my supervision during his third-year undergraduate project.
  - Experiments involving *Emiliania huxleyi* and *Phaeodactylum tricornutum* (including flow cytometry data shown in Figure 11, B and LC-MS data shown in Figure 17, A) were performed by Despoina Sousoni.
  - High-resolution mass-spectrometry data shown in Figure 12, B were collected by Lijiang Song, Head of Mass Spectrometry Facility (Department of Chemistry, University of Warwick), but sample preparation and data analysis were performed by myself.

- **Chapter 3:**
  - Proteomics samples were run by Cleidiane Zampronio, Chief Technician at the WPH Proteomics Facility (University of Warwick), although sample preparation and data analysis were performed by myself.

PUBLISHED WORK

Parts of this thesis have been published by the author as follows:

- Data presented in Chapter 2 and Chapter 3 (**Appendix 1**):

Chhun A[#], Sousoni D, Aguilo-Ferretjans M, Lijiang S, Corre C[#], Christie-Oleza JA[#]: Phytoplankton trigger the production of cryptic metabolites in the actinobacteria *Salinispora tropica*. (*Submitted*) Preprint available on *BioRxiv*, doi: 10.1101/2020.05.18.103358.

SUMMARY

The alarming rise of antimicrobial resistance in pathogenic strains has fuelled tremendous research efforts towards the discovery of novel bioactive molecules from untried ecological niches. In this regard, the world's oceans have revealed to be a remarkable resource of new bacterial taxa with promising biosynthetic potential. Study of the secondary metabolism of the marine actinobacterium *Salinispora*, for instance, has shown the genus to be an exceptional trove of unique and bioactive natural products, rivalling the significance of its terrestrial counterpart.

The isolation of new secondary metabolites from members of the genus *Salinispora* and other microorganism is, however, currently limited because most of the biosynthetic gene clusters (BGCs) encoded in their genomes are not expressed under standard laboratory conditions. This is well exemplified in *Salinispora*, as a staggering 80% of its BGCs are still orphan (*i.e.* not linked to their products). This observation warrants the development of new approaches to unlock the biosynthetic potential of the genus.

This thesis is devoted to investigating novel ways to activate, interrogate, and manipulate the biosynthetic potential of *Salinispora tropica* CNB-440. First, we demonstrate how co-cultivation of *S. tropica* with phytoplankton could be used to elicit the production of novel cryptic compounds in the actinobacterium. Our data also reveal that *S. tropica* exhibits antimicrobial activity against a range of eukaryotic and prokaryotic marine phototrophs *via* an uncharacterized mechanism.

Second, we report the first proteome dataset available in the genus *Salinispora*, that we explored in order to identify candidate secondary pathways responsible for the biosynthesis of the detected cryptic molecules and/or the antimicrobial activity observed in co-culture. Using high-throughput proteomics, we provide evidence that the orphan *nrps1* BGC is active and upregulated upon exposure to phytoplankton. We also suggest a potential mechanistic understanding of the antimicrobial effect seen in co-culture.

Finally, we implemented for the first time the CRISPR/Cas9 system in a member of the genus *Salinispora*, as a promising tool to link specific BGCs to the detected molecules and/or observed bioactivity described in our study. As a proof of concept, we successfully engineered *S. tropica* by deleting an entire BGC and a PPTase from its genome.

ABBREVIATIONS

A	Adenylation
ACP	Acyl Carrier Protein
AMR	Antimicrobial Resistance
ASW	Artificial Sea Water
AT	Acyltransferase
BGC	Biosynthetic Gene Cluster
BPC	Base Peak Chromatogram
C	Condensation
CoA	Coenzyme A
DAD	Diode-Array Detector
DAP	Diaminopimelic acid
DNA	Deoxyribonucleic Acid
FDA	US Food and Drug Administration
FDR	False Discovery Rate
HMM	Hidden Markov Models
HPLC	High-Pressure Liquid Chromatography
HSD	Honestly Significant Difference
KS	Ketosynthase
LB	Luria-Bertani medium
LC	Liquid Chromatography
LFQ	Label-Free Quantification
MB	Marine Broth
MRB	Multidrug Resistant Bacteria
MRSA	Methicillin-Resistant *Staphylococcus aureus*
MS	Mass Spectrometry
NMR	Nuclear Magnetic Resonance
NRPS	Nonribosomal Peptide Synthethase
PCP	Peptidyl Acyl Carrier

PCR	Polymerase Chain Reaction
PKS	Polyketide Synthase
PPant	Phosphopantetheine
PPTases	PhosphoPantetheinyl Transferases
rRNA	Ribosomal Ribonucleic Acid
SUPSYN	Supernatant of *Synechococcus*
TAR	Transformation-Associated Recombination
TE	Thioesterase
UV-VIS	Ultra violet-Visible

CHAPTER 1 | INTRODUCTION

1. A BRIEF HISTORY OF ANTIBIOTICS

Human health has been shaped by the use of drugs for millennia, starting with traditional medicines that have harnessed plant-derived molecules to treat various human illnesses. The *Artemisia* plant had been, for instance, used by Chinese herbalists as a remedy thousands of years ago, long before artemisinin was extracted from the plant and used as an anti-malarial drug (Cui & Su, 2009). More recently in history, the discovery of the microbe-derived antibiotic penicillin by Alexander Fleming in 1929 (Fleming, 1929) has been one of the most significant breakthroughs in modern medicine. Its successful use to treat bacterial infections has saved countless lives and has marked the dawn of the 'Golden age' of antibiotic discovery. This era, spanning from 1940 to 1962, witnessed the discovery of most of the microbial natural scaffolds from which pioneering drugs used today have been based upon. Antibiotics introduced during this period were mostly sourced from the specialized metabolism of bacteria and fungi and are grouped into different chemical classes, including β-lactams, aminoglycosides, glycopeptide and macrolides (Aminov, 2010; Brown & Wright, 2016). The identification of novel scaffolds following the golden era has, however, been virtually null with the latest class being reported in 1987; even if their representative antibiotics were ultimately marketed in the early 2000s (**Fig. 1**; Coates, Halls, & Hu, 2011; Silver, 2011).

The decline of the discovery rate of novel antimicrobials has become especially critical since it has been paralleled by a growing public health crisis caused by antimicrobial resistance (AMR) (Carlet et al., 2011). While AMR is a natural phenomenon whereby bacteria evolve mechanisms (*i.e.* by random point mutations or horizontal gene transfer) to survive antimicrobials exposure, the inappropriate use of antibiotics has set an unprecedented selective pressure upon pathogens that fuelled the rapid advent of multidrug resistant bacteria (MRB), rendering entire classes of antibiotics useless. For instance, a group of pathogenic bugs collectively named ESKAPE (*Enterococcus faecium*, *Staphylococcus aureus*, *Klebsiella pneumoniae*, *Acinetobacter baumanni*, *Pseudomonas aeruginosa* and *Enterobacter* spp.), have developed resistance mechanisms to the most commonly used antibiotics and are responsible for an increasing number of nosocomial infections (De Oliveira et al., 2020; Rice, 2008). Overall, it has been estimated that MRB

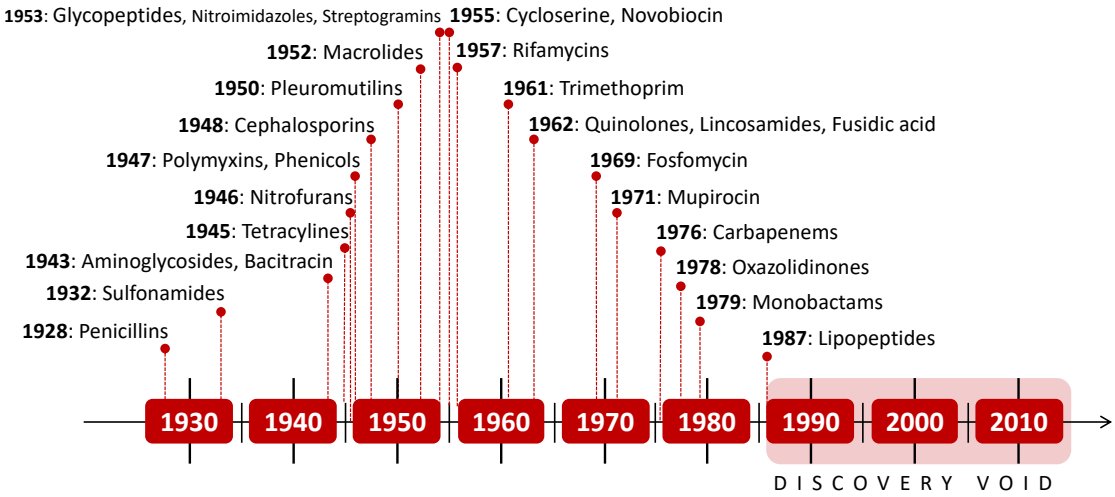

Figure 1 | Timeline of the discovery of the antibiotic classes in clinical use. The 'discovery void' represents the period since when the last antibiotic class successfully used as a treatment has been discovered or patented. Figure is adapted from Silver, 2011.

caused about 25,000 deaths across Europe in 2007 and 35,000 more in the U.S. (Colomb-Cotinat et al., 2016), and these numbers are set to worsen in the future. A review commissioned by the United Kingdom government indeed estimated that AMR could cause about 10 million deaths annually by 2050 (de Kraker et al., 2016; O'Neill, 2014), highlighting the urgency with which novel bioactive compounds are needed.

2. EXPLOITING NATURAL PRODUCTS FOR DRUG DISCOVERY

Natural products have undisputedly played a pivotal role in the discovery and development of medicines like antibiotics (Dias et al., 2012). These organic compounds derive from the primary or rather secondary metabolism of living entities, including plants, animals and microorganisms. Primary metabolites are directly involved in the growth, development or reproduction of an organism (*e.g.* polysaccharides, nucleic and fatty acids). In contrast, secondary metabolites are low molecular mass compounds (*i.e.* molecular weight < 3,000) often characteristic of a narrow range of species, with cryptic physiological functions deemed non-essential for the viability of the producing organism. Instead, they play a role in the adaptation to its environment and may be involved in defence or communication mechanisms (Dias et al., 2012). While natural products can be sorted into four main chemical classes (*i.e.* polyketides, nonribosomal peptides, terpenoids and steroids, alkaloids) (McMurry, 2009), their remarkable structural

diversity makes them a valuable reservoir of bioactive molecules with potential clinical relevance. The number of natural products discovered to this day exceeds 1 million, of which approximately 20-25% show biological activity ranging from anti-cancer, immunosuppressant or antibiotics (Demain & Sanchez, 2009). These bioactive compounds have continued to enter clinical trials to provide new drugs, as a comprehensive analysis of new medicines approved by the US Food and Drug Administration (FDA) between 1981 and 2014 showed that 33% of those small molecule-based medicines were natural products or derivatives of natural products (**Fig. 2**; Newman & Cragg, 2016).

Despite the contribution of natural product research for the development of novel drugs, low-throughput fermentation processes and the rediscovery of already known secondary metabolites led to a noticeable disinterest of most biopharmaceutical companies for this field in the late 20th century (Brown & Wright, 2016; Christopher Walsh, 2017). This was further aggravated by the advances at the time of alternative discovery platforms, driven by high-throughput screening and combinatorial synthesis, which were thought to be a more productive approach to drug discovery. However, low returns from the aforementioned alternative strategies, coupled with the growing demand for new drugs caused by the AMR crisis, eventually resulted in a renewed enthusiasm to exploit the diversity of natural products for drug discovery (Pham et al.,

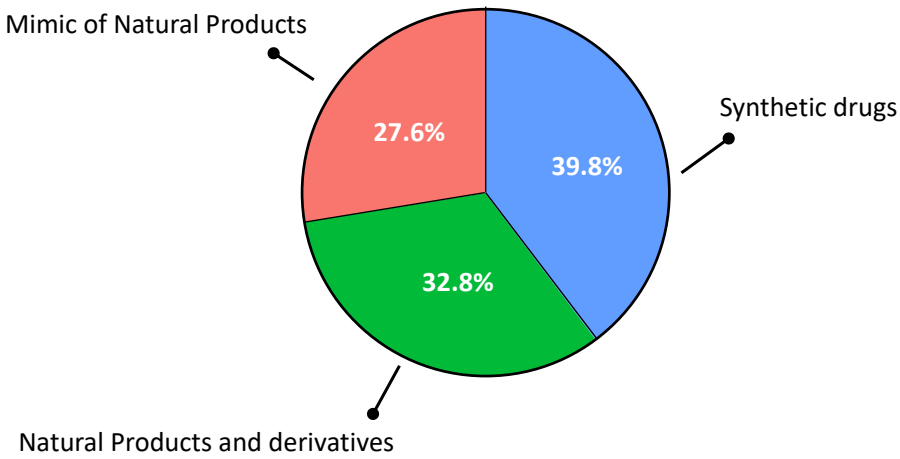

Figure 2 | Sources of all small-molecule drugs approved by the U.S. FDA. Approved from 1981 to 2014, with *n* = 1,211. Mimic of Natural Products refers to synthetic compounds showing competitive inhibition of the natural product substrate. Figure is adapted from Newman & Cragg, 2016.

2019; Shen, 2015). In particular, the significance of small molecules derived from microbial sources was supported by improvements in sequencing technologies, allowing genome sequencing of various microbes such as the soil actinomycete *Streptomyces coelicolor*, which revealed an untapped wealth of secondary metabolites awaiting to be uncovered (Baltz, 2019; Bentley et al., 2002).

3. ACTINOBACTERIA - A WEALTH OF BIOACTIVE COMPOUNDS

Actinobacteria are an extremely diverse phylum of Gram-positive bacteria with a high G-C content, including rod-shaped and filamentous cells. Although they are ubiquitous of soil and water ecosystems, soil actinomycetes have been historically the most prolific source of clinically-relevant natural products. In particular, species from the genus *Streptomyces*, which are aerobic soil-dwelling filamentous bacteria reproducing by sporulation, account for most of the bioactive compounds discovered to date.

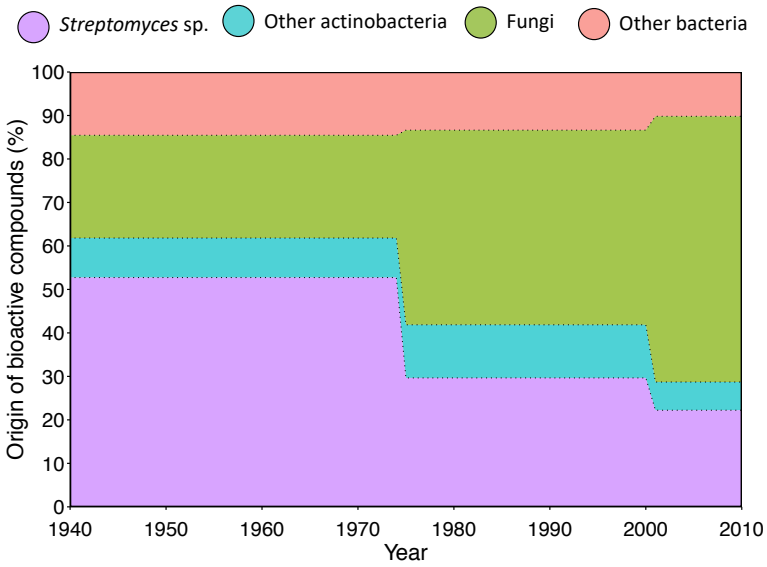

Figure 3 | Distribution of the reported bioactive microbial natural products according to their origin (1940-2010). Figure is adapted from Bérdy, 2012.

During the mid-1900s, more than 60% of bioactive microbial metabolites were sourced from actinobacteria and almost exclusively from *Streptomyces* spp. (**Fig. 3**; Bérdy, 2012). Although this proportion decreased in recent years in favour of fungi-derived metabolites, actinobacteria still account for a significant portion of the pool of reported bioactive molecules, making up to 30% of all the molecules discovered during the 2001 to 2010 period (**Fig. 3**). Overall, it has been estimated that from the 33,500 bioactive

metabolites that have been reported from microbes so far, 45% are produced by actinomycetes, of which 76% were isolated from *Streptomyces* spp. (Bérdy, 2012). More specifically, the *Streptomyces* genus alone yielded over two-third of all antibiotics used today, as the main antimicrobial chemical scaffolds derive from *Streptomyces*-isolated compounds (Bérdy, 2005; Genilloud, 2017; Takahashi & Nakashima, 2018). For instance, the β-lactam cephamycin was isolated from *Streptomyces clavuligerus* (Ward & Hodgson, 1993), the aminoglycoside neomycin from *Streptomyces fradiae* (Dulmage, 1953), the macrolide erythromycin from *Streptomyces erythreus* (Weber et al., 1985), the glycopeptide vancomycin from *Streptomyces orientalis* and tetracycline from *Streptomyces aureofaciens* (Darken et al., 1960) (**Fig. 4**).

The identification of novel secondary metabolites from this extensively studied soil-dwelling genus has, however, slowed down over the last few decades because of the recurring rediscovery of already known compounds (Coates et al., 2011). This resulted in a growing interest to explore the bacterial diversity of overlooked ecological niches and taxonomic groups, with the rationale that ecologically distinct microorganisms produce

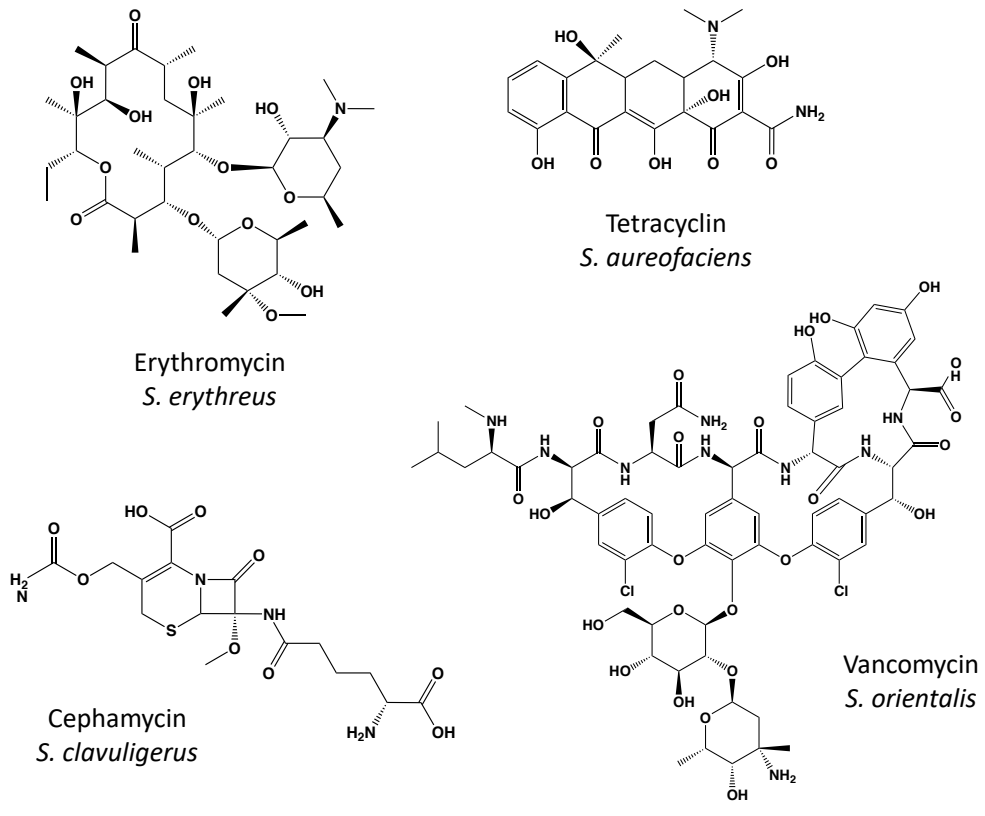

Figure 4 | Structures of representative antibiotics discovered in *Streptomyces.*

equally distinct natural products (Bull & Goodfellow, 2019; Molinski et al., 2009; Z. E. Wilson & Brimble, 2009). The world's oceans, covering 70% of the Earth's surface, have typically been poorly studied ecosystems, in part because of limited technologies and equipment allowing the exploration of this vast habitat. Our knowledge of the marine environment has nonetheless improved dramatically over the years and we now know that complex and diverse microbial communities inhabit the oceans. One millilitre of seawater commonly hosts about one million microorganisms, while their abundance in ocean-bottom sediments reaches up to one billion cells per millilitre (Whitman et al., 1998). From the study of these marine communities emerged numerous interesting novel compounds and bacterial species for drug discovery, including the promising actinobacterial genus *Salinispora* (Baltz, 2008; Fenical & Jensen, 2006; Manivasagan, Kang, et al., 2014; Manivasagan, Venkatesan, et al., 2014).

4. THE MARINE ACTINOBACTERIUM *SALINISPORA*

Soil actinobacteria are known to produce resilient spores that withstand harsh conditions and remain viable although dormant for years (Cross, 1981). It has therefore been assumed that actinomycetes recovered from marine environments over the years were simply the result of spores washed up from land into the sea. This paradigm changed, however, upon the description in 2002 of a persistent and widely distributed actinomycete taxon exclusively reported from the ocean, named *Salinispora* (Mincer et al., 2002). Bacteria from this newly discovered genus, closely related to *Micromonospor*a, were the first seawater-obligate marine actinomycetes to be

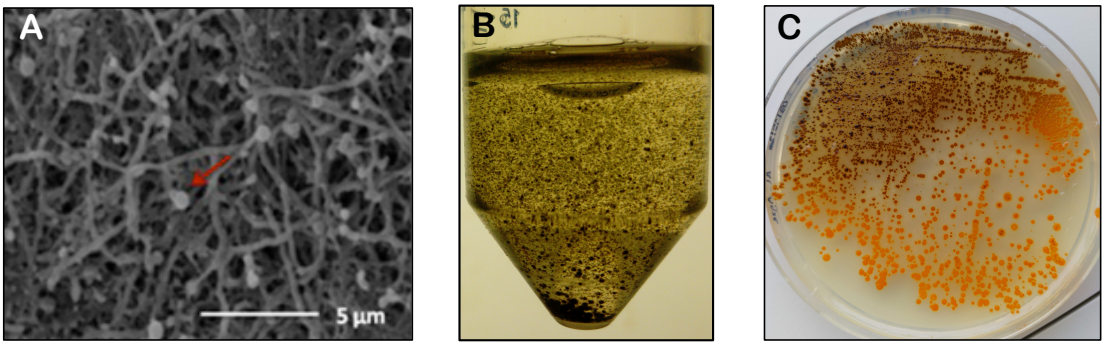

Figure 5 | Growth and morphology of *Salinispora*. (A) SEM of *S. arenicola* M413 mycelia with spores forming at the tip of the mycelium, indicated by the red arrow. Picture is extracted from Hewavitharana, Webb, Shaw & Fuerst, 2013. **(B)** Photograph of a 7-day old liquid culture of *S. tropica* CNB-440 in marine broth. **(C)** Photograph of a 22-day old culture of *S. tropica* CNB-440 on A1-agar plate.

described. It was later shown that they require sodium salts and that a low-ionic-strength environment leads to cell lysis (Tsueng & Lam, 2008). Further studies identified the loss of the *mscL* gene, which encodes a transmembrane protein involved in alleviating osmotic downshock, to be responsible for *Salinispora*'s salt requirement, thereby providing the first evidence that certain actinobacteria specifically adapted to marine ecosystems (Bucarey et al., 2012; Penn & Jensen, 2012).

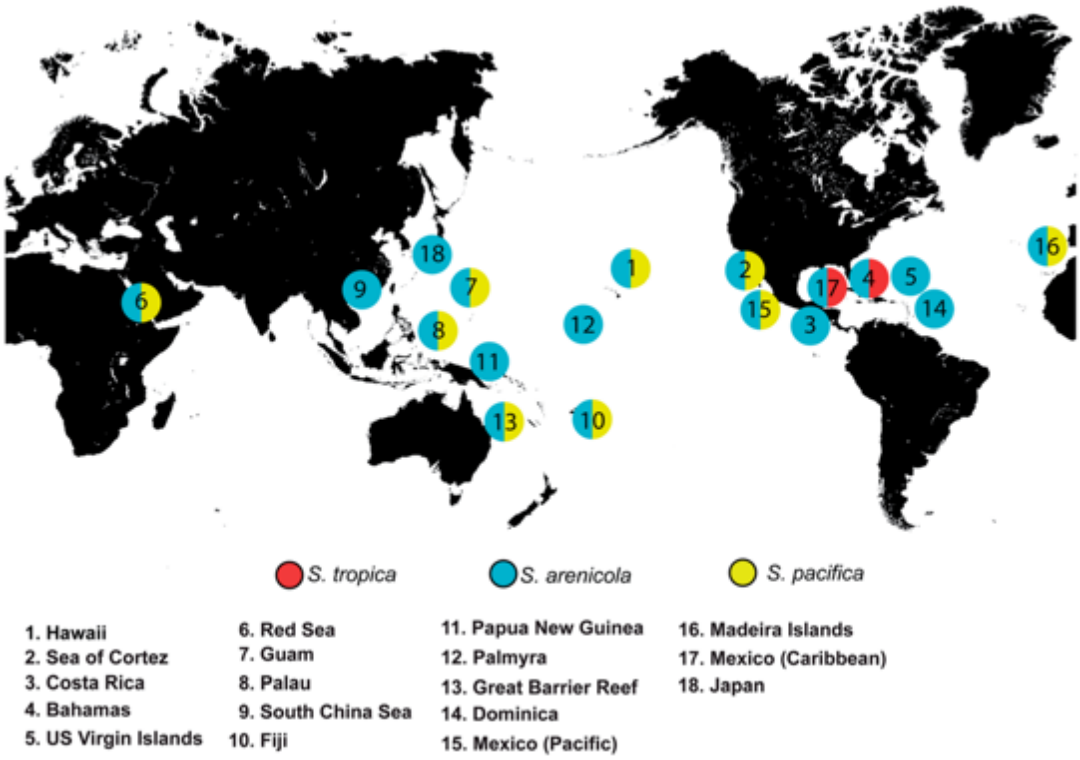

Figure 6 | Locations from which the genus *Salinispora* has been reported. Figure is extracted from Jensen, Moore & Fenical, 2015.

Salinispora are aerobic, Gram-positive heterotrophs that form a branched mycelium with a lack of aerial hyphae, they grow as dense aggregates in liquid and display a pigmentation ranging from orange to black, due to sporulation (**Fig. 5**) (Ng et al., 2013). Phylogenetic analyses of nearly complete small subunit rRNA and *gyrB* sequences of the first *Salinispora* isolates revealed that they formed a clade of closely related strains, with a 16S rRNA gene sequence identity greater than 99% (Jensen & Mafnas, 2006). While the genus is officially comprised of three formally described species, *Salinispora tropica*, *Salinispora arenicola* and *Salinispora pacifica* (Ahmed et al., 2013; Maldonado et al., 2005), recent phylogenomic analyses based on average nucleotide identity of 119 strains suggested more species-level diversity, with the existence of 10 different candidate

species (Millan-Aguinaga et al., 2017). To date, *S. tropica* is the species with the most limited geographic distribution and has been reported only from the Caribbean (Bahamas and Yucatán), while *S. pacifica* and *S. arenicola* are broadly distributed throughout tropical and subtropical oceans (**Fig. 6**). Originally recovered from marine sediments of shallow waters (1-30 meters depth) (Mincer et al., 2002), *Salinispora* has since then been found in far greater depths (1-1,100 meters), and isolated from the microbiota of ascidian, seaweeds, marine sponges and corals (Asolkar et al., 2010; Jensen et al., 2005; Ocampo-Alvarez et al., 2020). The cosmopolitan distribution of *Salinispora* in the marine ecosystem raised questions about whether this diversity could be reflected in the genus secondary metabolic potential, similarly to what has been observed for soil actinobacteria (van der Meij et al., 2017).

Genome sequencing of the type strain *S. tropica* CNB-440^{T} in 2007 brought a first answer to these questions by providing a valuable insight into the biosynthetic capacity of the genus (Udwary et al., 2007). Analysis of its genome revealed a strikingly rich predicted secondary metabolome, with the detection of many natural product gene clusters accounting for 10% of its entire genome. Interestingly, a significant portion of these identified genomic clusters were not only found to feature polyketide synthase (PKS) and nonribosomal peptide synthetases (NRPS) systems (responsible for the biosynthesis of two of the most important classes of bioactive natural products) but they also appeared to be completely new biosynthetic loci (Udwary et al., 2007). Altogether, these observations supported the idea that novel microbial taxa from untried ecological niches could represent a wealth of unique molecules for drug discovery, by revealing the genus *Salinispora* as a remarkable potential source of new secondary metabolites rivalling its terrestrial counterpart.

5. NATURAL PRODUCTS ISOLATED FROM *SALINISPORA*

Since its discovery, the genus *Salinispora* has proven to be a significant source of novel bioactive molecules with the isolation of numerous secondary metabolites, of which a majority were unique to the genus and showed a range of biological activities relevant for pharmaceutical applications (**Table 1**). For instance, the siderophore deferoxamine (Roberts et al., 2012), the immunosuppressant lymphostin (Miyanaga et al., 2011) and

Table 1 | Natural products reported from the genus *Salinispora*.

Compound name	*Salinispora* species			Biosynthetic class	Activity	References
	trop	*paci*	*aren*			
Arenamide			+	NRPS	NFkB inhibitor	Asolkar *et al.*, 2009
Arenicolide			+	PKS	*ND*	Williams *et al.*, 2007
Arenimycin			+	PKS	Antimicrobial/Cytotoxic	Asolkar *et al.*, 2010
BE-43547			+	PKS-NRPS	Hypoxia-selective toxicity	Villadsen *et al.*, 2016
Cyanosporaside		+		PKS	Cytotoxic	Oh *et al.*, 2006
Cyclomarazine			+	NRPS	Antimicrobial	Schultz *et al.*, 2008
Cyclomarin			+	NRPS	Anti-inflammatory	Schultz *et al.*, 2010
Deferoxamine	+	+	+	Hydroxamate	Siderophore	Roberts *et al.*, 2012
Enterocin		+		PKS	Antimicrobial	Bonet *et al.*, 2015
3-hydroxy-*N*-methyl-2-oxindole			+	*ND*	*ND*	da Silva *et al.*, 2019
4-hydroxy-pyran-2-one			+	*ND*	*ND*	da Silva *et al.*, 2019
Ikarugamycin			+	PKS-NRPS	Antimicrobial	Greunke *et al.*, 2017
Isopimara-8,15-dien-19-ol			+	Terpene	*ND*	Xu *et al.*, 2014
Lomaiviticin	+	+		PKS	Cytotoxic	He *et al.*, 2001
Lymphostin	+	+	+	PKS-NRPS	Immunosuppressant	Miyanaga *et al.*, 2011
6-methoxy-*N*-methylisatin			+	*ND*	Antimicrobial	da Silva *et al.*, 2019
Mevinolin			+	PKS	Cholesterol-lowering agent	Bose *et al.*, 2014
Pacificanone		+		PKS	*ND*	Oh *et al.*, 2008
Retimycin			+	NRPS	Cytotoxic	Duncan *et al.*, 2015
Rifamycin			+	PKS	Antimicrobial	Kim *et al.*, 2006
Rosamicin		+		PKS	Antimicrobial	Awakawa *et al.*, 2015
Salinaphthoquinones			+	*ND*	Antimicrobial	da Silva *et al.*, 2019
Salinichelin		+	+	Hydroxamate-NRPS	Siderophore	Bruns *et al.*, 2018
Saliniketal			+	PKS	Ornithine decarboxylase inhibitor	Williams *et al.*, 2007
Salinilactam	+			PKS	*ND*	Udwary *et al.*, 2007
Salinilactone			+	*ND*	Antimicrobial	Schlawis *et al.*, 2018
Salinipostin	+	+		Butyrolactone	Cytotoxic/antimalarial	Schulze *et al.*, 2015
Salinipyrone		+		PKS	*ND*	Oh *et al.*, 2008
Saliniquinone			+	PKS	Cytotoxic	Murphy *et al.*, 2010
Salinisporamide	+	+		PKS-NRPS	Cytotoxic	Feling *et al.*, 2003
Sioxanthin	+	+	+	Terpene	*ND*	Richter *et al.*, 2015
Sporolide	+			PKS	HIV reverse transcriptase	Buchanan *et al.*, 2005
Staurosporine			+	Alkaloid	Protein kinase inhibitor	Jensen *et al.*, 2007
Thiolactomycin		+		PKS-NRPS	Fatty acid synthesis inhibitor	Tang *et al.*, 2015
Tirandalydigin		+		PKS-NPRS	RNA polymerase inhibitor	Castro-Falcón *et al.*, 2016

Bold = novel compound; *trop* = *S. tropica; paci* = *S. pacifica; aren* = *S. arenicola;* + = Compound detected from this species; *ND* = not determined.

the terpenoid sioxanthin (Richter et al., 2015) are produced by all three *Salinispora* species (**Table 1**).

Although the two formers were previously reported from other microbes, sioxanthin was a new and unusual glycosylated carotenoid, associated with *Salinispora*'s orange pigmentation (**Fig. 7**). Interestingly, in contrast with the aforementioned compounds, it was shown that most of the metabolites reported from the genus are species-specific

and that these functional patterns could be characteristics of ecotypes rather than due to geographical isolation (Jensen & Mafnas, 2006; Jensen et al., 2007; Penn et al., 2009). Lomaiviticin (**Fig. 7**) was the first molecule reported from *Salinispora* and was isolated from *S. pacifica* before the genus was actually formally described. The isolate from which lomaiviticin was discovered was indeed thought to be a new species of *Micromonospora*, until 16S analysis later revealed the strain to be *S. pacifica* (He et al., 2001; Janso et al., 2014). Similarly to lomaiviticin, cyanosporaside and salinipyrone were two novel polyketides characteristic of *S. pacifica*, with the two formers exhibiting interesting cytotoxic activity (Oh et al., 2006, 2008). *S. arenicola* is the most widely distributed and abundant species of the genus (**Fig. 6**), and it is also a notable prolific producer of novel natural products (**Table 1**). For instance, the new polyketide molecules saliniquinone and arenimycin were both derived exclusively from *S. arenicola* and were found to have cytotoxic and antimicrobial activities, respectively (Asolkar et al., 2010; Murphy et al., 2010). Interestingly, arenimycin (**Fig. 7**) was shown to be effective against rifampicin- and methicillin-resistant *Staphylococcus aureus* (MRSA), a growing threat to human health involved in the AMR crisis (Chua et al., 2011). The novel non-ribosomal peptide

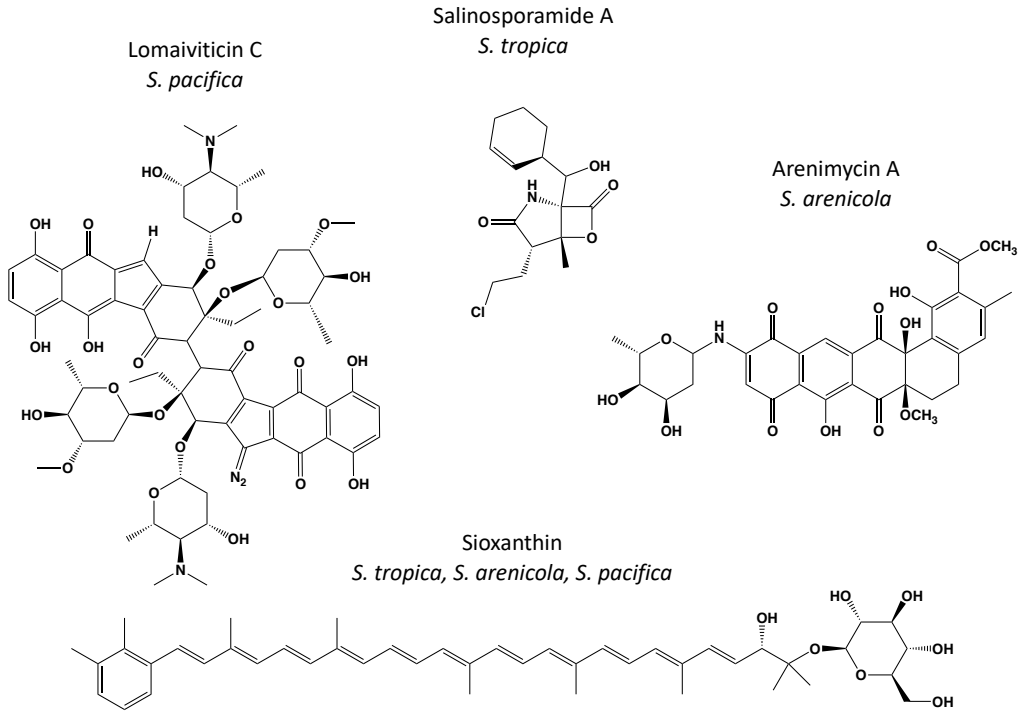

Figure 7 | Structures of secondary metabolites reported from the genus *Salinispora*.

compounds retimycin and arenamide were also derived only from *S. arenicola*, and exhibited promising cytotoxic activity (Asolkar et al., 2009; Duncan et al., 2015).

Among the catalogue of natural products discovered from *Salinispora*, salinosporamide is so far the most significant family of molecules obtained from the genus (**Fig. 7**; Gulder & Moore, 2010). Salinosporamide A was isolated from *S. tropica* in 2003, and has since then been extensively studied, leading to the identification of many analogues (Denora et al., 2007; Feling et al., 2003; Reed et al., 2007). The compound possesses a unique fused γ-lactam-β-lactone bicyclic ring pharmacophore with potency to inhibit the 20S proteasome, a target in cancer chemotherapy (Crawford et al., 2011). For this reason, it quickly entered phase I clinical trials for the treatment of different myeloma under the name Marizomib, given by the FDA (Harrison et al., 2016; Macherla et al., 2005). Due to its lipophilic structure, which allows it to pass the blood-brain barrier, the biopharmaceutical company Celgene has acquired the rights to Marizomib in 2016, and is currently investigating the molecule's potency to treat glioblastoma in a phase III clinical trial set to be completed in 2023 (ClinicalTrials.gov identifier NCT03345095). If salinosporamide is then approved, it will become the first marine natural product from a microbial source to be developed as a drug (Pereira, 2019).

Salinispora has undisputedly provided a remarkable abundance of novel natural products so far, most of which are bioactive and clinically useful. It is clear, however, from sequencing and subsequent analyses of *Salinispora*'s genomes, that the biosynthetic potential of the genus still remains exceedingly underexplored as many identified biosynthetic loci encoding secondary metabolites await to be characterized.

6. ORPHAN BIOSYNTHETIC GENE CLUSTERS

Most secondary metabolites are biosynthesized by multi-modular enzyme complexes encoded by groups of genes co-localized in the genome, referred to as a biosynthetic gene clusters (BGCs). Based on the type of molecule produced, different classes of BGC exist, with NRPS- and PKS-type systems being the most widely characterized and responsible for the formation of nonribosomal peptides and polyketides, respectively (Fischbach & Walsh, 2006). These natural products are essentially constructed through the elongation of a chain of covalently bound building blocks, being acyl-coenzyme A (CoA) for polyketides and amino or carboxylic acids for nonribosomal peptides, following

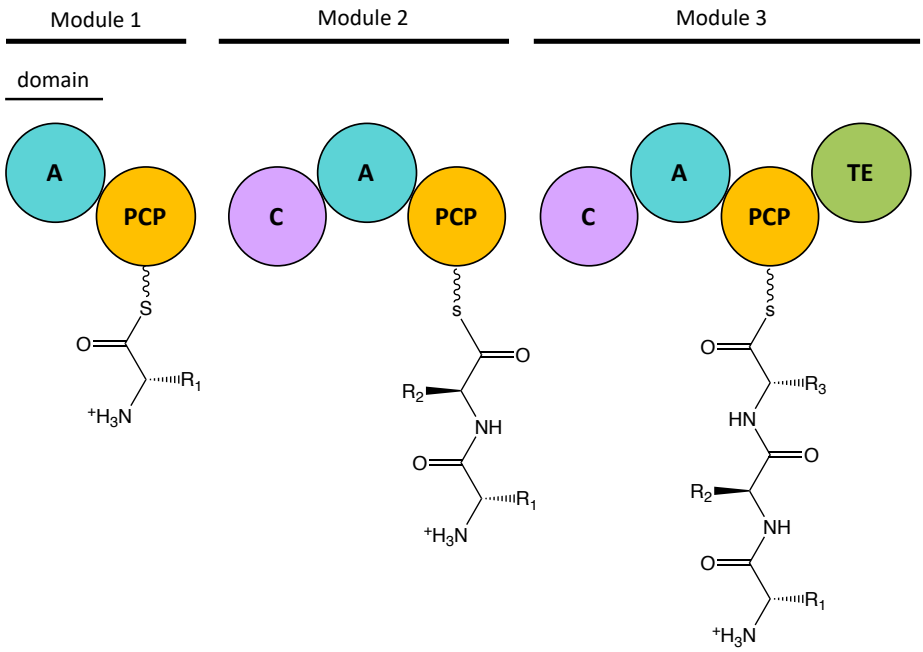

Figure 8 | General organization of a NRPS assembly line. Each module is responsible for adding one amino-acid to the growing oligopeptide where the adenylation (A) domains select and activate amino-acids in a specific manner by converting them into their corresponding aminoacyl thioester, which will then be loaded onto the PCP domains. The condensation (C) domain catalyzes the formation of a peptide bond between the PCP-bound amino-acid and the growing peptide chain of the upstream module. The thioesterase (TE) domain releases the mature oligopeptide from the NPRS assembly line.

an assembly line logic allowed by functional domains organized within the BGC (Scott & Piel, 2019; Walsh, 2008). For instance, a type I modular PKS consists of multiple catalytic units called modules, each responsible for the incorporation of one monomer. The modules are themselves composed of core domains involved in the different steps of the assembly line, namely an acyltransferase (AT) domain, an acyl carrier protein (ACP) and a ketosynthase (KS) domain (Tibrewal & Tang, 2014). Briefly, the AT domain will select and load the acyl-CoA monomer onto the ACP, which tethers substrates and growing polyketide intermediates. The KS domain will then catalyse the condensation reactions to bind the nascent natural product and the extender unit (Khayatt et al., 2013). Similarly, a NRPS module consists of an adenylation domain, a peptidyl carrier protein (PCP) and a condensation domain, which will serve analogous roles as the AT domain, the ACP and the KS domain, respectively (**Fig. 8**; Mootz et al., 2000). In addition to those biosynthetic genes required for the actual production of the molecule, BGCs also typically include

genes involved in expression regulation, self-resistance and export of the produced compound (Corre et al., 2008; Medema et al., 2015; Tenconi & Rigali, 2018).

Overall, the highly structured organization of BGCs facilitates their identification and characterization from the wealth of genomics data provided by next-generation sequencing technologies (Walsh & Fischbach, 2010). Genome mining of BGCs for natural product discovery has especially been propelled by the advent of bioinformatics pipelines such as antiSMASH, which allows fast identification and annotation of BGCs (Blin et al., 2019; Medema et al., 2011). More recently, the field has also seen the development of other platforms, like ARTS (Mungan et al., 2020) and BiG-SCAPE/CORASON (Navarro-Muñoz et al., 2020), for the prediction of the mode of action of BGC-encoded compounds *via* the identification of antibiotic resistant genes and for the clustering and classification of BGCs. While allowing the discovery of many novel natural products, these extensive genome mining efforts have simultaneously revealed an intriguing fact – a typical actinobacteria has the genetic potential (*i.e*. BGCs) to produce on average 10 times more secondary metabolites than what had been detected

Table 2 | Biosynthetic gene clusters of *Salinispora tropica* CNB-440. Table shows the characterized (orange) and orphan (green) BGCs of *S. tropica* CNB-440.

BGC name	Biosynthetic class	Product	Genetic location (strop_)	Size (kb)	Reference
sal	polyketide/non-ribosomal peptide	salinosporamide	RS05130-RS05275	41.8	Feling *et al.*, 2003
lom	polyketide	lomaiviticin	RS10930-RS11215	62.2	Kersten *et al.*, 2013
des	hydroxamate	desferrioxamine	RS12775-RS12855	19.2	Roberts *et al.*, 2012
spo	polyketide	sporolide	RS13560-RS13730	49.2	Dineshkumar *et al.*, 2014
slm	polyketide	salinilactam	RS13850-RS13965	82.0	Udwary *et al.*, 2007
lym	polyketide/non-ribosomal peptide	lymphostin	RS15295-RS15350	25.0	Miyanaga *et al.*, 2011
terp1	terpenoid	sioxanthin	RS16250-RS16295	10.4	Richter *et al.*, 2015
spt	butyrolactone	salinipostin	RS20900-RS20940	11.1	Amos *et al.*, 2017
terp2	terpenoid	sioxanthin	RS22405-RS22445	11.7	Richter *et al.*, 2015
pks1	polyketide	*NA*	RS02980-RS03095	30.9	*NA*
nrps1	non-ribosomal peptide	*NA*	RS03375-RS03535	37.5	*NA*
amc	carbohydrate	*NA*	RS11765-RS11795	6.6	*NA*
bac1	ribosomal peptide	*NA*	RS11800-RS12275	19.2	*NA*
pks3	polyketide	*NA*	RS12510-RS12630	23.3	*NA*
sid2	non-ribosomal peptide	*NA*	RS13260-RS13385	40.7	*NA*
sid3	non-ribosomal peptide	*NA*	RS13985-RS14120	29.2	*NA*
sid4	non-ribosomal peptide	*NA*	RS14125-RS14260	40.8	*NA*
bac2	ribosomal peptide	*NA*	RS14265-RS15290	19.0	*NA*
pks4	polyketide	*NA*	RS21120-RS21540	10.0	*NA*
nrps2	non-ribosomal peptide	*NA*	RS22250-RS22350	34.7	*NA*

from traditional screening and chemical analysis (Palazzotto & Weber, 2018). Those biosynthetic loci that are detected bioinformatically but for which no natural product has been assigned yet are called orphan BGCs. It is generally considered that they are either transcriptionally silent (*i.e.* poor or conditional level of expression or inactivation of their biosynthetic genes) or that the molecules they produce are difficult to detect and isolate (*i.e.* compound instability, limited sensitivity of detection methods or absence of bioactivity to screen for) (Rutledge & Challis, 2015).

The significance of orphan BGCs as a tremendous and untapped resource of novel bioactive compounds is well exemplified in the genus *Salinispora*. A recent study analyzing the draft genomes of 119 strains showed that, among the 176 distinct BGCs bioinformatically identified, a staggering 80% of those were still orphan (Letzel et al., 2017). As an illustrative case, the genome of the type strain *S. tropica* CNB-440 harbors at least twenty putative BGCs, but of these, only nine have been assigned to a natural product so far (**Table 2**). Discovering new secondary metabolites from the remarkable pool of orphan BGCs that remain to be characterized has become a focus of natural product research, with the development of means to activate such silent clusters being one of the biggest challenges of these research efforts (Onaka, 2017; Ren et al., 2017).

7. UNLOCKING MICROBIAL BIOSYNTHETIC POTENTIAL

In response to the growing number of orphan BGCs reported, researchers have developed pleiotropic and pathway-specific approaches to activate those silent clusters (Rutledge & Challis, 2015). Some successful examples of pathway-specific methods include the expression of entire BGCs in a heterologous host and the manipulation of transcription factors activating their expression. For instance, capture of a silent NRPS cluster from the marine actinomycete *Saccharomonospora* using transformation-associated recombination (TAR) cloning, followed by the deletion of a regulatory gene and subsequent expression of the refactored cluster into the host *S. coelicolor,* resulted in the discovery of the antibiotic taromycin (Yamanaka et al., 2014). A recent study from our group similarly used TAR cloning to capture a silent gene cluster from a genetically intractable *Streptomyces* strain, before inactivating a transcriptional repressor *via* CRISPR/Cas9 editing to trigger the production of scleric acid in *Streptomyces albus* (Alberti et al., 2019). Although these pathway-specific approaches have proven

successful, their implementation can present several limitations as they require the BGC of interest to be: (i) controlled by an identifiable transcription factor, (ii) amenable to genetic manipulation and (iii) of a reasonable size (<40 kb), as methods for capture and heterologous expression typically become less efficient as the size of the cluster increases (Rutledge & Challis, 2015). Additionally, such methods are by definition targeted and can hardly be applied in a high throughput manner or when little is known about the BGCs and their regulation.

In contrast, pleiotropic approaches can be used to trigger global changes in the regulation of biosynthetic loci, regardless of their sizes and without requiring any prior knowledge on their genetics, and do so in genetically intractable organisms. Most natural products are specialized molecules resulting from the myriad of inter- and intraspecies interactions that occur in the natural environment of the producing organisms. When they are grown axenically *in vitro*, many of the activating signals (*e.g.* signalling molecules, nutrients or cell-cell contacts) are therefore absent, leading to silent BGCs. Consequently, one of the most efficient and fruitful pleiotropic methods described in the literature utilizes co-cultivation of different microbes to elicit novel secondary metabolite biosynthesis (Bertrand et al., 2014; Slattery et al., 2001; Wakefield et al., 2017). Finally, the advent of -omics technologies (*i.e.* genomics, transcriptomics, proteomics etc.) have been instrumental in improving our understanding of secondary metabolites pathways and the discovery of new natural products (Bumpus et al., 2009; Chen et al., 2013; Palazzotto & Weber, 2018).

While these different methods have been applied successfully to various microorganisms and especially to *Streptomyces* sp. (Abdelmohsen et al., 2015; Onaka, 2017; Reen et al., 2015; Rutledge & Challis, 2015), their use in the genus *Salinispora* remains in its infancy. To the best of our knowledge, only a couple of studies employed heterologous expression of silent BGCs from *S. pacifica and S. arenicola* into *Streptomyces* host strains, to uncover the compounds enterocin and isopimara-8,15-dien-19-ol, respectively (Bonet et al., 2015; Xu et al., 2014). The co-inoculation of *Salinispora* with other microbes has, on the other hand, been more used but with little success. For instance, growing *S. arenicola* with the fungus *Emericella* sp. induced the production of the molecule emericellamide but in the latter instead of the former (Oh et al., 2007). More recently, Patin and colleagues co-cultured different *S. arenicola and S. tropica* strains with various

marine heterotrophs isolated from sediments but these interactions did not yield any new natural product (Patin et al., 2018; Patin et al., 2016). They showed, however, that *S. tropica* intriguingly exhibited antimicrobial activities against some marine heterotrophs without being able to identify the killing agent. These studies notably provided a first insight on the ecological significance of the bioactive compounds issued from members of the genus *Salinispora* and of their interactions with the microbial communities residing in marine sediments (Patin et al., 2017). Lastly, comparative transcriptomics analysis of several strains of *Salinispora* resulted in the discovery of the salinipostin molecule in *S. pacifica* (Amos et al., 2017) but it is so far the only study of the type in the genus.

8. CONCLUSION

The alarming increase of AMR has brought to light the urgency with which we need to discover novel active compounds, while the recurring rediscovery of already known natural products has drawn the interest of researchers towards untapped ecological niches to isolate unique molecules (Bull & Goodfellow, 2019). The marine actinobacterium *Salinispora* certainly drew particular attention upon its isolation almost two decades ago. The study of its secondary metabolome has since proven the genus to be an exceptional source of novel and bioactive natural products, set to rival the significance of soil actinomycetes (Jensen et al., 2015).

The discovery of new small molecules from *Salinispora* and other microbes is, however, currently hampered because most BGCs encoded by these microorganisms are not expressed under standard laboratory conditions (*i.e.* monocultures) (Walsh & Fischbach, 2010). This derives, in part, from our poor understanding of their natural interactions within their environments. The astonishing proportion of these orphan BGCs in *Salinispora* warrants the development of untried approaches to unlock the biosynthetic potential of the genus. Also, although a few studies investigated *Salinispora*'s impact on heterotrophic bacterial communities in marine sediments (Patin et al., 2017), very little is known of its interactions with other microbial communities (*i.e.* phototrophs), while there is growing evidence that *Salinispora* has a more cosmopolitan ecological distribution than what was previously thought (Ocampo-Alvarez et al., 2020).

RESEARCH AIMS FOR THE PH.D. THESIS

The present Ph.D. thesis aimed at exploring novel ways to activate, interrogate, and manipulate the biosynthetic potential of the marine actinobacterium *S. tropica* CNB-440.

The objectives of the research carried out were thus threefold.

- Firstly, to investigate the potency of co-culturing marine phytoplankton with *Salinispora* to stimulate its biosynthetic activity, using metabolomics.

- Secondly, to identify expression of candidate BGCs using high-throughput proteomics.

- Thirdly, to establish new strategies to influence secondary metabolite production in *Salinispora* at the genetic level, using the genome engineering CRISPR/Cas9 technology for multiple-gene deletion.

The following chapters will introduce the results obtained from these three research objectives.

CHAPTER 2 |

PHYTOPLANKTON TRIGGER THE PRODUCTION OF CRYPTIC METABOLITES IN THE MARINE ACTINOBACTERIUM *SALINISPORA TROPICA*

INTRODUCTION

Soil actinomycetes are a rich source of drug-like natural products, to which we owe up to 70% of all microbial antibiotics used today (Bérdy, 2012). Identification of novel secondary metabolites from this extensively studied family has, however, stalled over the last few decades as a result of the recurring rediscovery of already known compounds. This has led in recent years to a thriving interest for the study of new microorganisms, with the rationale that ecologically distinct microorganisms produce equally distinct secondary metabolites (Bull & Goodfellow, 2019; Molinski et al., 2009; Wilson & Brimble, 2009). For instance, the heterotrophic bacteria *Salinispora* drew particular attention when discovered as it was the first obligate marine actinomycete described (Jensen et al., 1991; Mincer et al., 2002) and has since proven to be an important source of new natural products for the pharmaceutical industry (Asolkar et al., 2010; Buchanan et al., 2005; Feling et al., 2003; Maldonado et al., 2005).

Despite the increasing number of novel strains identified with promising biosynthetic capacities, many hurdles in natural product discovery remain. Most of these microbial secondary metabolites are encoded by groups of colocalized genes, called biosynthetic gene clusters (BGCs), which are now more easily identified because of the improvement in sequencing technologies and bioinformatic tools (Medema et al., 2011). The majority of these identified BGCs, however, have yet to be linked to their products and are called orphan BGCs. They are generally considered to be either silent - because of a low level of expression or inactivation of their biosynthetic genes - or the metabolites they produce are cryptic - difficult to detect and isolate (Reen et al., 2015; Rutledge & Challis, 2015). The observation of numerous orphan BGCs in genome-sequenced microorganisms has resulted in a growing interest in developing biological or chemical means to activate such clusters (Abdelmohsen et al., 2015; Onaka, 2017). One of the simplest and most efficient methods described in the literature relies on co-cultivation

of different microbes to elicit novel natural product biosynthesis (Bertrand et al., 2014; Slattery et al., 2001; Wakefield et al., 2017).

The genome of the marine actinomycete *Salinispora tropica* comprises at least 20 putative BGCs of which 11 are orphan (Penn et al., 2009; Udwary et al., 2007). Recent studies have shown that *Salinispora* co-inoculated with various marine heterotrophs could produce one or several antimicrobial compounds, which remain uncharacterized as traditional analytical chemistry methods did not allow their identification and no candidate BGC was proposed (Patin et al., 2018; Patin et al., 2016). While co-culturing appears to be a promising means to activate orphan BGCs in *Salinispora*, it remains an underexplored technique to unravel the biosynthetic potential of this genus.

Here we report the discovery of novel cryptic secondary metabolites produced by *S. tropica* CNB-440. By using state-of-the-art metabolomics, we investigated how marine microbial phototrophs and their photosynthate induce the production of new metabolites in *S. tropica*. This strategy confirms microbial interactions as a promising and simple approach for future discovery of novel natural products.

MATERIAL AND METHODS

1. Culture conditions and cell abundance monitoring

1.1. Strains and growth media

Axenic marine phototrophs *Synechococcus sp.* WH7803, *Emiliania huxleyi* RCC1242 and *Phaeodactylum tricornutum* CCAP1055/1 were routinely grown in Artificial Seawater (ASW, Wilson et al., 1996), K-media (Probert & Houdan, 2004), and F/2 media (Guillard, 1975), respectively. Cultures were set up in Falcon 25 cm^2 rectangular culture flasks with vented caps containing 20 mL of media and incubated at a constant light intensity of 10 µmol photons m^{-2} s^{-1}, at 22 °C with orbital shaking (140 rpm). The type strains *Salinispora tropica* CNB-440^T (DSM No. 44818), *Salinispora arenicola*^{T} CNH-643 (DSM No. 44819) and *Salinispora pacifica* CNR-114 (DSM No. 45546) were grown in marine broth (MB, Difco), and incubated at 30 °C with orbital shaking (220 rpm). The *S. tropica* mutants *salA*$^-$ and *salL*$^-$ were generously provided by the Moore Laboratory, USA (Eustáquio et al., 2009; Eustáquio & Moore, 2008). Marine broth was supplemented with 50 µg mL^{-1} apramycin or 1.1 g L^{-1} Tris base, when required. ASW was supplemented with 10 µg mL^{-1} rifamycin SV or 3, 10, 50 or 100 µg mL^{-1} Fe(III), as required.

1.2. Co-culture setup

Salinispora cells were grown to late exponential phase in 10 mL of MB before washing them three times with sterile mineral media, as appropriate for each phototroph, and finally resuspending the washed cell pellet in 10 mL of mineral media. Exponentially growing axenic phototroph cells and the washed *Salinispora* were co-inoculated in fresh media to a concentration of 10% (v/v) and 20% (v/v), respectively. *Salinispora* cells were also washed and resuspended in a conditioned *Synechococcus* supernatant (SUPSYN), when required for the metabolomic analyses. To obtain the conditioned supernatant, *Synechococcus* cultures were incubated for 35 days as described above before centrifugation (4000 x *g* for 10 minutes at room temperature) and further filtration through 0.22 μm pore size filters to remove cells and particulate organic matter. Washed *Salinispora* cells were used to inoculate SUPSYN and MB, and cultures were incubated at 22 °C with shaking (140 rpm) and a light intensity of 10 μmol photons m^{-2} s^{-1}. For the physically separated *Synechococcus*-*Salinispora* co-cultures using the porous filters, cells were grown in 24 mm transwell with 0.4 μm pore polycarbonate membrane inserts (Corning). *Synechococcus* cells were inoculated in the well to a concentration of 20% (v/v) and *Salinispora* in the insert to a concentration of 55% (v/v).

1.3. Flow cytometry

Phototroph cell abundance was monitored using their autofluorescence by flow cytometry using a LSR Fortessa Flow Cytometer (BD) instrument, and the BD FACSDiva acquisition software (BD). Cells were detected and gated using excitation 488 nm – emission 710/50 nm at voltage 370 V, and ex. 640 nm – em. filter 670/14 nm at voltage 480 V. To remove any *Salinispora* cell aggregates that would block the flow cell, samples were pre-filtered through a sterile mesh with pore size of 35 μm (Corning) prior to analysis.

2. Metabolomic analysis

2.1. Sample preparation

The culture supernatants were analyzed by non-targeted metabolomic using either raw or concentrated supernatants. Raw supernatants were collected by sampling 200 μL of 0.22 μm-filtered culture milieu, prior to being mixed with an equal volume of HPLC-grade

methanol. For concentrating the supernatant, cells from 10 to 100 mL of cultures were removed by centrifugation (4,000 x *g* for 15 minutes) followed by a filtering step using 0.22 µm vacuum filter bottle system (Corning). Pre-purification of the compounds of interest from the supernatants was carried out by solid phase extraction using C18-silica. Using a 90:10 A/B mobile phase (where A is water with 0.1% formic acid and B is methanol with 0.1% formic acid) the undesired polar molecules and salts passed through the silica while the compounds of interest were retained and later collected following elution with a 10:90 A/B mobile phase. The obtained fractions were dried under reduced pressure at 40 °C (in a speed-vac) and resuspended in 1-3 mL of 50:50 HPLC-grade methanol/water solution. All samples were stored in snap-seal amber glass vials (Thames Restek) and kept at -20 °C until analysis.

2.2. Low-resolution LC-MS

Metabolites present in the cultures were routinely analyzed by reversed-phase liquid chromatography (LC). A Dionex UltiMate 3000 HPLC (ThermoScientific) coupled with an amaZon SL Ion Trap MS (Bruker) was used. A Zorbax Eclipse Plus C18 column with dimensions 4.6 mm x 150 mm, 5 µm particle size (Agilent Technologies) was employed for metabolite separation with a linear gradient of 95:5 A/B to 30:70 A/B over 5 minutes, followed by second linear gradient to 20:80 A/B over 10 minutes with a flow rate of 1 mL min^{-1} (Mobile phase A: water with 0.1% formic acid, B: methanol with 0.1% formic acid). The mass spectrometer (MS) was operated in positive ion mode with a 100-1000 *m/z* scan range. The injected volume was 10 µL at a temperature of 25 °C. Data was processed with the Bruker Compass DataAnalysis software version 4.2 (Bruker).

2.3. High-resolution LC-MS

To acquire molecular formulae information, samples were analyzed using an Ultra-high resolution MaXis II Q-TOF mass spectrometer equipped with electrospray source coupled with Dionex 3000RS UHPLC was employed (Bruker). A reverse phase C18 column (Agilent Zorbax, 100x2.1 mm, 1.8 µm) and a guard column (Agilent C18, 10x2.1 mm, 1.8 µm) were used for separation applying a linear gradient of 95:5 A/B to 0:100 A/B over 20 minutes (Mobile phase A: water with 0.1% formic acid, B: acetonitrile with 0.1% formic acid). The injected volume was 2 µL, and the flow rate was 0.2 mL min^{-1}. At the beginning

of each run, 7.5 µL of 10 mM of sodium formate solution was injected for internal calibration. The mass spectrometer was operated in positive ion mode with a 50-2500 *m/z* scan range. MS/MS data was acquired for the three most intense peaks in each scan.

3. Isolation and bioactivity assay of metabolites

3.1. Metabolites purification by HPLC

For metabolite purification for Nuclear Magnetic Resonance (NMR) analysis, organic extracts of co-cultures grown for 35 days were prepared as described in sections 1.2. and 2.1., with the following modifications: (i) four litres of co-cultures were obtained as 40 independent 100-mL cultures implemented in 250-mL conical flasks. Cultures were incubated for 35 days at 22 °C with shaking (140 rpm) and a light intensity of 10 µmol photons m^{-2} s^{-1}; (ii) Following pre-purification of the compounds by C18-silica solid phase extraction, the obtained extracts were dissolved in ca. 6 mL of 50:50 HPLC-grade methanol/water solution.

The isolation of molecule **6** from the organic extract was performed by reverse-phase HPLC, with a time-based pre-purification step followed by a UV-VIS-based separation step. An Agilent 1200 HPLC equipped with a binary pump and a Diode-Array Detector (DAD) was used. An Agilent Prep-C18 column with dimension 21.2 mm x 150 mm, particle size 5 µm (Agilent Technologies) was employed for metabolite separation with a linear gradient of 50:50 A/B to 20:65 A/B over 24 minutes with a flow rate of 5 mL min^{-1} (Mobile phase A: water with 0.1% formic acid, B: methanol with 0.1% formic acid). Samples were run as several rounds of 1,500 µL injected volume. The fraction containing the cryptic molecule **6** was collected between 2 to 6 minutes in the run, using an automated fraction collector. The resulting fraction was dried under reduced pressure at 40 °C (in a speed-vac) and resuspended in 600 µL of 50:50 HPLC-grade methanol/water solution.

Molecule **6** was further purified from the obtained sample by absorbance at 310 nm from 8.5 to 10 minutes in the run, using the same linear gradient as above. Sample was run as several rounds of 400 µL injected volume. Between runs, 50:50 HPLC-grade methanol/water solution was added to the ~200 µL of dead volume left from the sample to restore the 600 µL volume. Dilution was repeated up to four times. The threshold of the DAD for collection was set to values ranging from 15 to 500 mAU, as appropriate for the sample.

3.2. Bioactivity assay of organic fractions

The fractionation of organic extracts, obtained as explained in section 2.1 from 20-mL cultures, was done using reverse-phase HPLC. An Agilent 1200 HPLC equipped with a binary pump was used. An Agilent Prep-C18 column with dimension 21.2 mm x 150 mm, particle size 5 µm (Agilent Technologies) was employed for metabolite separation with a linear gradient of 50:50 A/B to 20:80 A/B over 25 minutes with a flow rate of 5 mL min^{-1} (Mobile phase A: water with 0.1% formic acid, B: methanol with 0.1% formic acid). Fractions were collected with 2 minutes time slices, using an automated fraction collector. Samples were run as several rounds of 1,500 µL injected volume. Matching fractions were pooled and dried under reduced pressure at 40 °C (in a speed-vac) and resuspended in 200 µL of sterile ASW, resulting in 12 fractions concentrated 100X.

To test the culture extract-issued fractions for bioactivity, exponentially growing axenic *Synechococcus* cells were inoculated in 5 mL of fresh ASW to a concentration of 10% (v/v). The resulting cultures were spiked with 200 µL of either ASW, or a 100X HPLC-fraction, for a final concentration of 4X. Cells were incubated at 22 °C with shaking (140 rpm) and a light intensity of 10 µmol photons m^{-2} s^{-1}.

3.3. Disc diffusion test

The 50X organic extracts used for the assay were generated as explained in section 2.1 from 20-mL cultures, and resuspended in a final volume of 400 µL of 50:50 HPLC-grade methanol/water solution. To grow phototrophic cells into solid media, 40 mL of exponentially growing axenic *Synechococcus* cells were first concentrated by centrifugation (4,000 x *g* for for 5 minutes), before discarding the supernatant. Cells were resuspended in the remaining media (~200 µL) and mixed together with 20 mL of freshly autoclaved ASW-0.2% agarose (still liquid). The cell-medium mixture was poured into plates and let to set/dry for 2 hours prior to being used. Autoclaved antibiotic assay discs (diam. 6 mm, Whatman) were coated with either an axenic *Synechococcus* culture organic extract (50X), a *Salinispora-Synechococcus* co-culture organic extract (50X), 10 µg mL^{-1} gentamycin or ASW with 1% methanol. Coated discs were placed onto the inoculated plates using flamed-sterilized tweezers. Plates were incubated at 22 °C under a light intensity of 10 µmol photons m^{-2} s^{-1}.

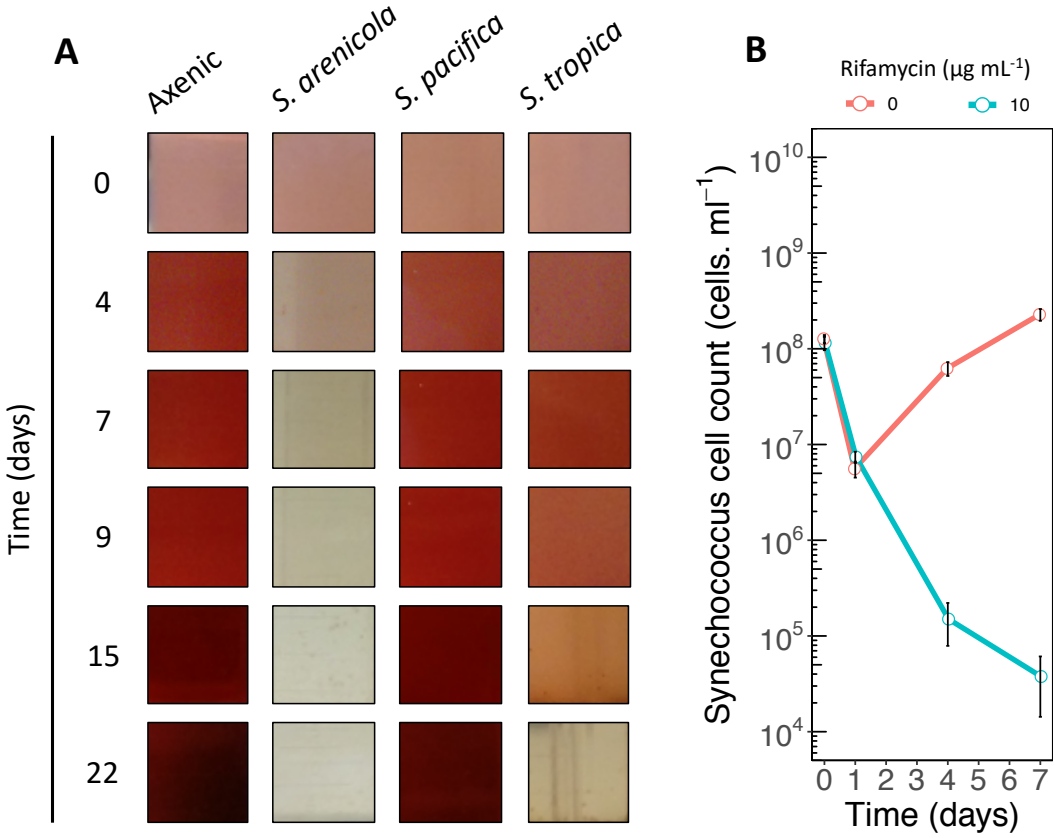

Figure 9 | *S. arenicola* and *S. tropica* have antimicrobial activity on *Synechococcus* in co-culture. (A) *Synechococcus* grown in axenic culture and in co-culture with three species of *Salinispora*. Photographs of representative cultures of three biological replicates are shown. Red pigmentation is characteristic of healthy *Synechococcus* cells, while cell bleaching (white cultures) indicates dead cells. (B) *Synechococcus* is sensitive to rifamycin. *Synechococcus* cell count over time in culture media with 0 (red line) or 10 (blue line) µg mL^{-1} of the antibiotic rifamycin. Graph shows mean ± standard deviation of three biological replicates.

RESULTS

Salinispora tropica has antimicrobial activity on a diverse range of marine phototrophs

We co-inoculated the cyanobacterium *Synechococcus* sp. WH7803 with three representative species of the genus *Salinispora*, namely *Salinispora arenicola*, *Salinispora pacifica* and *Salinispora tropica*. Unlike other heterotrophs, which usually enhance the growth of phototrophic organisms when in co-culture (*e.g.* Christie-Oleza et al., 2017; Sher et al., 2011), both *S. arenicola* and *S. tropica* showed a clear antimicrobial activity against *Synechococcus* (**Fig. 9, A**). Although we were able to monitor the phototroph's inhibition, we were unable to assess the growth profile of *Salinispora* in the co-culture due to its growth as dense cell aggregates preventing traditional monitoring techniques (*e.g.* optical density, colony forming unit or flow cytometry). While *S. arenicola* is known

to biosynthesize the antibiotic rifamycin (Asolkar et al., 2010), to which we confirmed *Synechococcus* is sensitive (**Fig. 9, B**), no antimicrobial compound has yet been characterized in *S. tropica* CNB-440. We were therefore interested in characterizing the nature of *Synechococcus* growth inhibition by *S. tropica*.

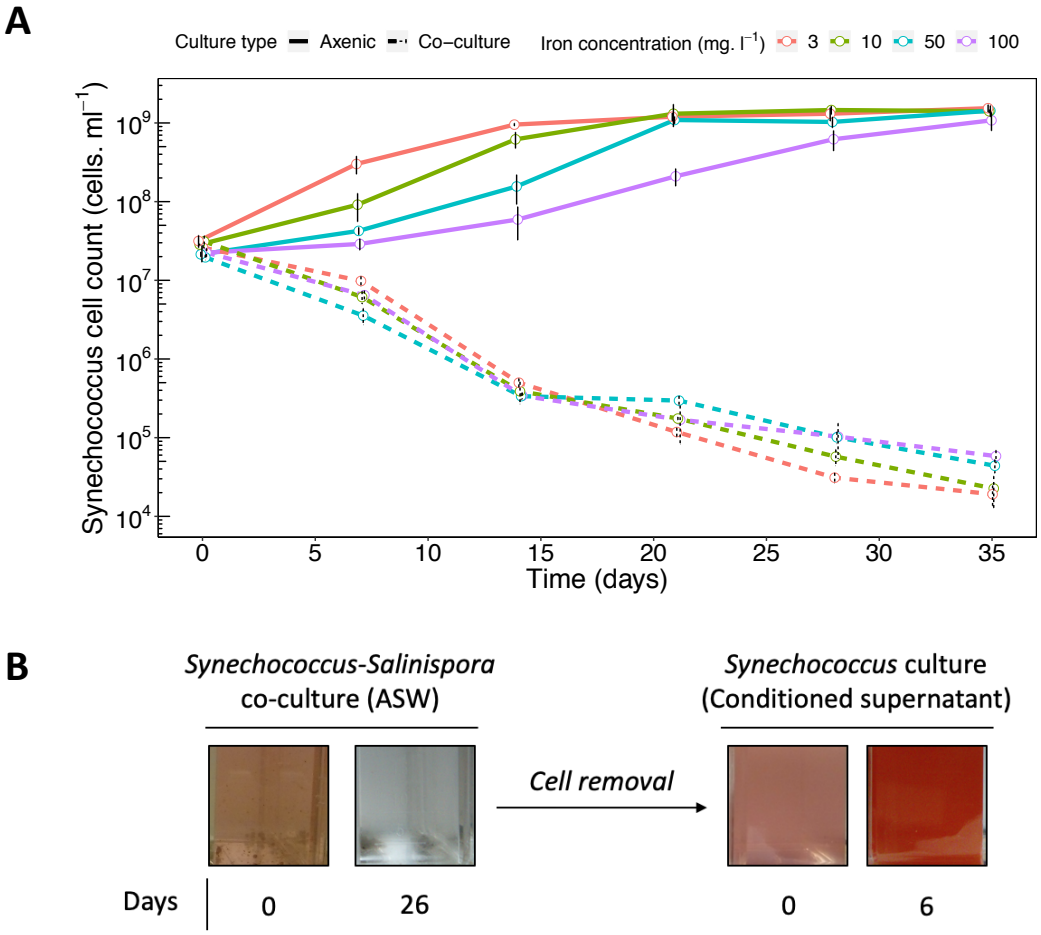

Figure 10 | *Synechococcus* inhibition by *S. tropica* is not mediated by iron or nutrient depletion. **(A)** Monitoring of *Synechococcus* population grown axenically or in co-culture with *S. tropica*, in media supplemented with 3, 10, 50 or 100 mg L^{-1} Fe(III). Graph shows mean ± standard deviation of three biological replicates. **(B)** *Synechococcus* grown axenically in a conditioned supernatant (right panel), obtained from a *Synechococcus-Salinispora* co-culture after the death of the phototroph (left panel). Photographs of representative cultures from three biological replicates are shown. Red pigmentation is characteristic of healthy *Synechococcus* cells, while cell bleaching (white cultures) indicates dead cells.

Previous studies have shown that *S. tropica* is able to outcompete other heterotrophs in co-culture by secreting the siderophore desferrioxamine leading to iron depletion (Patin et al., 2016; Roberts et al., 2012). To evaluate whether iron sequestration could explain the negative interactions observed in the present phototroph-*Salinispora* system, we

supplemented the co-cultures with increasing concentrations of iron (**Fig. 10, A**). The results obtained suggest that the antimicrobial phenotype was not due to siderophore activity, as saturating amount of iron could not rescue the growth of the phototroph.

We also assessed whether general nutrient depletion by *S. tropica* could be responsible for the phototroph growth defect. For this, we incubated *S. tropica* and *Synechococcus* together until bleaching of the latter. Remaining cells were filtered out to obtain a sterile

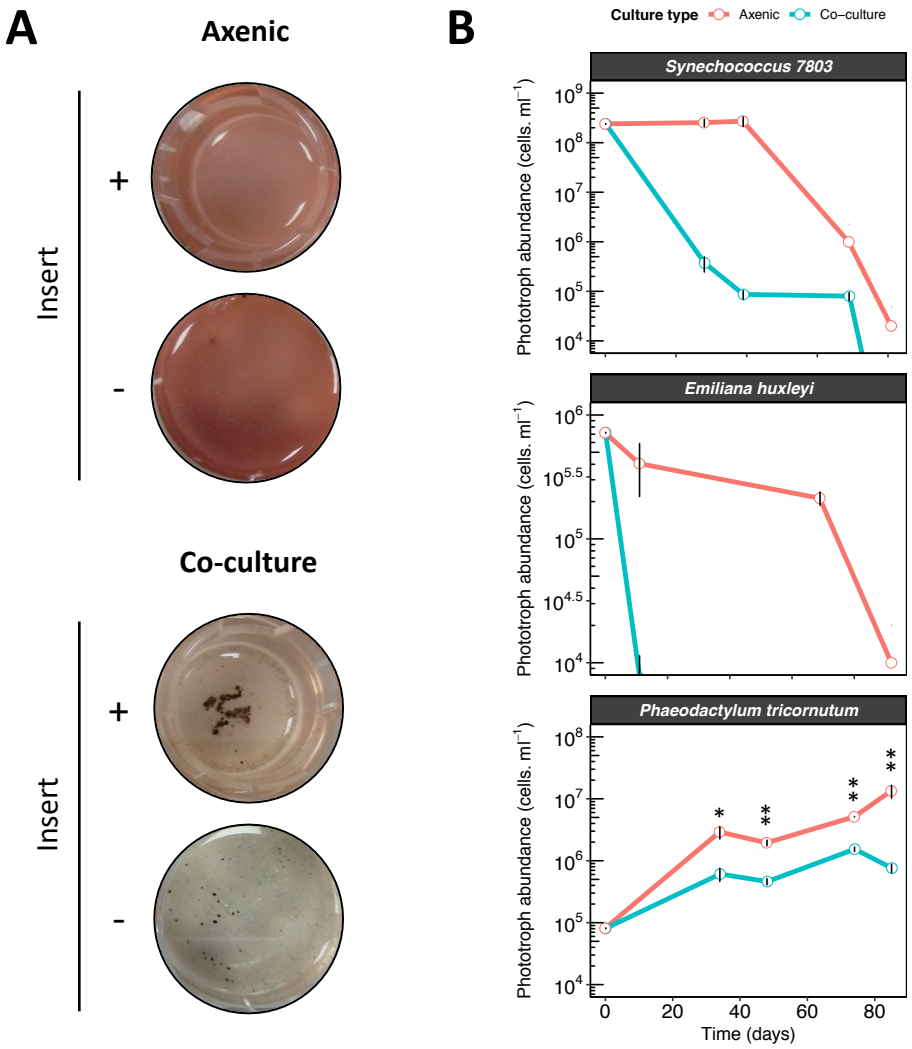

Figure 11 | *Salinispora tropica* inhibits the growth of several phytoplankton *via* the secretion of an antimicrobial molecule. (A) *Synechococcus* growth inhibition by *S. tropica* mediated by a diffusible molecule. The cyanobacterium was grown axenically and in co-culture with *S. tropica,* separated by a 0.4 µm pore membrane insert. Photographs of representative cultures of three biological replicates are shown, 7 days after inoculation. Red pigmentation is characteristic of healthy *Synechococcus* cells, while cell bleaching indicates cell death. (B) *S. tropica* inhibits marine phototrophs growth in co-culture. Cultures of three marine phototrophs grown axenically (red lines) and in co-culture with *Salinispora tropica* (blue lines). Graph shows mean ± standard deviation of three biological replicates. Statistically significant cell abundance are indicated (T-test, significant * at *p*-value < 0.05 and ** at *p*-value < 0.01).

conditioned supernatant, in which we inoculated axenically fresh *Synechococcus* cells (**Fig. 10, B**). The conditioned supernatant allowed rapid growth of the phototroph, suggesting that nutrient depletion did not drive the death of the first *Synechococcus* cells co-inoculated with *S. tropica* in this medium.

We then hypothesized that a yet unknown antimicrobial compound, to which our photosynthetic microorganism is sensitive to, could be produced by *S. tropica.* To test this assumption, we setup co-cultures in which *S. tropica* and *Synechococcus* were physically separated by a porous filter, preventing direct cell-to-cell interactions while allowing the diffusion of small molecules (**Fig. 11, A**). *S. tropica* was still able to impair *Synechococcus* proliferation in these experimental conditions, confirming that a secreted molecule was causing the death of the phototroph.

We were interested in testing the efficacy of this secreted compound against different types of phytoplankton. We therefore co-inoculated *S. tropica* with three phototrophic model species, namely the cyanobacterium *Synechococcus* sp. WH7803, the coccolithophore *Emiliania huxleyi* and the diatom *Phaeodactylum tricornutum*. They all showed a strong decline in the presence of *S. tropica*, being especially remarkable for the two former species (**Fig. 11, B**). While also affected, the diatom *P. tricornutum* was not killed by *S. tropica* but, instead, its cells densities were significantly maintained one order of magnitude lower than when incubated axenically. Altogether, our observations revealed that *S. tropica* produced a yet unknown antimicrobial molecule effective against both eukaryotic and prokaryotic phytoplankton.

Phototrophs elicit the production of novel cryptic metabolites in *S. tropica*

We analyzed the co-culture supernatants using non-targeted metabolomics to identify the pool of secondary metabolites secreted by *S. tropica* in response to the different phototrophs. The *Synechococcus*-*S. tropica* co-culture revealed eight molecular ions that were not present in the respective axenic cultures (**Fig. 12, A**). These molecules were further characterized by high-resolution MS/MS analysis, from which we generated empirical chemical formulae, allowing us to assign most of them to two subgroups of related compounds being: (i) ions **1**, **2**, **5** and **8**; and (ii) ions **4**, **6** and **7** (**Fig. 12, B**).

Ions **1**, **2**, **5** and **8** were derivatives of salinosporamide; a well-characterized molecule produced by *S. tropica* that presents a unique fused γ-lactam-β-lactone bicyclic ring stru-

A

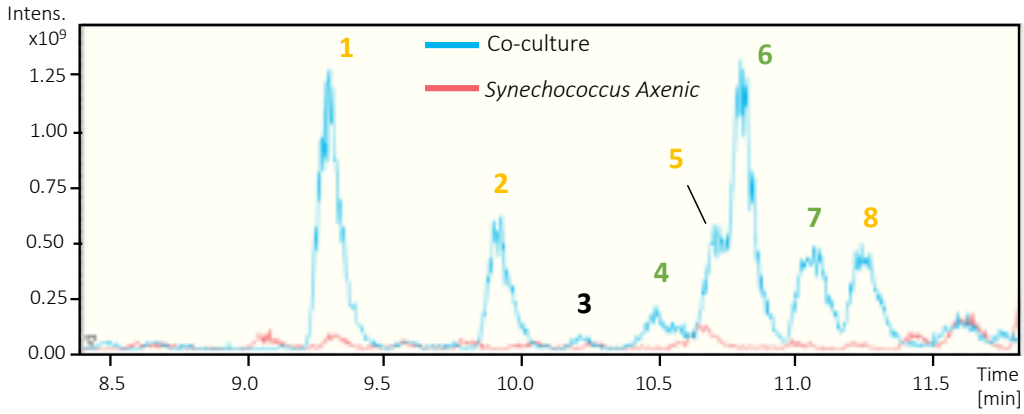

B

MS Peak	Observed *m/z*	Chemical formulae for $[M+H]^+$ (calculated *m/z*; err [ppm])	MS/MS
1	399.2135	$[C_{19}H_{31}N_2O_7]^+$ (399.2126; -2.4)	**296.1498** 271.1295 186.0765 168.0659
2	401.2294	$[C_{19}H_{33}N_2O_7]^+$ (401.2292; -2.8)	**298.1657** 273.1453 255.1348 152.0712
3	438.1701	$[C_{28}H_{24}NO_4]^+$ (438.1700; -0.3)	194.0817 177.1279
4	464.2509	$[C_{22}H_{34}N_5O_6]^+$ (464.2504; -1.2)	**276.16** 171.088 154.0615
5	296.1499	$[C_{15}H_{22}NO_5]^+$ (296.1492; -2.1)	296.1499 318.132 168.066
6	435.2609	$[C_{22}H_{35}N_4O_5]^+$ (435.2602; -1.7)	372.229 **276.1599** 142.0979
7	449.2764	$[C_{23}H_{37}N_4O_5]^+$ (449.2758; -1.3)	156.1135
8	298.1653	$[C_{15}H_{24}NO_5]^+$ (298.1649; -1.5)	320.1447 298.1654 170.0815

Figure 12 | Metabolome of the *S. tropica-Synechococcus* co-cultures. (A) *S. tropica* produces detectable small molecules in co-culture with *Synechococcus*. Overlaid base peak chromatograms (BPCs) of *Synechococcus* culture concentrated supernatants, when grown for 35 days in artificial sea water (ASW) either axenically (red) or in co-culture with *S. tropica* (blue). Peaks characteristic of the co-culture condition are labelled from 1 to 8. Color of the labels indicate groups of related compounds. **(B)** Molecular ions detected by LC-MS in *S. tropica-Synechococcus* co-culture. Table shows molecular ions detected by high-resolution LC/(+)ESI-MS. Peak numbering is based on HPLC retention time and colors indicate groups of related compounds. Observed *m/z* values and predicted chemical formulae for $[M+H]^+$ are provided. Observed mass of main ions obtained after MS2 fragmentation are given.

-cture (Feling et al., 2003), and that is now being tested as a drug because of its anti-cancer properties. Molecules **5** and **8** are consistent with known degradation products of salinosporamide A and B, respectively (Denora et al., 2007; **Fig. 13**), while molecules **1** and **2** are proposed to result from the nucleophilic addition of Tris (the buffering agent used in the ASW culture medium) to the lactone ring of salinosporamide A and B, respectively (**Fig. 13**). These salinosporamide sub-products were further confirmed by their absence when (i) Tris was not added (**Fig. 14, A**), or (ii) salinosporamide mutants that no longer produced these metabolites, *i.e. salA*$^{-}$ and *salL*$^{-}$ (Eustáquio et al., 2009), were used (**Fig. 14, B**). In order to test the activity of salinosporamide and its derivatives

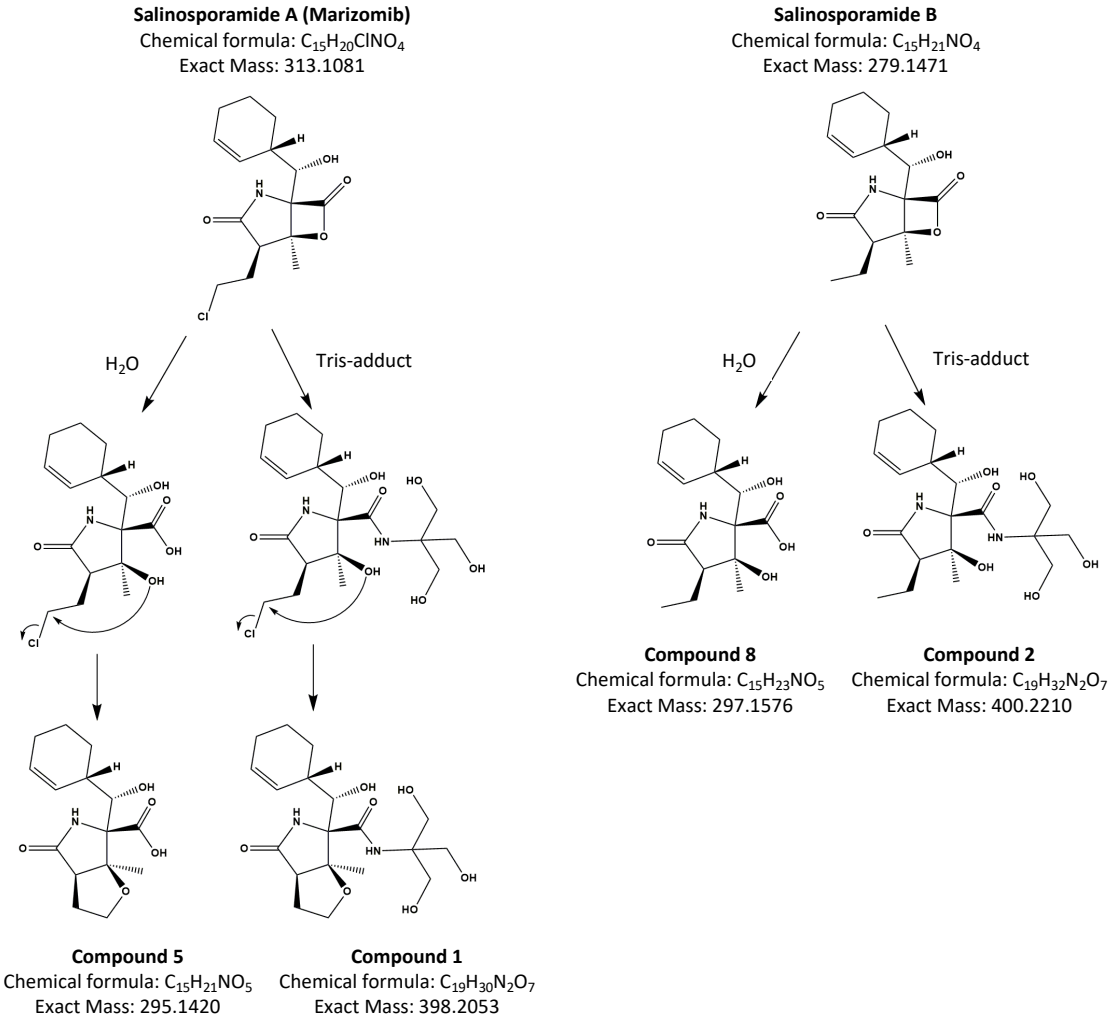

Figure 13 | Chemical structure of salinosporamide A and B, with their respective degradation products. Salinosporamide A ($C_{15}H_{20}{}^{35}ClNO_4$; mass 313.11) either hydrolyzes to form the molecule NPI-0065, **5** ($C_{15}H_{21}NO_5$; mass 295.14) or reacts with Tris to form the hypothetical molecule **1** ($C_{19}H_{30}N_2O_7$; mass 398.21). Salinosporamide B ($C_{15}H_{21}NO_4$; mass 279.15) either hydrolyzes to form the molecule **8** ($C_{15}H_{23}NO_5$; mass 297.16) or reacts with Tris to form the hypothetical molecule **2** ($C_{19}H_{32}N_2O_7$; mass 400.22).

on the phototrophs, we co-cultured *Synechococcus* with both salinosporamide mutants. Salinosporamide and its derivatives were not responsible for the antimicrobial activity as both deficient mutants were still able to inhibit the phototroph (**Fig. 15**).

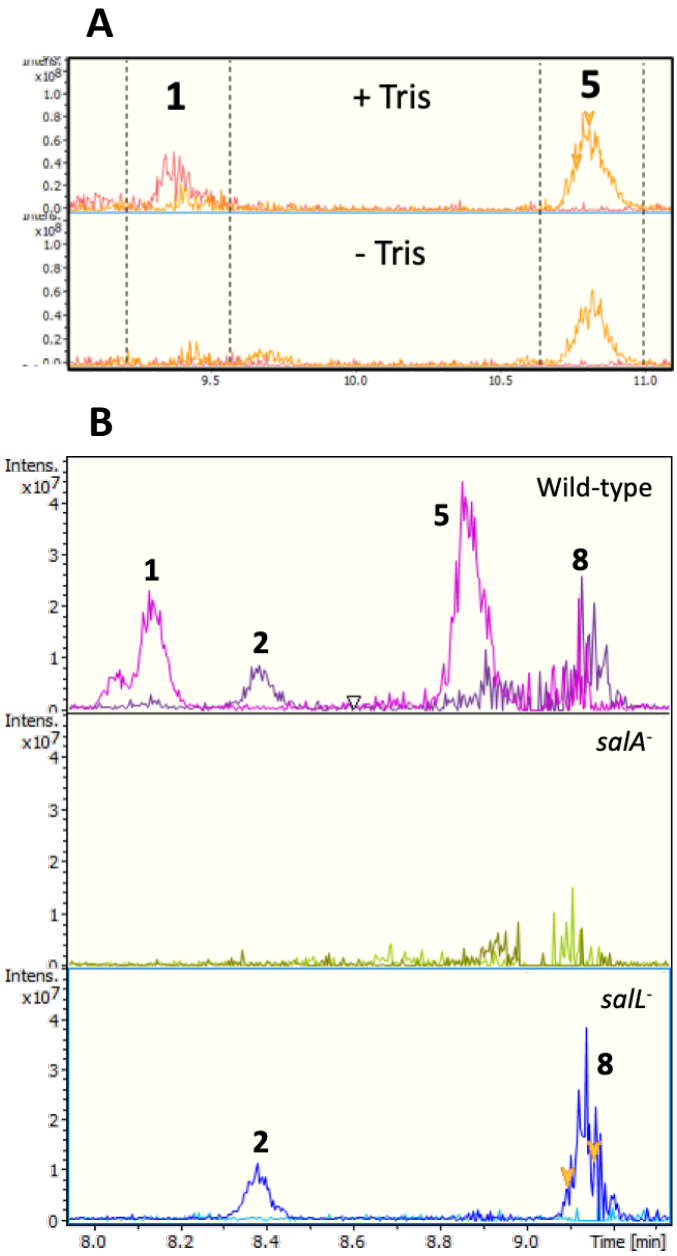

Figure 14 | Molecules 1, 2, 5 and 8 are degradation products of the analogs salinosporamide A and B. (A) Culture supernatant of *S. tropica* grown in marine broth (top panel) or marine broth supplemented with Tris (bottom panel). In red is shown the extracted ion chromatogram for molecule **1**, with *m/z* 399 (± 0.5). In orange is shown the extracted ion chromatogram for molecule **5**, with *m/z* 296 (± 0.5). **(B)** Extracted ion chromatograms of molecules **1**, **2**, **5** and **8** (EIC 399; 401; 296; 298 ± 0.5) in the culture supernatant of *S. tropica* wild-type (top panel), and the salinosporamide mutants *salA*$^{-}$ (middle panel) and *salL*$^{-}$ (bottom panel). The *salA*$^{-}$ strain does not produce salinosporamide A or any derivatives, while the *salL*$^{-}$ strain still produces the analog salinosporamide B.

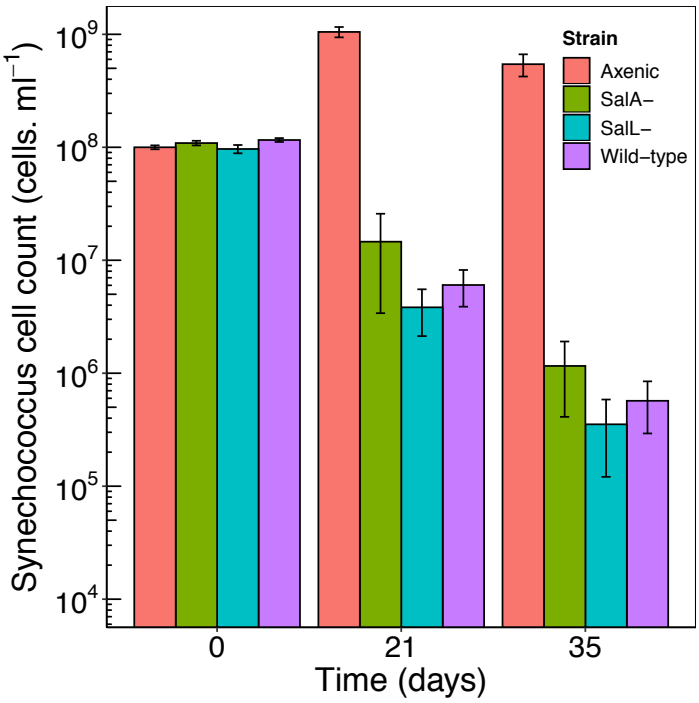

Figure 15 | Monitoring of *Synechococcus* grown in axenic culture and in co-culture with the wild-type, *salA*$^-$ or *salL*$^-$ *S. tropica* strains. Graph shows mean of triplicates ± standard deviation.

The second group of ions *i.e.* peaks **4**, **6** and **7**, were also related. Molecule **6** gave a *m/z* value of 435.2609 $[M+H]^+$. Based on the accuracy of this value and the isotopic pattern the empirical chemical formula $C_{22}H_{35}N_4O_5$ was predicted by the DataAnalysis software. The predicted formula for molecule **4** suggests that, with a 28.9900 Da mass difference when compared to **6**, the compound had lost one hydrogen and gained one nitrogen and one oxygen (**Fig. 16**). MS/MS analyses confirmed that both molecules **4** and **6** had an identical molecular fragment (*i.e. m/z* 276.1600 ± 0.0001 $[M+H]^+$, with the empirical chemical formula $C_{16}H_{22}NO_3$), indicating that the two molecules share a core backbone (**Fig. 16; Appendix 2**). Similarly, molecule **7** had the same chemical formula as **6** but with the addition of a methyl group (14.0155 Da mass difference; **Fig. 16**). Finally, MS/MS fragmentation of the three molecules **4**, **6** and **7** resulted in the related molecular fragments *m/z* 171.088, 142.0979 and 156.1135, respectively, which showed differences in masses and empirical formulae identical to that observed between their corresponding parent ions (**Fig. 16; Appendix 2**). Molecule **3** did not share an obvious link to any other metabolites and, therefore, was considered a new biosynthesized product of *Salinispora* (**Fig. 12, B**). Most interestingly, the search for compounds with the same molecular formulae as **3**, **4**, **6** or **7** in multiple databases (*e.g.* Reaxys, SciFinder,

Dictionary of NP) returned no known natural product, suggesting that they are novel compounds.

Intriguingly, the production of these novel compounds was triggered by the presence of the phototrophs as they were only detected in the co-cultures of all three phototrophs (**Fig. 12, A**; **Fig. 17, A**), but not when grown in mono culture – as shown by the absence of these metabolites when *S. tropica* was grown alone in mineral ASW or nutrient rich media MB (**Fig. 17, B and C**). Furthermore, we confirmed that the supernatant of a phototroph culture – containing photosynthate – was enough to induce such metabolite production (**Fig. 17, C**).

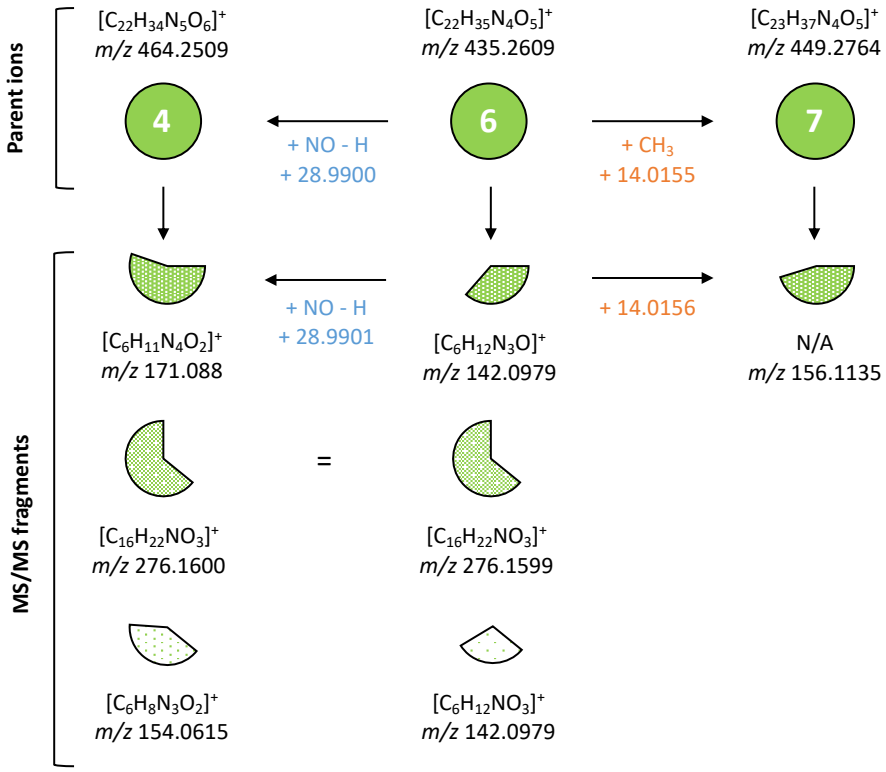

Figure 16 | The cryptic molecules 4, 6 and 7 are related. Schematic of the cryptic compounds and their corresponding daughter ions generated by MS/MS. Observed *m/z* values detected by high-resolution LC/(+)ESI-MS and predicted chemical formulae for [M+H]+ are provided. N/A indicate chemical formulae that could not be generated by the DataAnalysis software.

The cryptic compounds have a characteristic 310 nm absorbance spectrum

In order to characterize the cryptic molecules, we were interested in testing whether they had antimicrobial activity. For this, fractions obtained from high-pressure liquid chromatography (HPLC) separation of the organic extract of the co-culture supernatant

were spiked into axenic *Synechococcus* cultures but none exhibited antimicrobial activity against the phototroph (**Fig. 18, A**), although we confirmed that the cryptic molecule **6** was present in the fraction 2 (**Appendix 3**). We hypothesized that the synergistic effect of multiple molecules could be required to observe antimicrobial effect and/or that instability of the antimicrobial compounds could lead to low concentrations and prevent

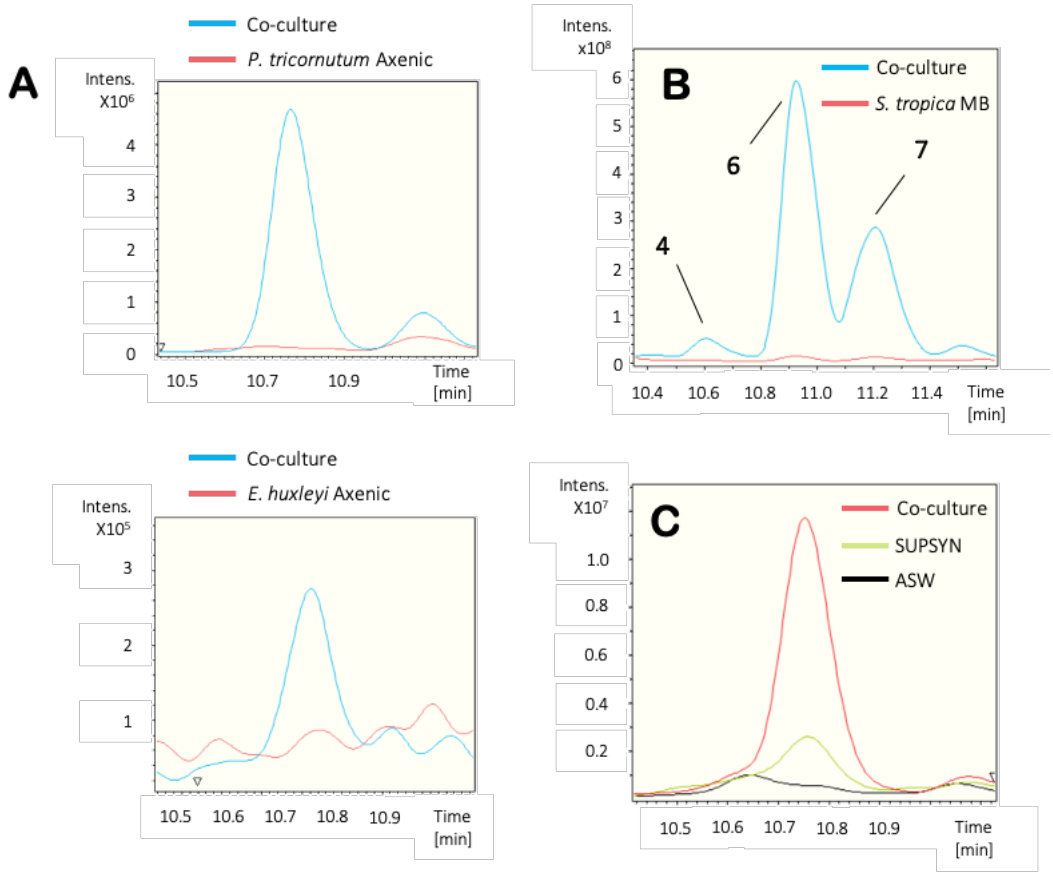

Figure 17 | Marine phototrophs trigger the production of cryptic molecules in *S. tropica*. **(A)** Other marine phototrophs also trigger the production of metabolite **6** by *S. tropica* as observed in Fig. 12, A. Figure shows extracted ion chromatograms for the molecule **6** EIC 435.2 ± 0.1 in the supernatants of the phototrophs (*P. tricornutum*, top panel; *E. huxleyi*, bottom panel) grown axenically (red) and in co-culture with *S. tropica* (blue). **(B)** The production of the related molecules **4**, **6** and **7** is dependent on the presence of photosynthate rather than high-nutrient availability. Graph shows extracted ion chromatograms for all three cryptic molecules EIC (464.2; 435.2; 449.2) ± 0.5 in the concentrated supernatants of *S. tropica* grown axenically for 35 days in marine broth (*S. tropica* MB, red) or in co-culture with *Synechococcus* in ASW (Co-culture, blue). **(C)** Cryptic molecule production is triggered by nutrients released by *Synechococcus* rather than cell-to-cell interactions. Graph shows extracted ion chromatograms for the cryptic molecule **6** (EIC 435.2 ± 0.5) in the supernatant of *S. tropica* grown axenically for 14 days either in artificial sea water (ASW, black line) or in a conditioned *Synechococcus* supernatant (SUPSYN, green line); and in co-culture with *Synechococcus* (Co-culture, red line). SUPSYN is equivalent to the '*Synechococcus* Axenic' condition in Fig. 12, A; cryptic metabolites were only detected after *S. tropica* incubation.

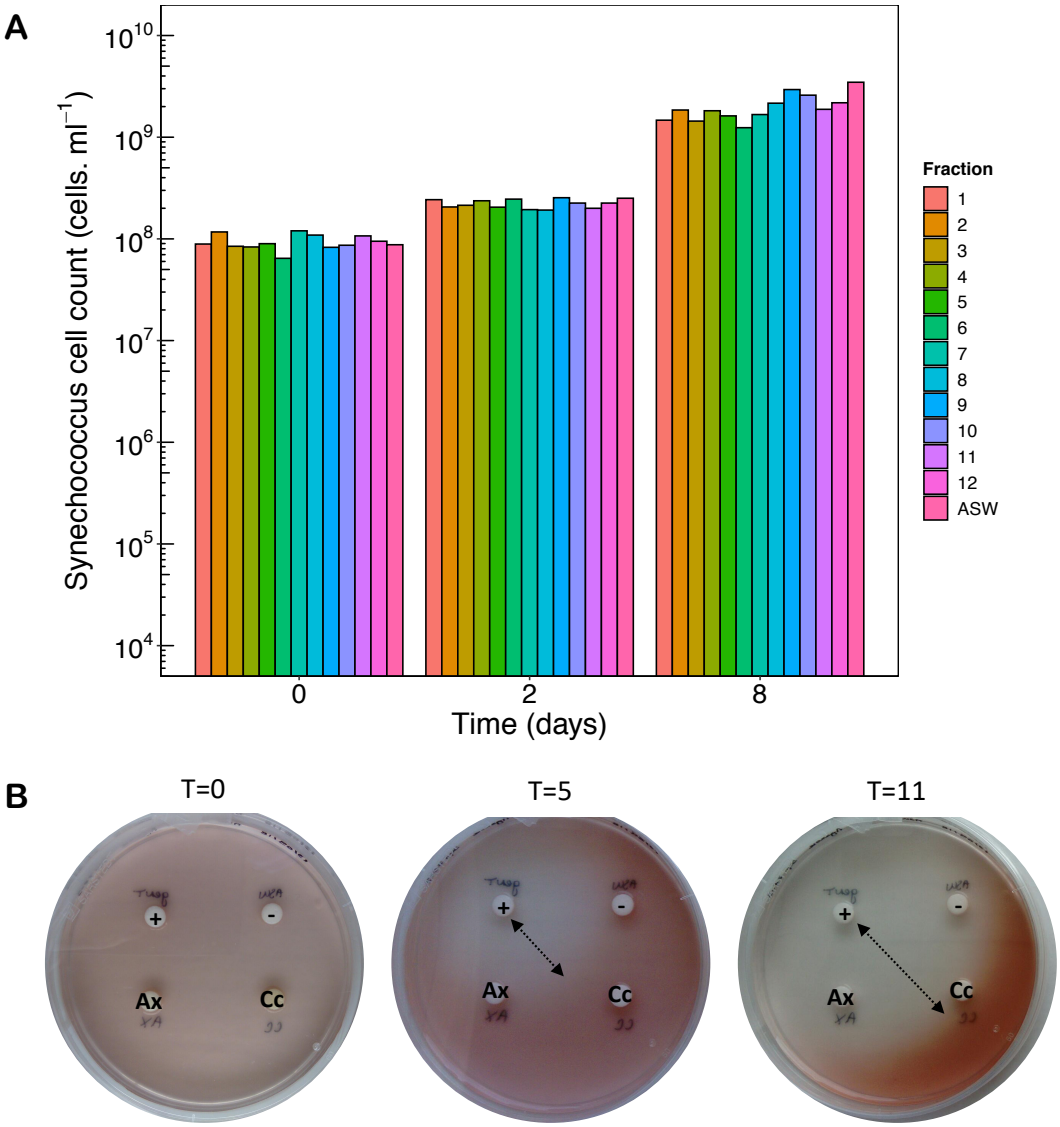

Figure 18 | Bioactivity-guided assays of co-culture organic extracts. (A) Fractionated co-culture extracts do not exhibit antimicrobial activity against *Synechococcus*. Fractions obtained from the HPLC separation of an organic extract of a co-culture supernatant after 35 days of incubation were spiked in axenic *Synechococcus* cultures, at a concentration of 4X. Fraction numbering is based on the HPLC elution time. ASW indicates the control culture in which only ASW was spiked-in. **(B)** Total extracts of *Salinispora* supernatants do not show antimicrobial activity against *Synechococcus*. Photographs of a representative plate from three biological replicates are shown. Indicated times (T) correspond to days of incubation. Arrows highlight inhibition zones. Discs were coated with either a 50X axenic *Synechococcus* culture organic extract (Ax), a 50X *Salinispora-Synechococcus* co-culture organic extract (Cc), 10 µg mL^{-1} gentamycin (+) or ASW with 1% methanol (-).

their activity. In an attempt to address these potential issues, we performed a disc diffusion assay against *Synechococcus* growing onto solid media, using a crude organic extract of the co-culture supernatant. We reasoned that this assay minimized dilution

and processing of the co-culture extract, as well as allowed testing of the collective pool of secreted molecules. Unfortunately, the unfractionated extract similarly showed no antimicrobial activity against the phototroph (**Fig. 18, B**).

While we were unable to link the killing phenotype observed in our co-culture with the cryptic compounds, we worked toward the elucidation of their chemical structures for further characterization. This required first the development of a purification method tailored for the molecules of interest, applicable to large volumes of culture supernatant. We successfully generated 4 L of co-culture supernatant, from which we isolated molecule **6** using a two-step HPLC protocol based on the polarity and light absorption of the analytes, as compound **6** had a characteristic UV-VIS absorption at 310 nm (**Fig. 19**). Despite multiple attempts, however, we obtained no informative signal from NMR analysis of the isolated cryptic molecule because of low titers of the compounds (**Appendix 4**), preventing so far the determination of its structure.

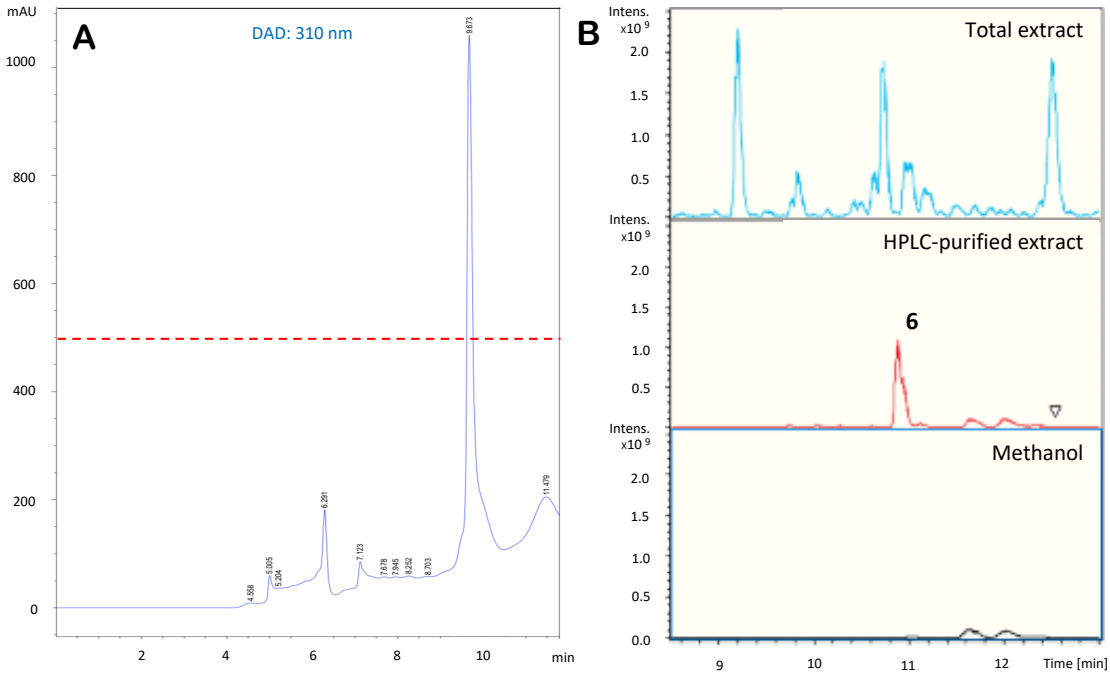

Figure 19 | Isolation of the cryptic compound 6 from the co-culture extract. (A) The molecule **6** can be purified by HPLC from the fraction obtained after a first time-based isolation step, using its absorbance at 310 nm. Graph shows HPLC chromatogram from DAD 310 nm. Red line indicates detector threshold for collection (500 mAU). **(B)** The resulting fraction (HPLC-purified extract) is a pure sample of **6**, compared to the original co-culture extract (Total extract) and a control sample of 50:50 H_2O/MetOH (Methanol). Graph shows LC-MS BPC.

DISCUSSION

We show that *S. tropica* is able to inhibit the growth of both marine cyanobacteria and eukaryotic phototrophs by some yet unidentified mechanism (**Fig. 11, B**). This observation broadens the potential role and impact that members of the *Salinispora* genus have on marine microbial communities. Members of the three *Salinispora* species are widely-distributed bacteria found in all tropical and subtropical oceans (Bauermeister et al., 2018; Mincer et al., 2002). While mostly inhabiting marine sediments, bacteria from this genus have also been isolated from the microbiota of seaweeds, marine sponges and more recently corals (Asolkar et al., 2010; Jensen et al., 2005; Ocampo-Alvarez et al., 2020). In marine sponges, it is suggested that they influence the sponge microbiota through the production of acyl homoserine lactone molecules and antibiotics (Bose et al., 2017; Singh et al., 2014). Similarly, different species of *Salinispora* were shown to possess distinct mechanisms to outcompete co-occurring marine heterotrophs in sediments, *i.e.* through the production of siderophores to deplete iron or antimicrobial molecules (Patin et al., 2017; Tuttle et al., 2019), although no antimicrobial compound has yet been identified for *S. tropica* (Patin et al., 2018). We herein provide the first evidence that *Salinispora* might not only directly influence heterotrophic communities, but also kill both prokaryotic and eukaryotic phytoplankton to which they are exposed, *e.g.* when these sediment out of the water column (Guidi et al., 2016), grow in sunlit coastal sediments (Patin et al., 2017) or are part of the same coral-associated microbiota (Ocampo-Alvarez et al., 2020).

While we were successful in identifying and obtaining the molecular formulae of novel cryptic metabolites produced in response to phytoplanktonic photosynthate (**Fig. 12, B; Fig. 17**), we were unable to isolate and identify the compound responsible for the antimicrobial effect on the marine phototrophs by using traditional bioactivity-guided assays with crude or HPLC-fractionated co-culture extract (**Fig. 18**). This mechanism proved similarly elusive in previous studies, where *S. tropica* showed an antimicrobial activity on marine heterotrophs, but the molecule responsible was not identified (Patin et al., 2018; Patin et al., 2016). The parallelism between our observations and those described in the literature suggests that the active compound(s) may be the same. We reason that the compound's instability, low titers and/or synergic effect of several molecules required for activity could explain the difficulty in identifying the antimicrobial

agent and may require constant production of the compound to result in cell death. For instance, the large number of structurally-related metabolites resulting from the chemical reaction of salinosporamide with various compounds (*i.e*. water, Tris) may support this hypothesis, as the antimicrobial molecule may be similarly unstable. The diversity of products arising from a single BGC may also be due to the promiscuity of the biosynthetic enzymes utilizing structurally related primary precursors. This results in a range of compounds, each produced at lower titers than a single natural product, and ultimately hamper the isolation of sufficient amounts of the compounds of interest.

Similarly, the structure elucidation of the cryptic molecules has so far proven extremely challenging, as the quantities of compounds purified from 4-liter co-cultures were insufficient to generate informative signals by NMR. While solving the structures of other *Salinispora* molecules was typically made possible by the ease with which one can grow liters of axenic culture in rich broth (*e.g.* 20 L for salinosporamide; Feling et al., 2003), the cryptic metabolites reported here are only synthesised in response to a phototroph in a nutrient-limited media. Supporting the growth of marine phytoplankton in large cultures is arduous and it is hence remarkably difficult to obtain substantial volumes of *Salinispora*-phototroph co-cultures. The isolation method that we developed, based on the characteristic UV-VIS absorption of one of the compounds should, however, support future efforts made to purify larger amounts of the cryptic metabolites from scaled-up co-cultures and ultimately allow for their structure determination.

In conclusion, we show that *S. tropica* can produce a broad-range antibiotic able to affect both unicellular prokaryotes and eukaryotes alike, such as the marine diatom and coccolithophore tested in our study. Such a broad-range antimicrobial could suggest a mode of action affecting a common target present in both types of cells such as the proteasome, a proteolytic complex present in the three domains of life (Becker & Darwin, 2017). Finally, our study pioneers the use of phototrophs as a promising strategy to trigger novel natural products from marine actinobacteria, as our metabolomics analysis identified cryptic secondary metabolites produced in response to co-inoculated phytoplankton. Future work is, however, required to elucidate the structure of the new molecules and because of their elusive nature, research efforts should also focus on identifying candidate pathways responsible for their production (*e.g.* pathways upregulated in presence of photosynthate).

CHAPTER 3 |

ANALYSIS OF *SALINISPORA TROPICA*'S PROTEOME REVEALS AN ORPHAN NRPS GENE CLUSTER ENCODING A POTENTIAL PROTEASOME INHIBITOR

INTRODUCTION

Biosynthetic gene clusters (BGCs) are groups of co-localized genes encoding multi-modular enzyme complexes responsible for the synthesis of most natural products. For instance, a non-ribosomal peptide synthetase (NRPS)-type cluster traditionally consists of catalytic units, each responsible for the incorporation of one non-proteinogenic amino-acid to a growing oligopeptide (**Fig. 8**; Scott & Piel, 2019; Walsh, 2008). These modules are themselves composed of core domains (*e.g.* adenylation (A), peptidyl carrier protein (PCP) or condensation domain (C)) that are required for the assembly of the natural product (Mootz et al., 2000). In addition to those pivotal biosynthetic enzymes, BGCs typically encode proteins involved in regulation and export, as well as self-resistance in case of an antimicrobial metabolite (Corre et al., 2008; Medema et al., 2015; Tenconi & Rigali, 2018). The highly organized architecture of BGCs facilitates their identification and annotation by increasingly efficient bioinformatics pipelines (Blin et al., 2019; Medema et al., 2015; Mungan et al., 2020). Most of these biosynthetic loci that are reported bioinformatically have, however, yet to be assigned to their products and are named orphan BGCs. They are generally assumed to be either transcriptionally silent (*i.e.* poor or conditional level of expression or inactivation of their biosynthetic genes) or the molecules they produce are difficult to detect and isolate (*i.e.* compound instability, limited sensitivity of detection methods or absence of bioactivity to screen for) (Rutledge & Challis, 2015).

These issues are well exemplified in the marine actinomycete *Salinispora*, a remarkable producer of new secondary metabolites with drug-like properties (Asolkar et al., 2010; Gulder & Moore, 2010; Janso et al., 2014). Previous studies have shown that 10% of the type strain *S. tropica* CNB-440^{T} genome is dedicated to natural product biosynthesis with the identification of twenty putative BGCs, of which eleven are still orphan (**Table 2**; Penn et al., 2009; Udwary et al., 2007). In Chapter 2, we have used co-inoculation of *S. tropica* with phytoplankton as a means to activate those orphan clusters that are silent. We have

demonstrated that co-cultures not only triggered the production of cryptic compounds in *S. tropica*, but also revealed an antimicrobial activity exhibited by *S. tropica* against the phototrophs that we could not link to any molecule. While our work and that of others have focused on activating silent BGCs, little has been done to characterize those orphan BGCs as either being silent or producing cryptic molecules, and to propose candidate BGCs that could be linked to the bioactivity of undetectable metabolites. The only available study of the type in *Salinispora*, to date, is based on a comparative transcriptomics analysis of various *Salinispora* species that recently allowed the discovery of the compound salinipostin, as well as the report of seven transcriptionally silent BGCs (**Table 3**; Amos et al., 2017). Meanwhile, combining metabolomics with proteomics has proven successful in linking novel secondary metabolites to active orphan BGCs in several *Streptomyces* species, but has not yet been applied to the genus *Salinispora* (Bumpus et al., 2009; Chen et al., 2013; Gubbens et al., 2014; Owens et al., 2014; Schley et al., 2006).

Table 3 | Previously reported activity of orphan biosynthetic gene clusters in *S. tropica.*

BGC name	Biosynthetic class	Genetic location (strop_)	Size (kb)	Found transcriptionally silent*
pks1	polyketide	RS02980-RS03095	30.9	Yes
nrps1	non-ribosomal peptide	RS03375-RS03535	37.5	Yes
amc	carbohydrate	RS11765-RS11795	6.6	Yes
bac1	ribosomal peptide	RS11800-RS12275	19.2	No
pks3	polyketide	RS12510-RS12630	23.3	No
sid2	non-ribosomal peptide	RS13260-RS13385	40.7	Yes
sid3	non-ribosomal peptide	RS13985-RS14120	29.2	Yes
sid4	non-ribosomal peptide	RS14125-RS14260	40.8	Yes
bac2	ribosomal peptide	RS14265-RS15290	19.0	No
pks4	polyketide	RS21120-RS21540	10.0	No
nrps2	non-ribosomal peptide	RS22250-RS22350	34.7	Yes

* Based on the comparative transcriptomics analysis done by Amos *et al*. (2017), in *S. tropica* CNB-440 grown axenically in A1 medium in exponential phase.

Here, we report the first available proteomics dataset in *S. tropica* CNB-440 that we explored to identify candidate BGCs that could be linked to the antimicrobial activity exhibited by *Salinispora* in co-culture and/or responsible for the biosynthesis of the cryptic metabolites observed in our metabolomics study. Using comparative proteomics

analysis, we show that the orphan BGC *nrps1* is highly active and a promising candidate for the production of a potential antimicrobial proteasome inhibitor.

MATERIAL AND METHODS

1. Culture conditions

1.1. Strains and growth media

Axenic marine phototroph *Synechococcus sp.* WH7803 was routinely grown in Artificial Seawater (ASW, Wilson et al., 1996). Cultures were set-up in Falcon 25 cm^2 rectangular culture flasks with vented caps containing 20 mL of media and incubated at a constant light intensity of 10 µmol photons m^{-2} s^{-1}, at 22 °C with orbital shaking (140 rpm). The type strain *Salinispora tropica* CNB-440^T was grown in marine broth (MB, Difco), and incubated at 30 °C with orbital shaking (220 rpm).

1.2. Incubation setup

To compare the proteome of *Salinispora* incubated in MB, ASW and in the presence of photosynthate, cells were washed and resuspended in either MB, ASW or a conditioned *Synechococcus* supernatant (SUPSYN), as appropriate. Cells were first grown to late exponential phase in 10 mL of MB before washing them three times with MB, ASW or SUPSYN, and finally resuspending the washed cell pellet in 10 mL of the same media. Washed *Salinispora* cells were inoculated in 10 mL of fresh MB, ASW or SUPSYN media to a concentration of 25% (v/v), and cultures were incubated for 5 days at 22 °C with shaking (140 rpm) and a light intensity of 10 µmol photons m^{-2} s^{-1}.

To obtain the conditioned supernatant, *Synechococcus* cultures were incubated axenically for 35 days as described above ('Strains and growth media' section) before centrifugation (4000 x *g* for 10 minutes at room temperature) and further filtration through 0.22 µm pore size filters to remove cells and particulate organic matter.

2. Proteomic analysis

2.1. Preparation of cellular proteome samples

Cultures were set up as described above and incubated for 5 days after which cells were collected by centrifuging 10 mL of culture at 4,000 x *g* for 10 minutes at 4 °C. Cell pellets were placed on dry ice before storing at -20 °C until further processing. The cell pellets

were resuspended in 200 µL 1x NuPAGE lithium dodecyl sulfate (LDS) sample buffer (ThermoFischer Scientific), supplemented with 1% ß-mercaptoethanol. Cell pellets were lysed by bead beating (2x45 sec and 1x30 sec at 6.0 m/s) and sonication (5 min), followed by three successive 5-min incubations at 95 °C with short vortex steps in between. Cell lysates containing all proteins were loaded on an SDS-PAGE precast Tris-Bis NuPAGE gel (Invitrogen), using MOPS solution (Invitrogen) as the running buffer. Protein migration in the SDS-PAGE gel was performed for 5 min at 200 V, to allow removal of contaminants and purification of the polypeptides. The resulting gel was stained using SimplyBlue SafeStain (Invitrogen) to visualize the cellular proteome. The gel bands containing the cellular proteome were excised and stored at -20 °C until further processing.

2.2. Trypsin in-gel digestion and nano LC-MS/MS analysis

Polyacrylamide gel bands were destained and standard in-gel reduction and alkylation were performed using dithiothreitol and iodoacetamide, respectively; after which proteins were in-gel digested overnight with 2.5 ng μL^{-1} trypsin (Christie-Oleza & Armengaud, 2010). The resulting peptide mixture was extracted by sonication of the gel slices in a solution of 5% formic acid in 25% acetonitrile, and finally concentrated at 40 °C in a speed-vac. For mass spectrometric analyses, peptides were resuspended in a solution of 0.05% trifluoroacetic acid in 2.5% acetonitrile prior to filtering using a 0.22 µm cellulose acetate spin column. Samples were analyzed by nanoLC-ESI-MS/MS with an Ultimate 3000 LC system (Dionex-LC Packings) coupled to an Orbitrap Fusion mass spectrometer (Thermo Scientific) using a 60 minutes LC separation on a 25 cm column and settings as previously specified (Christie-Oleza et al., 2015).

2.3. Proteomic data analysis

Raw mass spectral files were processed for protein identification and quantification using the software MaxQuant (version 1.5.5.1; Cox & Mann, 2008) and the UniProt database of *S. tropica* CNB-440 (UP000000235). Quantification and normalization of spectral counts was done using the Label-Free Quantification (LFQ) method (Cox et al., 2014). Samples were matched between runs for peptide identification and other parameters were set by default. Data processing was completed using the software Perseus (version

1.5.5.3). Proteins were filtered by removing decoy and contaminants and were considered valid when present in at least two replicates for one condition. The relative abundance of each protein was calculated using protein intensities transformed to a logarithmic scale with base 2 and normalized to protein size. Variations in protein expression between the SUPSYN and MB conditions were assessed with a two-sample T-test, with a false discovery rate (FDR) *q*-value below 0.05 and a log(2) fold change above 2. When comparing the MB and ASW conditions against SUPSYN, variations in protein expression were analyzed by one-way ANOVA (with a FDR *q*-value below 0.05 and a log(2) fold change above 2) followed by Tukey's HSD post hoc test when ANOVA indicated significant differences.

Table 4 | Summary of the proteomic dataset.

Strain studied (No. of proteins)	Growth medium	Detected proteins (% of total proteins)	Detected proteins related to BGCs (% of total detected)	Relative abundance[a] (%)
S. tropica CNB-440 (4,522)	Marine Broth (MB)	1,869 (41.3)	179 (9.6)	9.6 ± 0.9
	Artificial Seawater (ASW)	1,797 (39.7)	172 (9.6)	11.4 ± 0.4
	Phototroph supernatant (SUPSYN)	1,831 (40.5)	181 (9.9)	15.0 ± 1.2

[a] Table shows the cumulated relative abundance of the detected proteins linked to biosynthetic gene clusters, indicated as mean ± standard deviation of three biological replicates. Tukey HSD test, ** significant at *q*-value < 0.01; *** significant at *q*-value < 0.001.

RESULTS

Overview of the *Salinispora tropica* proteome dataset

Having detected novel secondary metabolites produced by *S. tropica* in response to phototroph-released photosynthate, we set out to investigate how it affected the induction of its BGCs. To this end, we analyzed and compared the proteomes of *S. tropica* grown in presence of the phytoplankton photosynthate – *i.e.* in a conditioned *Synechococcus* supernatant (SUPSYN) where the cryptic molecules are produced – and in nutrient rich broth – *i.e.* marine broth (MB) where the cryptic molecules are not detected. Considering that the medium SUPSYN is effectively artificial seawater with some phototroph-released nutrients, we also incubated *S. tropica* in fresh artificial seawater (ASW) as a control. The rationale behind using the SUPSYN medium rather than

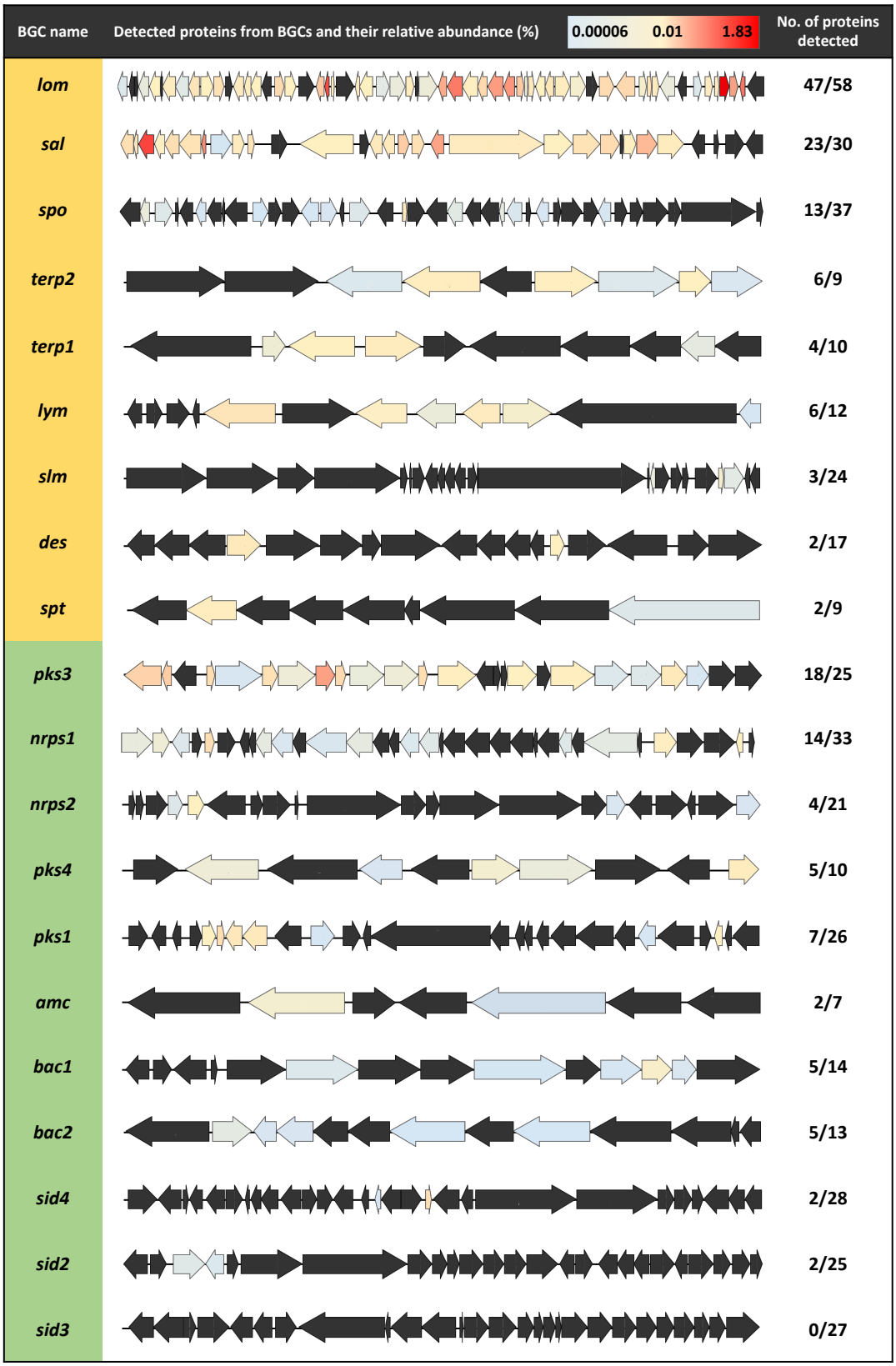

Figure 20 | Photosynthate allows expression of orphan biosynthetic gene clusters in *S. tropica*. Characterized (orange) and orphan BGCs (green) in *S. tropica* CNB-440 detected by high-throughput proteomics when grown with photosynthate (SUPSYN) for 5 days. Genes are colored according to the relative abundance of their corresponding proteins. Those that were not detected are represented in black.

co-inoculating *S. tropica* with *Synechococcus* was two-fold. First, it had the advantage to avoid *Synechococcus* proteins that may interfere with the correct detection of *Salinispora* proteins. Second, we reasoned that it would reduce potential variations in protein expression caused by *Synechococcus-Salinispora* cell to cell interactions and/or the limitation in carbon availability that would occur early in the co-culture in ASW.

Overall, the datasets obtained contain close to 1,900 proteins, representing about 40 % of the total expected proteome of *S. tropica* (**Table 4**). We found that 10 % of those detected proteins could be linked to BGCs (**Table 4**), a figure consistent with the estimated percentage of the *S. tropica* genome to be devoted to natural product assembly (Udwary et al., 2007). Interestingly, while the actual numbers of BGC-related proteins were similar in all three conditions tested, we found that their cumulative abundances accounted for a significantly higher proportion of the proteomes when cells were grown in presence of the phytoplankton's photosynthate compared to both MB and ASW (**Table 4**). As we believed this observation suggests that phototrophic cells prompt an increase of *S. tropica* secondary metabolism, we were interested in identifying which BGCs were expressed and influenced by photosynthate.

Photosynthate allows the expression of orphan gene clusters in *S. tropica*

We were able to detect proteins encoded by almost all of *S. tropica* BGCs regardless of the incubation medium, including 10 of its 11 orphans BGCs (**Fig. 20**). For instance, the already characterized BGCs *lom* and *sal* were abundantly detected with 81% (47/58) and 77% (23/30) of their encoded proteins detected, respectively, some representing high relative abundances within the proteome (**Fig. 20**). The BGC *lom* is linked to the cytotoxic glycoside lomaiviticin molecule (Kersten et al., 2013). However, this metabolite previously showed no antimicrobial activity on co-cultured heterotrophic organisms (Patin et al., 2018) and, hence, it is unlikely to cause the antimicrobial phenotype observed on the phototrophs in this study. The high abundance of the *sal* cluster producing the salinosporamide compound is expected given the high detection of this metabolite by LC-MS (see **Chapter 2**).

Among the orphan BGCs, of particular interest were *pks3* and *nrps1*, for which we detected 72% (18/25) and 42% (14/33) of their encoded proteins, respectively (**Fig. 20**). Moreover, the *pks3* BGC was noticeably highly detected as seven of its detected proteins

showed a relative abundance above 0.1% (**Fig. 20**). While it has been previously suggested that *pks3* may produce a spore pigment polyketide, very little experimental evidence is available in the literature, and the product of *pks3* had not been identified (Kersten et al., 2013). On the other hand, the non-ribosomal peptide synthetase (NRPS) gene cluster *nrps1*, which was previously shown to be silent at the transcriptional level (**Table 3**; Amos et al., 2017), surprisingly appeared to be highly active in our experimental setup. We were able to detect three of the cluster core biosynthetic proteins, namely a non-ribosomal peptide synthetase (A4X2Q0), an adenylation domain-containing protein (A4X2R4) and a condensation domain-containing protein (A4X2R5), with a relative abundance of 0.004%, 0.004% and 0.001%, respectively (**Table 5**). This orphan BGC has only been predicted to produce a non-ribosomal dipeptide (Penn et al., 2009).

Intriguingly, the most abundant protein detected from *nrps1* was an ATP-dependent Clp

Table 5 | Detected proteins from the *nrps1* orphan BGC in *S. tropica* grown with photosynthate.

Protein ID	*Homologue* (% identity/% similarity) *Organism* [Protein ID]	Putative function	Relative abundance (%; n = 3)
A4X2P5	*ridA* (33/54) *Bacillus subtilis* [P37552.3]	2-iminobutanoate/2-iminopropanoate deaminase	0.014
A4X2P8	MFS transporter (28/41) *Mycobacterium tuberculosis* [A0A0H3M5L9.1]	MFS transporter	0.018
A4X2Q0	***srfAB* (28/45) *Bacillus subtilis* [Q04747.3]**	**Non-Ribosomal Peptide Synthetase[a] [C-A-PCP]**	**0.004**
A4X2Q2	***fabG* (34/56) *Vibrio harveyi* [P55336.1]**	**Ketoreductase domain[a]**	**0.002**
A4X2R0	*fadE25* (24/40) *Mycobacterium leprae* [P73574.1]	Acyl-CoA dehydrogenase	0.003
A4X2R1	*YdiO* (28/42) *Escherichia coli K-12* [p0A9U8.1]	Acyl-CoA dehydrogenase	0.002
A4X2R4	***ProA* (gramicidin S synthase) (32/47) *Brevibacillus brevis* [P0C064.2]**	**Adenylation domain[a]**	**0.004**
A4X2R5	***AlaA* (gramicidin synthase subunit B) (26/45) *Brevibacillus parabrevis* [Q70LM6.1]**	**Condensation domain-containing protein[a] [C-PCP-TE]**	**0.001**
A4X2R7	*argG* (53/73) *Nitratiruptor sp.* [A6Q3P9.1]	Argininosuccinate synthase	0.001
A4X2R8	*Fmt* (32/48) *Stenotrophomonas maltophilia* [B2FIR3.1]	Methionyl-tRNA formyltransferase	0.004
A4X2S2	***clpP* (69/85) *Frankia casuarinae* [Q2J9A8.1]**	**ATP-dependent Clp protease proteolytic subunit[b]**	**0.121**
A4X2S4	*MjK1* (25/41) *Methanocaldococcus jannaschii* [Q57604.1]	Potassium channel protein	0.002
A4X2S5	*korB* (65/77) *Mycobacterium tuberculosis* [O53181.1]	2-oxoglutarate oxidorectudase subunit beta	0.006
A4X2S6	*korA* (66/78) *Mycobacterium tuberculosis* [O53182.3]	2-oxoglutarate oxidoreductase subunit alpha	0.004

[a] Core biosynthetic enzyme.

[b] Protein potentially involved in self-resistance to a proteasome inhibitor.

protease subunit (A4X2S2), with a relative abundance of 0.121% (**Table 5**), a protein that may be involved in conferring resistance to a BGC-encoded antimicrobial compound (Kirstein et al., 2009), as further discussed below in this Chapter.

Photosynthate increases the expression of the *nrps1* orphan gene cluster

Although all BGCs appeared to be similarly active between conditions with regards to the detection of their proteins (*i.e.* the same proteins were generally present in the different proteomes, rather than being conditional to one growth medium), a thorough comparative analysis of their expression levels revealed that phototroph-released nutrients could specifically trigger several proteins within a BGC (**Fig. 21**). For instance, the orphan *pks3* BGC showed an up-regulation of the production of pivotal enzymes for polyketide biosynthesis when cells were grown in the SUPSYN medium compared to MB. Namely, an acyl-CoA ligase (A4X7T8), a 3-ketoacyl-ACP synthase (A4X7U0) and a long-chain fatty acid-CoA ligase (A4X7U3) were up-regulated 3.1, 2.6 and 4.1-fold, respectively (**Fig. 21, A**). These variations in protein detection could not, however, be confidently attributed solely to the presence of photosynthate because they were also observed at similar levels between the MB and ASW conditions. This could indicate that the orphan *pks3* cluster's expression is regulated by nutrient availability as it is less active in a nutrient-rich broth like MB.

On the other hand, the activity of the BGC *nrps1* was more clearly influenced by photosynthate as 28% (4/14) of its detected proteins were significantly up-regulated in the SUPSYN medium *versus* MB (**Fig. 21, B**). They included three core biosynthetic enzymes, namely a non-ribosomal peptide synthetase (12.5-fold change; A4X2Q0), a ketoreductase domain-containing protein (1.6-fold change; A4X2Q2) and an adenylation domain-containing protein (3.4-fold change; A4X2R4). Furthermore, we were able to confirm that photosynthate specifically triggered an increase in the expression of at least three of them (*i.e.* A4X2Q0, A4X2Q2 and A4X2R0), as they exhibited a significant up-regulation in SUPSYN compared to the two other media, but abundances alike between ASW and MB (**Fig. 21, C**). For instance, the non-ribosomal peptide synthetase A4X2Q0 was up-regulated 5.5 and 12.5-fold in presence of the phytoplankton's photosynthate *versus* in ASW or MB, respectively, while showing comparable activity in the two latter conditions (**Fig. 21, C**).

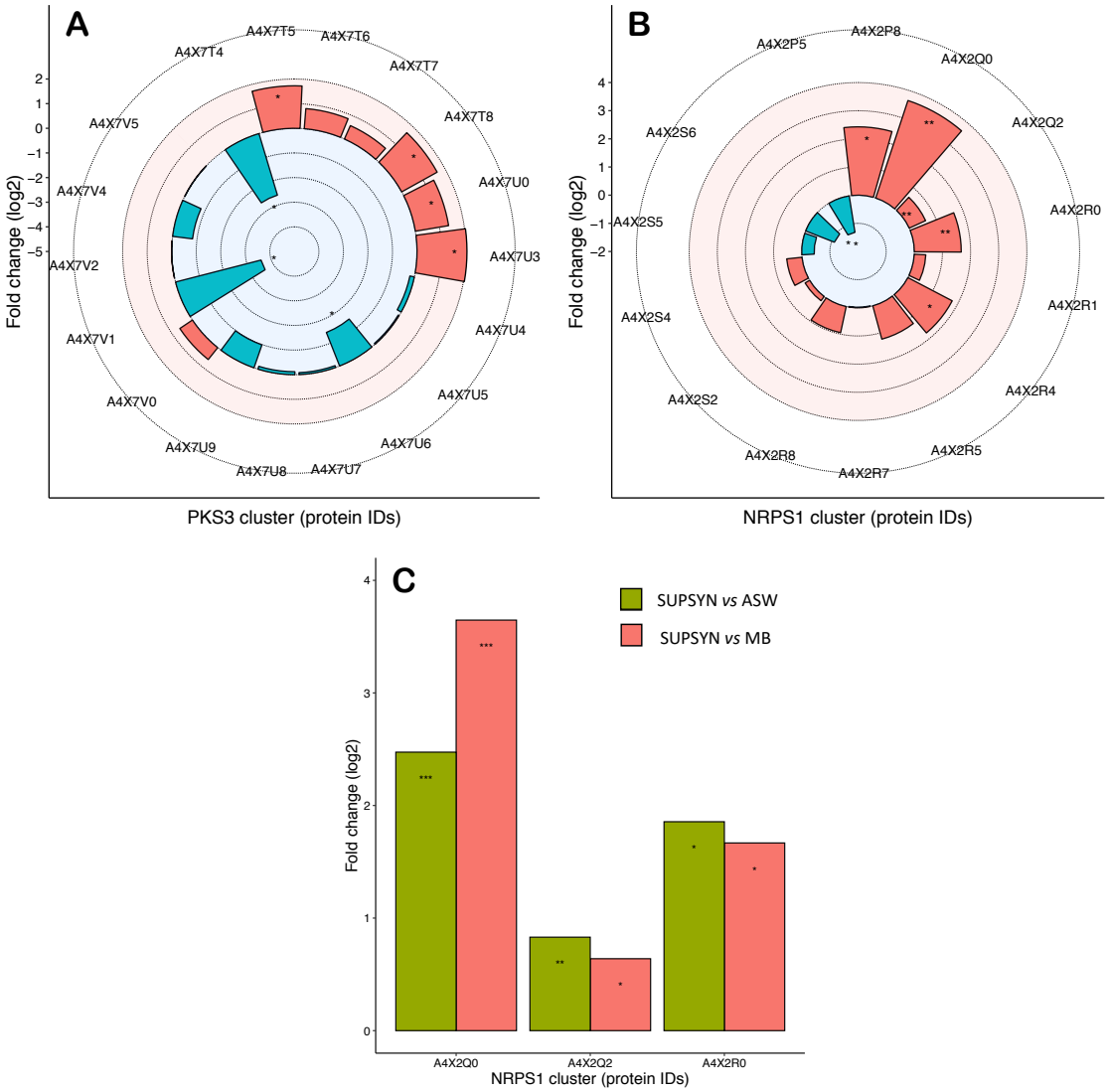

Figure 21 | Photosynthate increases the expression of the orphan *nrps1* BGC in *S. tropica*. Photosynthate and other nutrients influence several proteins from the orphan BGCs *pks3* **(A)** and *nrps1* **(B)**, in comparison with cells grown in MB. Up- (red) and down-regulated (blue) proteins in the presence of the photosynthate (SUPSYN) are shown. Statistically significant fold changes are indicated by an asterisk (T-test, significant at *q*-value < 0.05). Enzymes further analyzed for a post hoc test are indicated by a double asterisk. **(C)** Photosynthate specifically triggers an up-regulation of several proteins from the *nrps1* BGC. Up-regulated proteins in the presence of photosynthate compared to ASW (green) and MB (red) are shown. These proteins showed no significant difference between the MB and ASW conditions. Tukey HSD test, * significant at *q*-value < 0.05; ** significant at *q*-value < 0.01; *** significant at *q*-value < 0.001. Graphs show mean fold change of triplicates, as calculated by the Perseus software.

DISCUSSION

We here provide the first cellular proteome dataset for *S. tropica* CNB-440. Exploring its proteome exposed to photosynthate, we detected proteins encoded by almost all its BGCs, including most of its orphan BGCs (**Fig. 20**). This strengthens *S. tropica* potential

for novel natural product discovery, as most of these orphan BGCs may be poorly expressed or producing molecules difficult to detect, rather than to be silent or inactivated. Notably, while detection and relative abundance of proteins for the *lom* cluster strongly suggest production of lomaiviticin, we were not able to detect it in our experimental setup. In this regard, the *lom* BGC provides an interesting example of a small compound for which both protein and transcription levels indicate its biosynthesis, but analytical chemistry fails to allow its detection. This observation also challenges the assumption that most of the BGCs corresponding to un-detected molecules are silent, and highlight the necessity to improve isolation and detection of natural products, as it has previously been discussed (Amos et al., 2017). In comparison, the *sal* BGC, producing the salinosporamide compound, was one of the most highly expressed BGC as several of its proteins were detected with high relative abundance. This finding is in agreement with previous studies that have shown by transcriptomics that the BGC *sal* is highly and constitutively expressed when grown in nutrient rich A1 medium (Amos et al., 2017). Also, the high expression of this BGC correlated with a noticeable detection of salinosporamide derivatives by LC-MS. Therefore, the abundant detection of several orphans BGC proteins, including those from *pks3* and *nrps1* BGCs, may be interesting candidates responsible for the biosynthesis of the cryptic metabolites detected by LC-MS we reported in Chapter 2.

The proteins detected from the BGC *nrps1* are essential enzymes involved in non-ribosomal peptide biosynthesis, *i.e.* A4X2Q0, a non-ribosomal peptide synthetase (NRPS) made of a C-A-PCP domain; A4X2Q2, a ketoreductase domain-containing protein; A4X2R4, an adenylation domain-containing protein; and A4X2R5, a condensation domain-containing protein made of C-PCP-TE domain. The detection of these proteins therefore strongly suggests the actual synthesis of the non-ribosomal peptide and could well be the cryptic metabolites **4**, **6** and **7** detected by LC-MS (see **Fig. 12, B** from **Chapter 2**). The molecules indeed include four nitrogen atoms in their predicted molecular formulae and four identified A-domains, which are responsible for the selection and activation of the amino-acids monomers incorporated into the non-ribosomal peptide, are encoded in the *nrps1* BGC. Interestingly, while the substrate specificity of A4X2Q0's A-domain is alanine, the one of A4X2R4 and the two others could not be predicted. We also show that the proteins encoded by the *nrps1* BGC were more abundantly detected

with photosynthate (**Fig. 21**), which is consistent with our previous observation that the detection of the molecules is conditional to the presence of phytoplankton or their photosynthate. This correlation supports the orphan *nrps1* as a promising candidate for the production of the cryptic compounds and, potentially, the antimicrobial activity observed on co-cultured phototrophs.

Intriguingly, we detected from this same BGC a highly abundant ATP-dependent Clp protease proteolytic subunit (ClpP, A4X2S2) that may be providing *S. tropica* with self-resistance against the *nrps1* peptides. Virtually all organisms across the tree of life have a system for targeted proteolysis for protein turnover, with most bacteria, mitochondria and chloroplasts relying on a ClpP-type proteasome while eukaryotes, archaea and some actinobacteria typically possess the homologous 20S proteasome structure (Becker & Darwin, 2017; Snoberger et al., 2017). The ClpP proteasome is known to be the target for certain antibiotics, including the novel acyldepsipeptide (ADEP) class (Kirstein et al., 2009), and it is common to find alternative ClpP proteasomes encoded nearby the antibiotic-producing BGC to confer resistance to the host cell (Thomy et al., 2019). In a similar fashion, salinosporamide A is a 20S proteasome inhibitor, to which *S. tropica* is resistant because of an extra copy of the proteasome beta subunit gene within the salinosporamide-producing cluster (Kale et al., 2011). We can thus reasonably infer from the presence of *clpP* in the *nrps1* BGC that it is likely to produce an antibiotic targeting the ClpP proteasome, a class of antimicrobial compounds that has recently gained considerable attention as an attractive option to tackle multidrug resistant pathogens (Culp & Wright, 2017; Momose & Kawada, 2016; Moreno-Cinos et al., 2019). We here provide the first proteomic evidence that *S. tropica*'s *nrps1* is active and may produce a promising antimicrobial compound acting as a ClpP proteasome inhibitor. The synthesis of such an antibiotic would explain the antimicrobial effect of *S. tropica* on all marine phototrophs tested in our study (see **Chapter 2**) as they all rely on the ClpP proteolytic machinery (Andersson et al., 2009; Jones et al., 2013; Zhao et al., 2018).

We here provide a valuable insight into the biosynthetic potential of *S. tropica* with our proteomic dataset, as it revealed the expression of several orphan BGCs, including the *nrps1* cluster that was previously reported to be silent (Amos et al., 2017). We show that a protein-based study can help in the identification of candidate BGCs for the discovery of novel natural products. Our comparative proteomic analysis demonstrated that the

photosynthate released by primary producers influences the biosynthetic capacities of *S. tropica*, activating the expression of the orphan BGCs *nrps1*, a promising candidate for antibiotic production that could encode the detected cryptic molecules. Additional evidence, such as genetic inactivation of the *nrps1* BGC, will confirm this mechanism. For this, future work will involve the development of a genome engineering method in *S. tropica* that would allow the fast deletion of candidate BGCs, and support the bioactivity-guided screening of novel antimicrobials and their corresponding BGCs.

CHAPTER 4 |

GENOME ENGINEERING OF *SALINISPORA TROPICA* USING CRISPR/CAS9 FOR PPTASES AND BGCS DELETION

INTRODUCTION

The marine actinomycete *Salinispora* is a promising genus for the discovery of novel natural products, with anti-cancer and antibiotics compounds having been isolated from its three species (Asolkar et al., 2009; Feling et al., 2003; Janso et al., 2014; Nett & Moore, 2009). Although many new molecules have been sourced from this genus already, its full potential for secondary metabolite production remains to be exploited. Sequencing of the type strain *S. tropica* CNB-440^{T}, for instance, lead to the identification of twenty biosynthetic gene clusters (BGCs), of which eleven are still orphan (Penn et al., 2009; Udwary et al., 2007). Recent studies also showed that some strains exhibited antimicrobial activity in co-cultures against marine heterotrophs but traditional analytical chemistry methods failed to enable the identification of the molecule responsible (Patin et al., 2018; Patin et al., 2016). We have similarly reported in Chapter 2 that *S. tropica* inhibits phytoplankton's growth and that it produces cryptic compounds in response to the co-culture. Additionally, analysis of *S. tropica*'s proteome presented in Chapter 3 suggests that several of its orphan BGCs might well be active but their products have yet to be characterized (*e.g. pks3*, *nrps1* and *nrps2*). The link between these different observations remains to be established *via* the assignment of the antimicrobial activity observed in co-culture and/or the production of the cryptic compounds to one of *S. tropica* BGCs.

This strategy would rely on the ability to inactivate several BGCs in *S. tropica* using genome editing. Instead of individually deleting each BGC, however, one could inactivate groups of BGCs by targeting phosphopantetheinyl transferases (PPTases), a family of enzymes essential for the biosynthesis of secondary metabolites (Beld et al., 2014). All polyketide synthase (PKS) and non-ribosomal peptide synthetase (NRPS) systems, for instance, require the activity of PPTases, dedicated or not, to produce their natural products. Briefly, NRPS- and PKS-based biosynthesis relies on modules, where one module is responsible for the iterative addition of one building block (*i.e.* amino-acid and acyl-coenzyme A, respectively) to the nascent molecule. In NRPS systems, each module

comprises several protein domains, typically an adenylation, peptidyl carrier protein (PCP), condensation and thioesterase domains (**Fig. 8**; Mootz et al., 2000). Briefly, an amino-acid selected and activated by the adenylation domain is loaded onto the PCP domain. The condensation domain catalyzes the formation of a peptide bond between the PCP-bound amino-acid and the growing peptide chain of the upstream module. Finally, the thioesterase domain releases the mature oligopeptide from the NPRS assembly line (Fischbach & Walsh, 2006; Süssmuth & Mainz, 2017). This process is, however, possible only after a PPTase transfers a phosphopantetheine (PPant) moiety to the conserved serine of an inactive apo-PCP domain, resulting in its active holo-form (Beld et al., 2014; **Fig. 22**). The PPant then acts as a flexible 'arm' onto which the intermediates of the assembly lines are transiently held, allowing their shuttling to the neighbouring protein domains, making the molecule biosynthesis possible (Lambalot et al., 1996). PPTases are also known to possess broad specificity, with one PPTase often being able to activate a specific set of several BGCs, therefore representing a promising target to inactivate multiple BGCs by single gene deletion (Beld et al., 2014; Zhang et al., 2017).

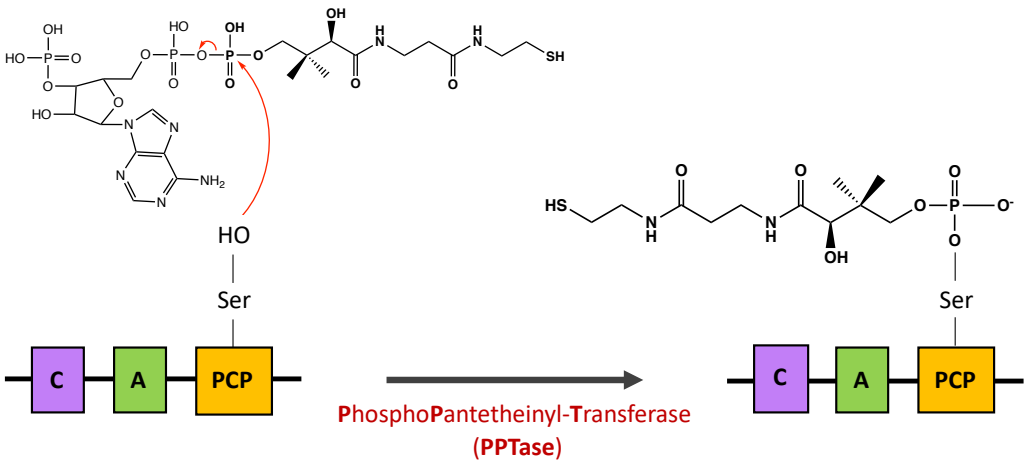

Figure 22 | PPTases are essential for the biosynthesis of all PKSs and NRPSs natural products. Scheme of PCP activation by a PPTase. PPTases modify PCP domains post-translationally by adding a PPant moiety to the conserved serine of inactive apo-PCPs, resulting in their active form holo-PCPs, allowing the loading and shuttling of intermediates which is pivotal to non-ribosomal peptide and polyketide natural product biosynthesis.

Gene integration and deletion in the genus *Salinispora* has previously been done to study various biosynthetic pathways, using well established methods based on integrative

vectors and PCR-targeted mutagenesis (Bucarey et al., 2012; Eustáquio et al., 2010). These techniques could be used to generate PPTase mutants, however, they present one or several of the following drawbacks: (a) integration of a selectable marker limiting the number of genomic modifications possible in a cell, (b) lack of stability of the single cross-over and (c) relatively time-consuming protocols requiring several steps to obtain marker-free mutants (Datsenko & Wanner, 2000; Gust et al., 2003; Kieser et al., 2000). While the CRISPR/Cas9 technology allows rapid generation of marker-less double cross-over mutants and has been applied successfully in soil actinobacteria, it has yet to be used in *Salinispora* (Alberti et al., 2019; Jinek et al., 2012).

Here, we implemented for the first time the CRISPR/Cas9 technology to perform whole-BGC and single-gene PPTase deletion in the genus *Salinispora*. We use a combination of metabolomics and proteomics to characterize a mutant strain deficient in the PPTase 2496. Our preliminary data suggests that PPTases in *S. tropica* are functionally redundant and that improving the CRISPR/Cas9 efficiency could lead to its successful use for the global inactivation of BGCs in the genus *Salinispora*.

Table 6 | Bacterial strains and plasmids used in this study.

Strain	Genotype	Reference or source
E. coli DH5α	F$^-$ *endA1 glnV44 thi-1 recA1 relA1 gyrA96 deoR nupG purB20* ϕ80d*lacZ*ΔM15 Δ(*lacZYA-argF*)U169, hsdR17($r_K^- m_K^+$), λ$^-$	New England Biolab (NEB)
E. coli ET12567-ΔDAP	*dam-13::Tn9, dcm-6, hsdM, hsdS, ΔdapA::(erm-pir);* contains pUZ8002	Allard *et al*., 2015
S. tropica CNB-440	Wild-type	Maldonado *et al*., 2005; DSM No.: 44818
S. tropica Δ2496	Derivative of *S. tropica* CNB-440, Δ*strop_2496* (PPTase 2496)	This study
S. tropica Δnrps2	Derivative of S. tropica CNB-440, Δ*strop_4429-4409* (BGC *nrps2*)	This study
Plasmid	**Description**	**Reference or source**
pCRISPomyces-2	Codon-optimized *cas9* from *Streptococcus pyogenes; lacZ* flanked by *BbsI* sites for Golden Gate cloning of crRNA; *XbaI* site for addition of homology arms; temperature-sensitive pSG5 origin and apramycin resistance marker	Cobb *et al*., 2015
pCRISPomyces-0685	Derivative of pCRISPomyces-2, targets PPTase 0685	This study
pCRISPomyces-0777	Derivative of pCRISPomyces-2, targets PPTase 0777	This study
pCRISPomyces-2496	Derivative of pCRISPomyces-2, targets PPTase 2496	This study
pCRISPomyces-2822	Derivative of pCRISPomyces-2, targets PPTase 2822	This study
pCRISPomyces-nrps1	Derivative of pCRISPomyces-2, targets the BGC *nrps1*	This study
pCRISPomyces-nrps2	Derivative of pCRISPomyces-2, targets the BGC *nrps2*	This study

MATERIAL AND METHODS

1. Strains and growth conditions

Retargeting of the pCRISPomyces-2 vector was performed using commercial chemically competent *E. coli* DH5α cells (NEB). Conjugation of retargeted pCRISPomyces-2 was done using *E. coli* ET12567-ΔDAP, a diaminopimelic acid (DAP)-auxotroph and methylation-deficient donor strain containing the RP4 conjugation machinery in the helper plasmid pUZ8002 (**Table 6**; Allard et al., 2015). The strain was kindly provided by the Roy laboratory (Canada). *E. coli* cells were routinely cultured in Luria-Bertani (LB) broth supplemented with 50 µg mL^{-1} kanamycin, 25 µg mL^{-1} chloramphenicol, 50 µg mL^{-1} apramycin and 60 µg mL^{-1} DAP, when required.

Salinispora tropica CNB-440 was routinely grown in marine broth (Difco) and incubated at 30 °C with shaking (220 rpm). Marine broth was supplemented with 100 µg mL^{-1} apramycin, when required. Setup of co-cultures with *Synechococcus* WH7803 and description of SUPSYN is described in the Material and Methods section of Chapter 2.

2. Construction of *S. tropica* mutants

2.1. Retargeting of pCRISPomyces-2

In order to knock-out the selected PPTases, we retargeted the pCRISPomyces-2 vector, a CRISPR/Cas9-based system optimized for genome editing of *Streptomyces*, following the author guideline provided in the supporting information (Cobb et al., 2015). Briefly, protospacer design was based on *S. tropica* CNB-440 genome (NC_009380), using the CRISPY-webtool (crispy.secondarymetabolites.org; Blin et al., 2016). Targets were STROP_RS03465 (strop_0685), STROP_RS03935 (strop_0777), STROP_RS12565 (strop_2496), STROP_RS14165 (strop_2822), STROP_RS03535 and STROP_RS03375 to delete the *nrps1* gene cluster, as well as STROP_RS22350 and STROP_22250 to delete the *nrps2* gene cluster. Protospacers for each target were selected to be: (a) 20-bp for the full sgRNA, (b) with the 3' protospacer adjacent motif (PAM) NGG, (c) on the non-coding strand, (d) unique in the genome even with 1-bp mismatch, and (e) located centrally within the target, when possible.

For PPTase deletion, selected protospacers were synthesized as two 24-bp oligonucleotides that were the reverse complement of each other, such that the annealed product resulted in double-stranded protospacers with BbsI-compatible

overhangs (**Appendix 5**). For BGC deletion, two guide RNA cassettes were required and protospacers were synthesized as a synthetic construct (**Appendix 5**). Protospacers and synthetic constructs were cloned into pCRISPomyces-2 using Golden Gate Assembly. To allow precise editing via homologous recombination, two ~ 1-kb arms corresponding to the sequences flanking the Cas9-induced deletion were cloned into the retargeted pCRISPomyces-2 plasmids using Gibson Assembly (**Appendix 5**).

2.2. Plasmid conjugation

For cell mating, 3 mL of donor *E. coli* ET12567-ΔDAP cells were grown overnight in LB medium. The overnight cultures were back-diluted into 10 mL of LB medium and grown to an optical density of 0.4-0.6. Medium used up to this stage was supplemented with the appropriate antibiotics and DAP. Donor cells were then washed three times with fresh LB medium to remove antibiotics, and then re-suspended in 500 µL of LB medium without antibiotics. Recipients for conjugation were spores of *S. tropica* CNB-440 collected from cells grown onto one A1- and one MB-agar plate for 30 days at 30 °C. Spores were isolated from mycelium in suspension by filtering through a sterile 10-mL syringe with added cotton wool. Spores were pelleted and resuspended into 500 µL of A1 medium.

Donor and recipient cells were mixed, pelleted, resuspended in about 50 µL of the remaining media and finally aliquoted onto solid MB media as 10 µL spots. Cells were incubated for 16-20 hours at 30 °C to allow mating. To select for successful plasmid conjugations, cells were re-suspended from the plates into 100 µL of MB medium, plated onto solid MB media supplemented with 100 µg/mL apramycin, and incubated at 30 °C for about 12 days.

2.3. Knock-out verification

Exconjugants were first grown in MB medium supplemented with apramycin to confirm resistance and plasmid acquisition. Genomic DNA was extracted from the resulting cultures using a DNeasy plant mini kit (Qiagen), modified with an additional bead beating step (2x45 sec and 1x30 sec at 6.0 m/s). Extracted DNA was used as template to check the deletion of the PPTases and BGCs by PCR using primers listed in **Appendix 6**. PCR-

amplified fragments containing the deleted junction were also verified using Sanger sequencing.

3. Mutant strain characterization

3.1. Cell counting *via* flow cytometry

Synechococcus cell abundance in co-culture was monitored using its autofluorescence by flow cytometry using a LSR Fortessa Flow Cytometer (BD) instrument, and the BD FACSDiva acquisition software (BD). Cells were detected and gated using ex. 488 nm – em. 710/50 nm at voltage 370 V, and ex. 640 nm – em. filter 670/14 nm at voltage 480 V. To remove any *Salinispora* cell aggregates that would block the flow cell, samples were pre-filtered through a sterile mesh with pore size of 35 µm (Corning) prior to analysis.

3.2. LC-MS analysis

Details of the preparation of metabolomics samples can be found in the Material and Methods of Chapter 2 (section 2). Briefly, the co-culture supernatants were analyzed after 35 days by non-targeted metabolomic using supernatant crude extracts. For this, cells from 10 mL of cultures were removed by centrifugation (4,000 x *g* for 15 minutes) followed by a filtering step using 0.22 µm vacuum filter bottle system (Corning). Pre-purification of the organic compounds from the supernatants was carried out by solid phase extraction using C18-silica, as described in Chapter 2 (section 2.1.). The obtained extract was dried under reduced pressure at 40 °C (in a speed-vac) and resuspended in 1 mL of 50:50 HPLC-grade methanol/water solution. All samples were stored in snap-seal amber glass vials (Thames Restek) and kept at -20 °C until analysis.

Metabolites were analyzed by reversed-phase liquid chromatography. A Dionex UltiMate 3000 HPLC (ThermoScientific) coupled with an amaZon SL Ion Trap MS (Bruker) was used. A Zorbax Eclipse Plus C18 column with dimensions 4.6 mm x 150 mm, 5 µm particle size (Agilent Technologies) was employed for metabolite separation with the same linear gradient specified in Chapter 2 (section 2.2.). The mass spectrometer (MS) was operated in positive ion mode with a 100-1000 *m/z* scan range. The injected volume was 10 µL at a temperature of 25 °C. Data was processed with the Bruker Compass DataAnalysis software version 4.2 (Bruker).

4. Proteomic analysis

Details of the preparation of cellular proteome samples can be found in the Material and Methods of Chapter 3 (section 2.1.). Briefly, cultures were set up as previously described and incubated for 5 days in MB. Protein extracts were purified from contaminants *via* SDS-PAGE gel migration. The gel bands containing the cellular proteome were excised and destained, followed by a standard in-gel reduction and alkylation using dithiothreitol and iodoacetamide, respectively. Proteins were then in-gel digested overnight and the resulting peptide mixture was extracted by sonication of the gel slices in a solution of 5% formic acid in 25% acetonitrile, and finally concentrated at 40 °C in a speed-vac.

For mass spectrometric analyses, peptides were resuspended in a solution of 0.05% trifluoroacetic acid in 2.5% acetonitrile prior to filtering using a 0.22 µm cellulose acetate spin column. Samples were analyzed by nanoLC-ESI-MS/MS with an Ultimate 3000 LC system (Dionex-LC Packings) coupled to an Orbitrap Fusion mass spectrometer (Thermo Scientific) using a 60 minutes LC separation on a 25 cm column and settings as previously specified (Christie-Oleza et al., 2015).

Raw mass spectral files were analyzed using Qual Browser from the software Xcalibur (version 2.2). Ions of interests were identified manually by plotting the appropriate mass ranges. Charge state was confirmed by calculating the mass differences observed between related peaks from isolated ion spectra (**Appendix 7**). Volcano plots were based upon data analyzed with Perseus, using the pipeline and settings previously described in Material and Methods of Chapter 3 (section 2.3.).

5. Bioinformatics

5.1. PPTase identification

Hypothetical PPTases in *S. tropica* CNB-440 are listed by Kim and colleagues in Table S1 of their study (*Distribution of PPTases in Actinomycetales microorganisms and some eubacteria*): strop_0685, strop_0777, strop_2496, strop_2822 and strop_3859 (Kim et al., 2018). To confirm that they are PPTases, we analyzed their sequence alignments, with the *sfp* from *Bacillus subtilis* as a reference (GenBank accession number AEK64474.1) using CLUSTAL multiple sequence alignment by MUSCLE (3.8) (https://www.ebi.ac.uk/Tools/msa/muscle/; Madeira et al., 2019) and ESPript (3.0) for annotation (http://espript.ibcp.fr; Robert & Gouet, 2014).

5.2. ACP/PCP identification

A Hidden Markov Models (HMM) profile for the ACP, PCP, ACPS, and ACP_beta domains was extracted from the "nrpspksdomains.hmm" file which is included in the antiSMASH software package using the binary program hmmfetch. These profiles were used to query the genome of *S. tropica* CNB-440 (UP000000235) using hmmsearch. The default threshold cutoffs were used for the query using the flag "—cut_tc." Hmmfetch and Hmmsearch are part of the hmmer suite of programs (http://hmmer.org/, v3.2.1)

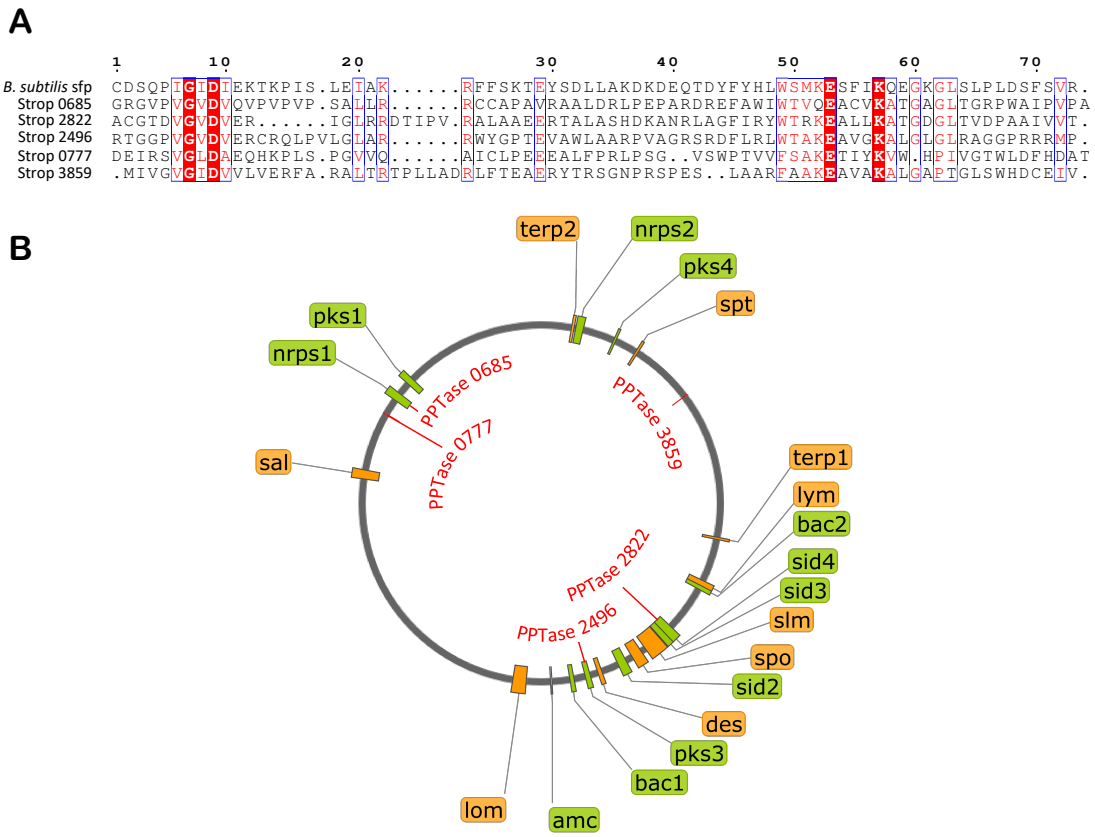

Figure 23 | *S. tropica* has four PPTases responsible for activation of its NRPSs and PKSs. (A) Amino-acid sequence alignments of identified PPTases in *S. tropica* CNB-440 with *B. subtilis* Sfp. Amino-acids with strict identity are highlighted in red. Amino-acids within a blue frame are similar across sequences. **(B)** Genomic map of *S. tropica* CNB-440, showing BGCs (outer ring) and identified PPTases locations (inner ring). Genome size is 5,183,331 bp. BGCs are labelled in orange if characterized and in green if orphan.

RESULTS

Identification of PPTases in *S. tropica* CNB-440

In order to delete PPTases for the broad inactivation of BGCs in *S. tropica*, we were interested in identifying and locating its PPTases linked to secondary metabolism only

(PKS and NRPS). There are indeed two subfamilies of PPTases: the AcpS-type is required for fatty acid biosynthesis (*i.e.* primary metabolism) and the Sfp-type for polyketide and non-ribosomal peptide biosynthesis (*i.e.* secondary metabolism; Beld et al., 2014; Lambalot et al., 1996).

Previous studies have identified bioinformatically at least five putative PPTases encoding genes in the genome of *S. tropica* CNB-440, namely *strop_0685*, *strop_0777*, *strop_2496*, *strop_2822* and *strop_3859* (Kim et al., 2018; Udwary et al., 2007). Alignment of their amino-acid sequences confirmed that they possess the highly conserved regions ppt-1 [(I/V/L)G(I/V/L/T)D(I/V/L/A)] and ppt-3 [(F/W)(A/S/T/C)xKE(S/A)h(h/S)K(A/G)] that are characteristic of PPTases (**Fig. 23, A**; Lambalot et al., 1996). Interestingly, mapping the PPTases to the *S. tropica* genome showed that they are all located within a BGC or nearby (*i.e. strop_0777* being 75 kb away from *nrps1*; *strop_0685* within *nrps1*; *strop_2496* within *pks3* and *strop_2922* within *slm*), with the exception of *strop_3859* which is 300-kb away from its closest BGC (*i.e. spt*; **Fig. 23, B**).

We found the location of the PPTases to be consistent with their putative function. The number of amino-acids *n* between the ppt-1 and ppt-3 motifs is specific to the PPTase subfamilies, with *n* between 42-48 aa for the AcpS-type and 38-41 aa for the Sfp-type. As such, we identified the PPTases 0685, 0777, 2496 and 2822 to be involved in secondary metabolism, with *n* = 38, 36, 39 and 38, respectively; and the PPTase 3859 to be involved in primary metabolism, with *n* = 42 (**Fig. 23, A**). Based on DNA sequence analysis and the genetic context of the identified PPTases, we ultimately hypothesized that the four PPTases 0685, 0777, 2496 and 2822 are responsible for the functional activation of *S. tropica*'s BGCs.

Genomic deletion of PPTases and NRPS clusters in *S. tropica* using CRISPR/Cas9

While previous studies used well-established integrative vectors and PCR-targeted mutagenesis to create *Salinispora* mutants, the CRISPR/Cas9 technology has, to date, not been applied in the genus *Salinispora* (Bucarey et al., 2012; Eustáquio & Moore, 2008). In order to knock-out the selected PPTases, we chose to use the pCRISPomyces-2 vector (**Fig. 24, A**), a CRISPR/Cas9-based system optimized for genome editing of *Streptomyces* (Cobb et al., 2015). We modified the pCRISPomyces-2 plasmid to delete the PPTases 0685, 0777, 2496 and 2822, by cloning in the corresponding protospacers and homology

arms (**Table 6**; **Fig. 24, B**). We also decided to delete the orphan *nrps1* and *nrps2* gene clusters based on proteomic data obtained by our group that suggested they could be linked to the cryptic molecules and/or the antimicrobial activity observed in co-culture (see **Chapter 3**). For this, we similarly retargeted the pCRISPomyces-2 vector for those BGCs and then worked towards transferring the six modified CRISPR vectors into *S. tropica*.

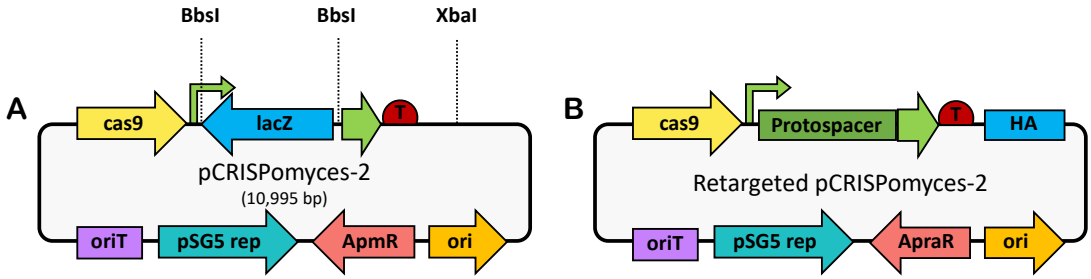

Figure 24 | Plasmid maps of the CRISPR/Cas9-based pCRISPomyces plasmids used for genomic deletion. (A) Map of the original pCRISPomyces-2 vector (Cobb *et al.*, 2015). **(B)** Generic map of the retargeted pCRISPomyces for deletion of PPTases constructed in this study. The endonuclease cas9 (cas9) is guided by a 20-bp CRISPR RNA (protospacer) completed with a guide RNA scaffold (green arrow). Homology arms (HA) used as editing template for homologous recombination can be cloned into the XbaI site. Apramycin resistance marker (ApraR) allows selection in both *E. coli* and *Streptomyces*. The colE1 origin (ori) allows for replication in *E. coli*, while the temperature-sensitive pSG5 rep enables replication in *Streptomyces*.

Although transfer of plasmids in *Salinispora via* conjugation has previously been reported, we found the successful implementation of this technique to be non-trivial. We were unable to obtain any exconjugant using a published protocol (Eustáquio & Moore, 2008) despite numerous attempts, which warranted extensive efforts into the development of a modified method efficient for the transfer of DNA in *S. tropica,* which we discuss in detail later in the thesis. Some differences were, for instance, the use of (i) an auxotrophic *E. coli* donor strain allowing screening of exconjugants without the addition of nalidixic acid, (ii) spores sourced from solid medium, (iii) cell spotting for mating and (iv) reduced apramycin concentration added in-plate rather than overlayed. Following this altered protocol, the conjugal transfer of our retargeted pCRISPomyces-2 plasmids to *S. tropica* yielded on average 1-8 exconjugants per plate. We successfully isolated exconjugants for all of our plasmids with the exception of pCRISPomyces-2822, resulting in the *S. tropica* strains 0685, 0777, 2496, nprs1 and nrps2.

We then screened the obtained exconjugants by PCR to confirm the deletion of the genomic regions of interest. We were able to isolate colonies of the strains *S. tropica* 0777, 2496 and nrps2, that appeared to have the expected deletions whereas the strains 0685 and nrps1 gave unexpected results. Indeed, when screening colonies of *S. tropica* 0685, we were intriguingly unable to amplify the region flanking the PPTase 0685 but we were able to in the wild-type strain (**Fig. 25, A**). While the integrity of the gDNA extracted from this strain was verified using a primer pair amplifying an untargeted region of the genome, no amplicon could be obtained with various oligonucleotide pairs binding up to

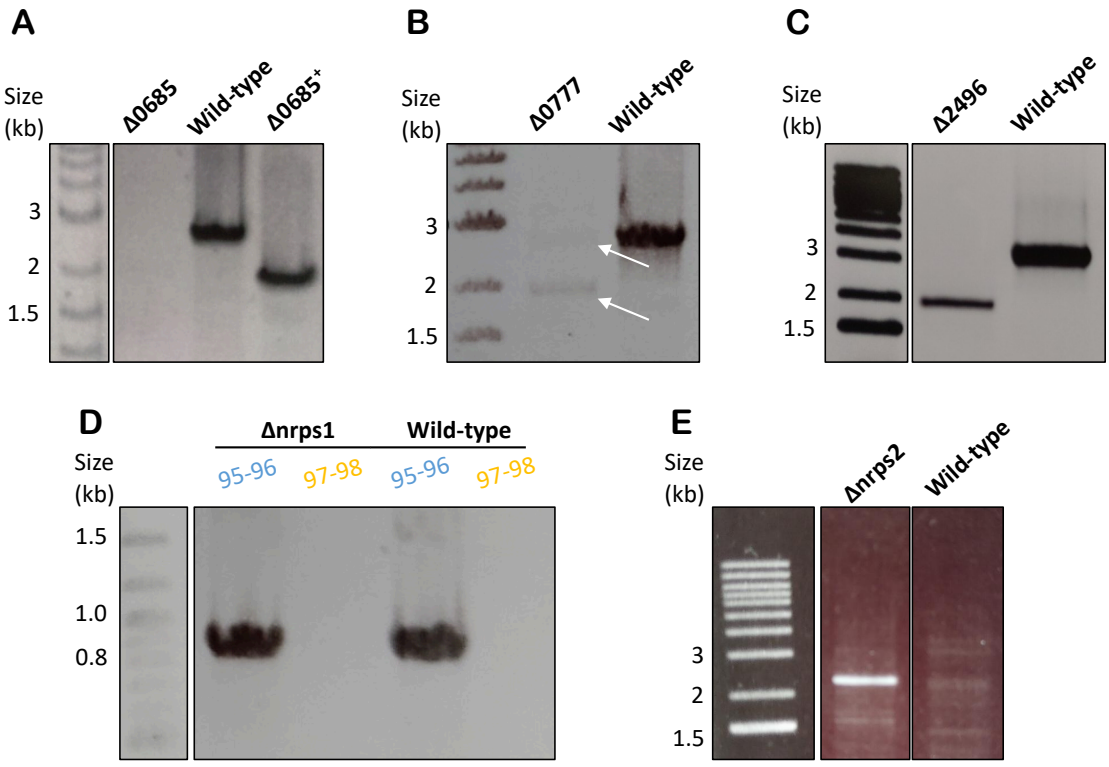

Figure 25 | PCR verification of exconjugants. (A) PCR check of PPTase 0685 deletion. Expected size for the wild-type strain is 2,622 bp and 1,940 bp for the ΔPPTase 0685 strain. Lane labelled Δ0685+ shows control PCR to confirm integrity of the gDNA used for lane labelled Δ0685, with another primer pair that binds outside the targeted region, with an expected amplicon of 1,947 bp. **(B)** PCR check of PPTase 0777 deletion. Expected size for the wild-type strain is 2,784 bp and 2,050 bp for the ΔPPTase 0777 strain. **(C)** PCR check of PPTase 2496 deletion. Expected size for the wild-type strain is 2,642 bp, and 2,142 bp for the ΔPPTase 2496 strain. **(D)** PCR check of BGC *nrps1* deletion. With the primer pair 95-96, which binds within the cluster, expected size for the wild-type strain is 892 bp and no amplicon for the Δnrps1 strain. With the primer pair 97-98, which binds outside the cluster, expected size for the wild-type strain is 40,700 bp and 571 bp for the Δnrps1 strain. **(E)** PCR check of BGC *nrps2* deletion. With the primer pair binding outside the cluster, expected size for the wild-type strain is 34,711 bp and 2,448 bp for the Δnrps2 strain. PCR products were run on a 1% agarose gel with a 1 kb plus ladder (Invitrogen).

2,4 kb away from the sites of deletion. This observation suggested an unsuspected recombination event that would require further investigation. Concerning the *nrps1* deletion, despite extensive screening, no apramycin-resistant clone of the strain *S. tropica* nrps1 tested showed the loss of the corresponding BGC (**Fig. 25, D**).

On the other hand, screening of the strains *S. tropica* 0777, 2496 and nrps2 showed the apparent deletion of the corresponding genomic regions (**Fig. 25, B, C and E**). As genome editing using CRISPR/Cas9 is marker-less, the obtention of mixed populations of wild-type and mutant cells is to be expected and has been previously reported (Cobb et al., 2015). We obtained such mixed population with the strain *S. tropica* 0777, as PCR screening revealed dual amplicons corresponding both to the correct deletion of the PPTase 0777 and the wild-type genomic region (**Fig. 25, B**). Isolation of the mutant cells from the wild-type population was carried out but unsuccessful. We were able to confirm, however, the successful genomic deletion of the entire *nrps2* gene cluster (> 34 kb deletion) and the PPTase 2496 (501-bp deletion), resulting in the two strains Δnrps2 and Δ2496, respectively (**Fig. 26**; **Table 6**). Regrettably, we worked with a mixed

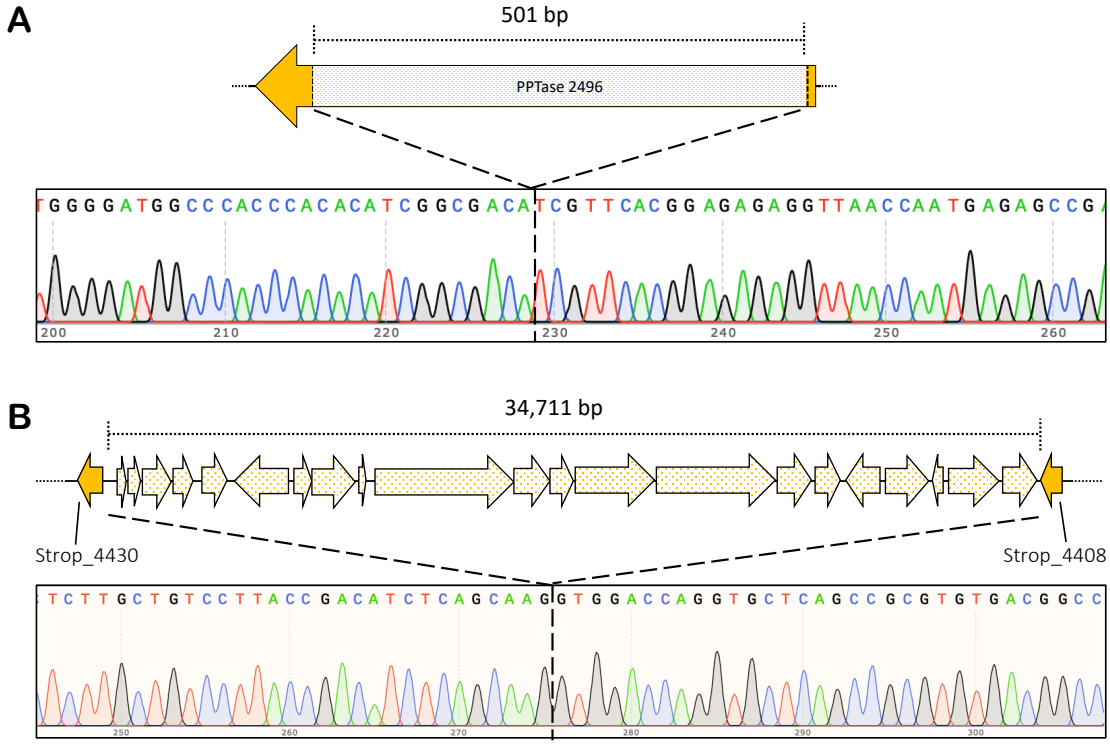

Figure 26 | Genomic deletion of the PPTase 2496 and *nrps2* BGC in *S. tropica*. The deleted regions of the PPTase 2496 **(A)** and the *nrps2* BGC **(B)** are depicted in shaded yellow, with their sizes indicated. Un-modified regions are filled in yellow. Sanger sequencing of the engineered genomic regions issued from the corresponding *S. tropica* Δ2496 and Δnrps2 strains are shown. Dotted lines show the position of the deletion.

population mutant/wild-type of the strain *S. tropica* nrps2, that we did not detect because of our primer design, and subsequent cultures lead to the loss of the recombinant strain. The reasons for the difficulties encountered in isolating the mutants are further discussed below in this Chapter. Meanwhile, the strain *S. tropica* Δ2496 was successfully isolated as a pure culture and used for the ensuing experiments.

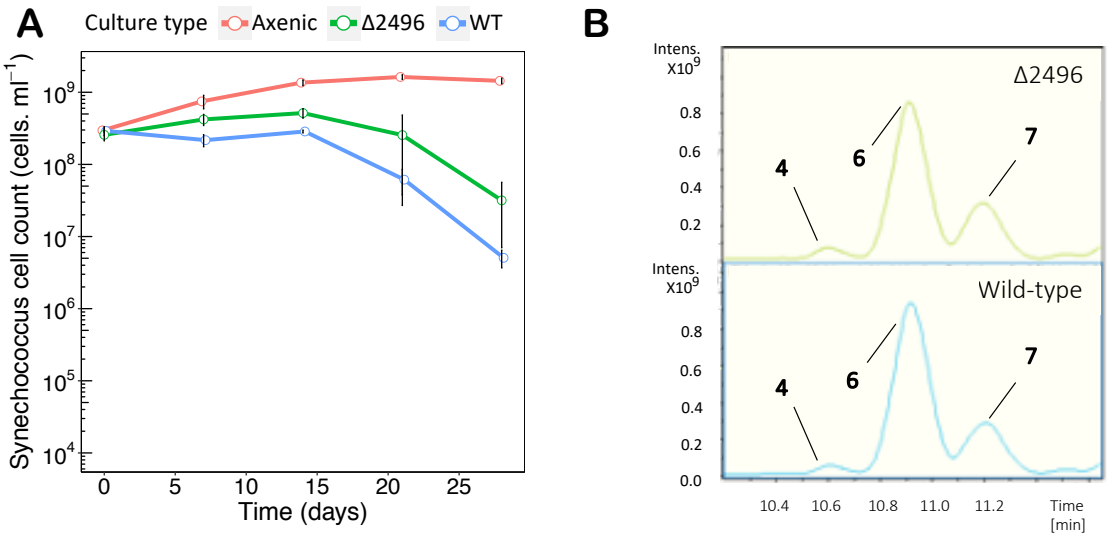

Figure 27 | The mutant strain *S. tropica* Δ2496 has the same antimicrobial activity and metabolome than the wild-type strain. (A) Both the wild-type (blue line) and Δ2496 (green line) *S. tropica* strains inhibit *Synechococcus* growth in co-culture. Graph shows mean ± standard deviation of three biological replicates. **(B)** The production of the cryptic molecules **4**, **6** and **7** is not abolished in the mutant strain *S. tropica* Δ2496. Graph shows extracted ion chromatograms for all three cryptic molecules EIC (464.2; 435.2; 449.2) ± 0.5 in the concentrated supernatants of the *S. tropica* wild-type strain (blue) or the Δ2496 strain (green) grown for 35 days in co-culture with *Synechococcus* in ASW.

Characterization of the *S. tropica* mutant strain Δ2496

Having shown the efficacy of CRISPR/Cas9 to generate knock-out mutants in *S. tropica*, we set out to determine whether the deleted PPTase 2496 could be linked to the biosynthesis of the cryptic molecules and/or the antimicrobial activity observed against phytoplankton (see **Chapter 2**). Interestingly, the gene encoding this PPTase is located within the orphan *pks3* BGC (**Fig. 23, B**), a cluster we have shown to be active that is thought to produce an unidentified spore pigment polyketide (Kersten et al., 2013). Due to this specific location, we hypothesized that the PPTase 2496 was likely to be responsible for the activation of the ACP/PCP domains of the *pks3* BGC, therefore directly impacting the biosynthesis of the *pks3*-encoded compound.

To test this, we first co-inoculated the phototroph *Synechococcus* with either the wild-type strain *S. tropica* CNB-440 or the mutant strain Δ2496 and compared their antimicrobial activity profile (**Fig. 27, A**). The PPTase-deficient mutant was still able to inhibit the growth of the phototroph, suggesting that the PPTase 2496 is not required for the antimicrobial ability of *S. tropica*. We also analyzed by LC-MS crude extracts obtained from the co-culture supernatants, allowing us to detect the cryptic compounds **4**, **6** and **7** produced by the mutant and wild-type strains alike (**Fig. 27, B**). Additionally, we studied their total metabolomes and looked for any differences (*i.e.* loss of molecule) but we could not identify such change. This observation similarly suggested that the deletion of the PPTase 2496 did not influence the secondary metabolism of *S. tropica*.

Considering the absence of differences in phenotype between the wild-type and Δ2496 *S. tropica* strains, we were interested in assessing by proteomics whether deletion of the PPTase 2496 actually prevented activation of the ACPs/PCPs of the *pks3* BGC.

The ACP domain of the *pks3* BGC is not activated only by the PPTase 2496

In order to investigate whether the PPTase 2496 was solely responsible for the activation of the *pks3* cluster, we used proteomics to detect the post-translational modifications of the ACPs/PCPs in the wild-type and mutant *S. tropica* strains. PPTases indeed activate apo-PCP domains into their active holo-form by covalently installing a PPant moiety to a conserved serine. As such, holo-PCPs can be detected in proteomics data by searching for the appropriate peptides bearing the added mass of a PPant group.

For this, we first identified all ACP/PCP domains in *S. tropica's* genome using an HMMER search combined with antiSMASH. The bioinformatic analysis carried out resulted in the detection of 41 putative ACPs/PCPs, of which one was located within the *pks3* cluster (**Fig. 28**). We found, indeed, a single ACP site in the strop_RS12595 gene with the highly conserved serine residue that we expected to be PPTase-modified. Based on the amino-acid sequence of the corresponding protein A4X7U8, we calculated the mass of the predicted peptide to contain the conserved serine residue after tryptic fragmentation (**Fig. 29, A**). Considering no miscleavage of the protein, the 26-amino-acid peptide is expected to weight 2640.3752 Da in its apo-form. Considering the PPTant moiety (*i.e.* 340.0858 Da) as well as the iodoacetamide derivation (*i.e.* 57.0215 Da) used in our sample preparation, we anticipated the mass of the holo-ACP fragment to be 3037.4825

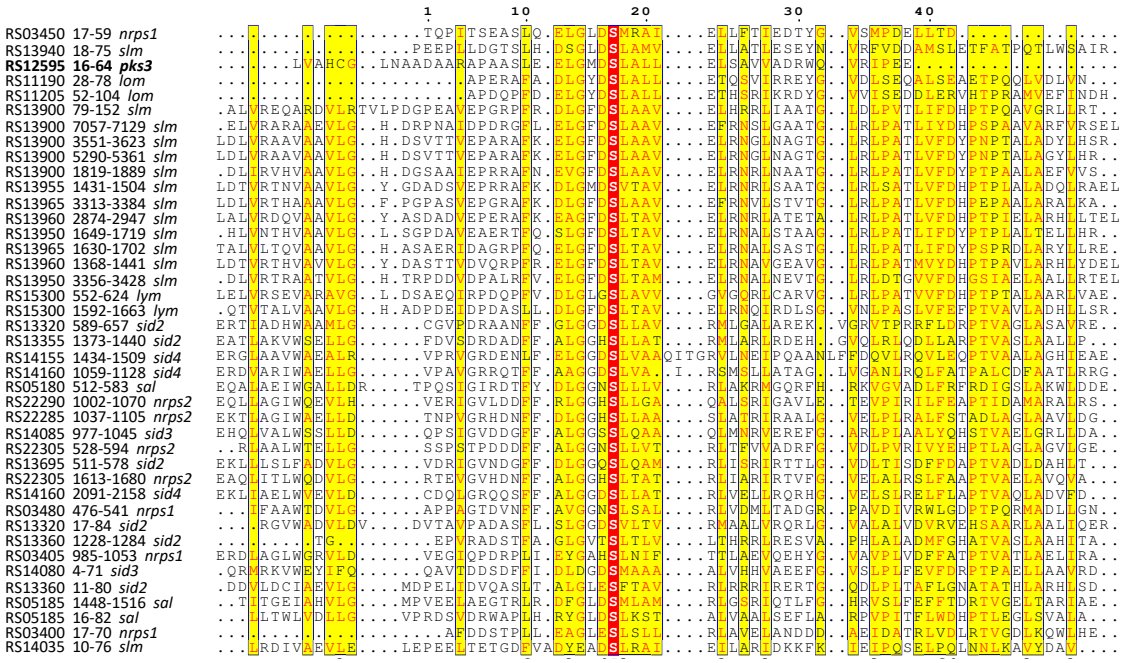

Figure 28 | Identification of putative ACP/PCP sites in *S. tropica*'s genome. Amino-acid sequence alignments of all ACPs/PCPs in *S. tropica* CNB-440. Sequences were identified based on an antiSMASH and HMMER search. The highly conserved serine residue expected to be modified by PPTases is highlighted in red. The ACP domain identified within the *pks3* BGC is in bold. Identifiers show locus name (strop_), ACP/PCP domain position (amino-acid number) and the gene cluster in which the sites are.

Da (**Fig. 29, B**). Finally, we calculated the mass over charge ratio (*m/z*) of the corresponding ions that would effectively be detected by the mass spectrometric instrument. The adducts had *m/z* 1519.7412, 1013.4942, 760.3706 and 608.4965 corresponding to 2, 3, 4 and 5 positive charges, respectively (**Fig. 29, C**).

We generated the proteomes of the wild-type and Δ2496 *S. tropica* strains and we looked for the ACP-peptide belonging to the *pks3* BGC. Surprisingly, we found in both strain its active form bearing the PPant moiety, at a retention time of 38 minutes (**Fig. 30**). The holo-ACP fragment was reliably detected by MS as its corresponding ions were identified for all four charge states calculated **(Fig. 30; Appendix 7**). This observation made in the PPTase 2496-deficient strain indicated that the *pks3*-encoded ACP is modified by functionally redundant PPTases, as its activation appeared independent of the PPTase 2496.

Deletion of the PPTase 2496 impacts the abundance of several *pks3*-encoded proteins

Lastly, we queried the total proteomes of the wild-type and Δ2496 *S. tropica* strains for any differences that may have resulted from the deletion of the PPTase. As expected, we

A

A4X7U8 (strop_RS12595)

MTVTDGRPLAADITDILVAHCGLNAADAAR**APAASLEELGMDSLALLELSAVVADR**WQVRIPEETGQLSIAGVADLVARGV
EPAGHTENDILIAAPLPLVWEVTNDVAGWPDLFTEYAVAEILHREGNTVRFRLTMHPDENGIAWSWVSERTADPDGREV
RAQRVEPGPFEYMRIHWRYVEEAGGTRMIWTQDFAMKTTAPLTNAEMTDRINANSAVQLAVIKEKIERRAAQETGAGDE

B

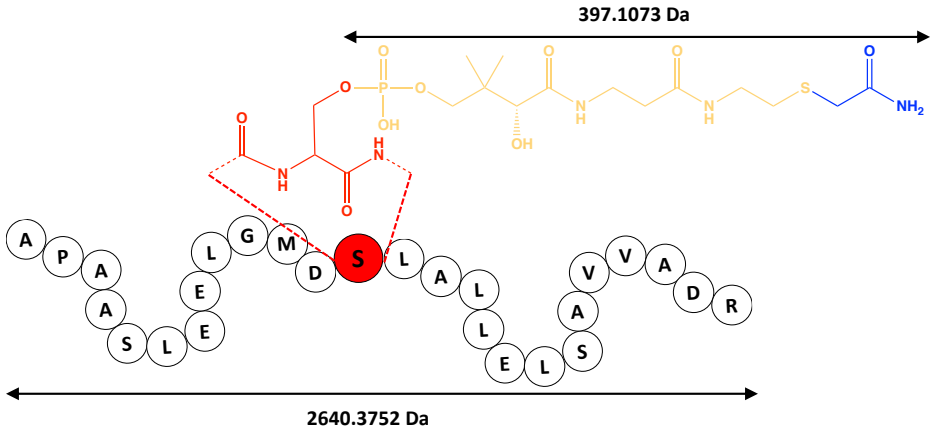

C

No. charges	APAASLEELGMDSLALLELSAVVADR (2640.3752 Da)		
	apo-ACP	**holo-ACP-(PPant)**	**holo-ACP-(PPant-IAA)**
1	2641.3752	2981.4610	**3038.4825**
2	1321.1876	1491.2305	**1519.7412**
3	881.1251	994.4870	**1013.4942**
4	661.0938	746.1153	**760.3706**
5	529.0750	597.0922	**608.4965**

Figure 29 | Mass of the ACP-peptide from the *pks3* BGC estimated for MS detection. (A) Amino-acid sequence of the protein A4X7U8 that belongs to the orphan *pks3* BGC. Sequence of the peptide resulting from tryptic digestion that contains the conserved serine residue (highlighted in red) predicted to bear the PPant moiety is underlined. **(B)** The peptide is also depicted with its serine residue (red) modified with a PPant group (orange) and with the iodoacetamide derivation (blue). **(C)** Calculated masses of the ions corresponding to the holo-ACP peptide derivatized with iodoacetamide (IAA) at different charge states.

found little variations in their proteomes but for five proteins that were downregulated in the mutant strain when grown in SUPSYN (**Fig. 31, A**).

Interestingly, three of these are encoded within the *pks3* BGC (*i.e.* A4X7U0, A4X7T8 and A4X7T5; **Fig. 31, B**). The protein A4X7T1 is most likely also involved in the *pks3* biosynthetic pathway, although not formally described as belonging to the cluster, because its corresponding gene is located directly downstream the BGC and is part of the same transcription unit as the genes encoding the three previously mentioned enzymes (**Fig. 31, B**). While an antiSMASH analysis coupled with a blastP search identified

A4X7U0 and A4X7T8 as core polyketide biosynthetic proteins, the function of A4X7T1 could not be predicted (**Table 7**). Additionally, this protein was the only one to be significantly less abundant in the mutant strain compared to the wild-type when cells were grown in MB (**Fig. 31, A**). The fifth downregulated enzyme A4X6H0 did not belong to any reported BGCs and was also of unknown function (**Table 7**).

The genes encoding the PPTase 2496 and the proteins A4X7U0, A4X7T8, A4X7T5 and A4X7T1 are remarkably oppositely oriented in the same bidirectional operon (**Fig. 31, B**). We therefore hypothesized that the proteins downregulation could be caused by an alteration of the genes' transcription, although the PPTase deletion conserved the entire intergenic region (*i.e.* sequence comprised between *strop_2495* and *strop_2496*) that should contain the bidirectional promoter. In an attempt to verify this, we screened the promoter region of the operon using various tools (*i.e*. GBpro Genome Browser, iPromoter-2L and BPROM) but they failed to identify any bacterial promoters or regulatory elements within the queried sequence. Future work based on

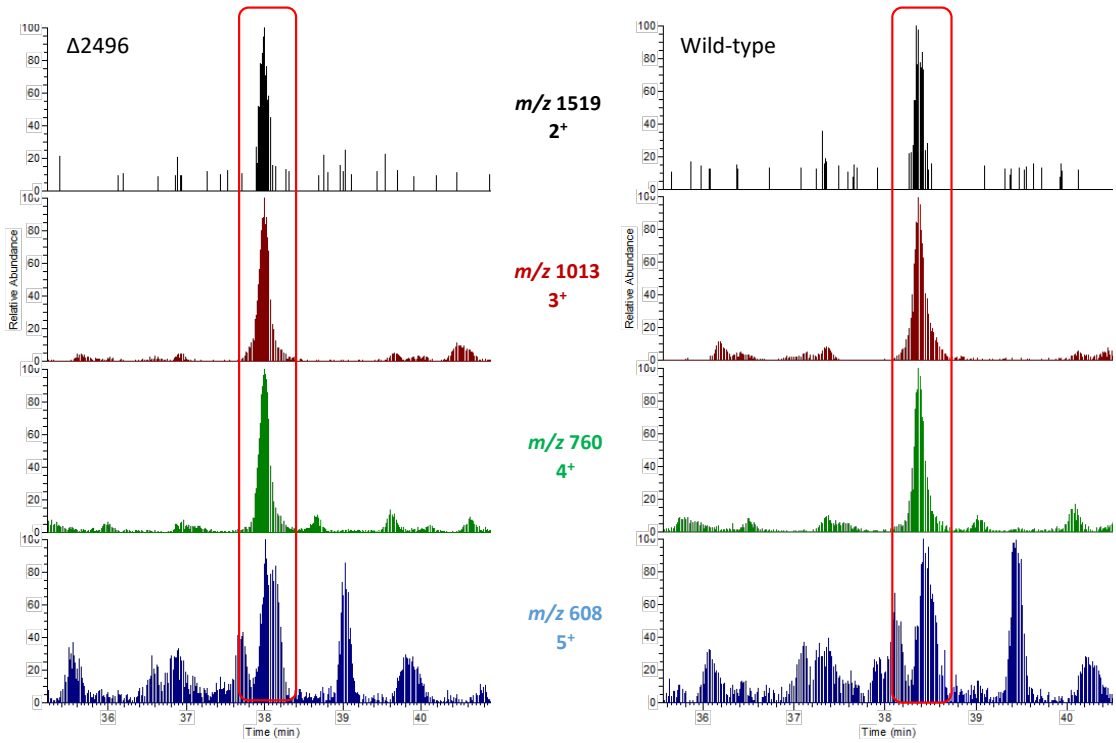

Figure 30 | Deletion of the PPTase 2496 does not abolish activation of the ACP site within the *pks3* BGC. MS analysis detecting the PPTase-modified peptide of protein A4X7U8, at different charge states, in the proteome of the *S. tropica* wild-type strain (Wild-type, right panel) or the ΔPPTase 2496 strain (Δ2496, left panel) grown axenically for 5 days in MB. Chromatograms show mass ranges *m/z* 1519.74-1520.74 (black), 1013.49-1014.49 (red), 760.37-761.37 (green) and 608.49-609.49 (blue).

complementation experiments should be carried out to confirm whether the observed downregulation of the *pks3* encoded proteins is due to a polar effect of the PPTase deletion.

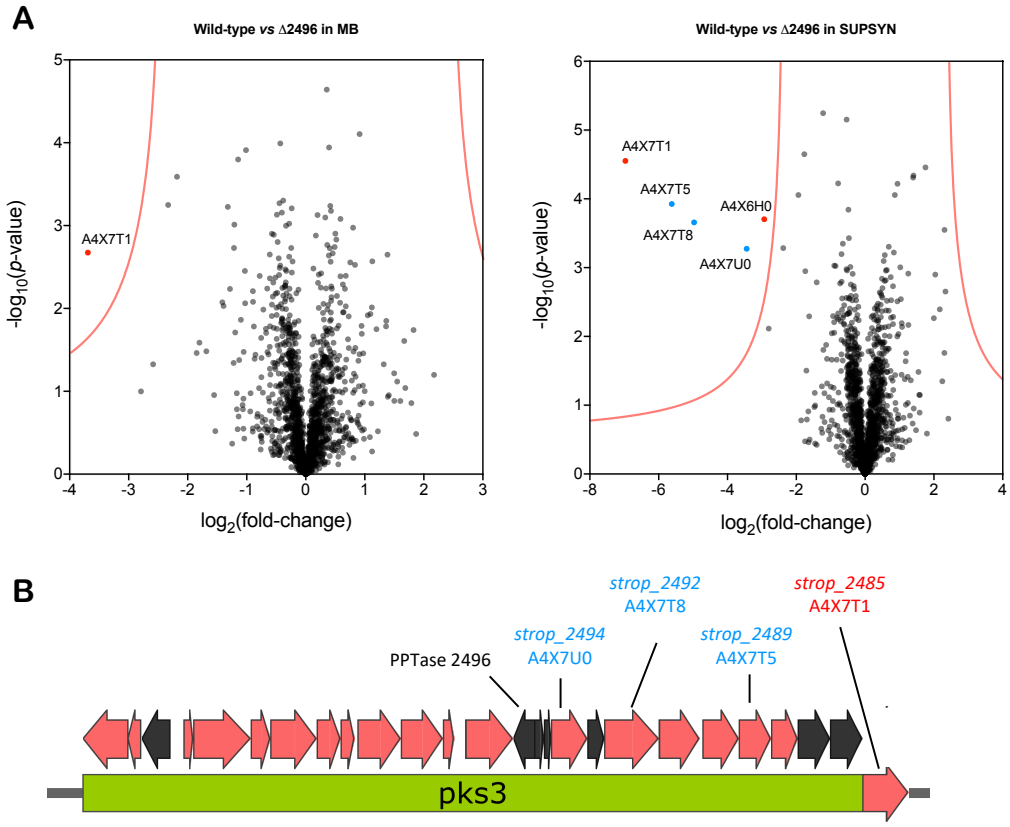

Figure 31 | Several *pks3*-encoded proteins are downregulated in the PPTase 2496-deficient strain. (A) Volcano plots of the comparative proteomic analysis of the *S. tropica* wild-type and ΔPPTase 2496 strains grown for 5 days in marine broth (MB, left panel) or in a phototroph supernatant (SUPSYN, right panel). Red curve represents a false discovery rate (FDR) of 0.05 and s0 of 2. The IDs of significantly differentially expressed proteins are given. These proteins are colored in red or blue if they are encoded within the *pks3* BGC. **(B)** Representation of the *pks3* cluster. Genes are depicted in red if their corresponding proteins were detected in the proteomic dataset. Those that were not detected are depicted in black.

DISCUSSION

We demonstrated for the first time the use of the CRISPR/Cas9 technology to genome engineer the genus *Salinispora.* We successfully deleted the PPTase 2496 and the entire *nrps2* gene cluster, representing more than 34 kb of the *S. tropica* genome (**Fig. 26**). These genomic deletions resulted in the two CRISPR-induced mutant strains Δ2496 and Δnrps2, respectively (**Table 6**).

Obtention of those mutant strains, however, has proven extremely challenging. First, conjugal transfer of plasmids into *S. tropica* failed using already established protocols (Eustáquio & Moore, 2008; Netzker et al., 2016) and required the development of a successful method *via* a lengthy trial and error approach. Based on the observations made from numerous attempts, we hypothesize that antibiotic concentrations, condition of cell mating and spore preparation are some key factors for efficient DNA transfer in *S. tropica*. Employing an auxotrophic donor strain, for instance, allowed us to decrease the amount of antibiotic used for exconjugant selection, which we believe concurrently helped to decrease the metabolic burden and stress on the recombinant cells (Allard et al., 2015). Also, spotting donor and recipient cells for mating increased cell-to-cell contact compared to spreading cells as a layer onto solid medium. Lastly, while the published protocol reports the obtention of spores from only 1 mL of a 3-day old *Salinispora* liquid culture in A1 medium (Eustáquio et al., 2009) we collected a very limited number of spores this way. Instead, we found that growing *Salinispora* as a dense cell lawn onto solid media for 30 days resulted in a far greater number of spores (despite being a longer process), as it is more commonly done with *Streptomyces* species (Shepherd et al., 2010).

Table 7 | Differentially expressed proteins in *S. tropica* Δ2496 *vs* wild-type.

Protein ID	*Homologue* (% identity/% similarity) *Organism* [Protein ID]	Putative function
A4X7U0	***fabF* (34/53) *Bacillus subtilis* [O34340.1]**	**Ketosynthase (KS)[a]**
A4X7T8	***hcl* (25/39) *Thauera aromatica* [Q9AJS8.1]**	**Acyltransferase (AT)[a]**
A4X7T5	*htxA* (27/41) *Pseudomonas stutzeri* [O69060.1]	Ketoglutarate-dependent hypophosphite dioxygenase
A4X7T1	NA[b]	NA
A4X6H0	NA[b]	NA

[a] Core biosynthetic enzyme.
[b] No significant similarity found based on the UniProtKB/SwissProt sequences database.

Although we were able to ultimately obtain a few successful exconjugants using our improved protocol of conjugation, the CRISPR/Cas9 system presented several drawbacks for the generation of mutants in *Salinispora*. The pCRISPomyces-2 vector contains a temperature-sensitive origin of replication allowing plasmid curing when growing cells at 39 °C or above (Cobb et al., 2015) but *S. tropica* does not grow at this temperature.

We have attempted plasmid curing by passaging isolated exconjugants in fresh medium without antibiotic selection for up to five months without success. Experiments described in this manuscript were therefore performed using the mutant *S. tropica* strain still bearing the pCRISPomyces plasmid, which could have impacted the cell fitness as well as caused additional undesired genomic deletions. Additionally, the absence of selection marker for the deletion event leads to the isolation of mixed populations of wild-type and mutant cells (Cobb et al., 2015). Our *S. tropica* ∆nrps2 strain was, for instance, lost through subculturing because of this marker-less editing. The *S. tropica* population bearing the pCRISPomyces-0777 vector was also made of mixed cells (**Fig. 25, B**). Unfortunately, we were unable to isolate a pure culture of the mutant due to the aggregation of *Salinispora* cells as both dense clumps in liquid and tough colonies on solid, preventing us from further characterizing the strain. Future knock-outs will therefore require a better separation technique of exconjugants to obtain pure cultures. Lastly, our difficulties in isolating *nrps1*- and PPTase 0685-deficient cells in any of the corresponding apramycin-resistant exconjugants that we tested, are most likely due to off-target or poor on-target performance of the CRISPR/Cas9 cleavage. This observation highlighted the importance to design multiple synthetic guide RNA for future genome editing attempts, as the efficiency and specificity of the Cas9 endonuclease varies depending on the protospacer target sequences selected (Fu et al., 2014; Graf et al., 2019).

Of the six genomic deletions tested, we finally only obtained the strain *S. tropica* ∆2496 as a pure culture, allowing us to assess its potential involvement in the biosynthesis of the cryptic molecules and/or antimicrobial activity observed against *Synechococcus*. Data revealed that the mutant strain has the same metabolome and killing phenotype as the wild-type *S. tropica* (**Fig. 27**). To understand this, we investigated whether the deleted PPTase 2496 was solely responsible for the activation of the *pks3*-encoded ACP domain we identified through bioinformatic analysis. Using proteomics to detect the post-translational modifications of this ACP site, we showed that it was activated through the addition of a PPant moiety in both the PPTase 2496-deficient and the wild-type strains (**Fig. 30**). PPTases are generally dedicated specifically to the biosynthesis of the molecule produced by the BGC in which their encoding genes are located, or to distinct sets of BGCs (Stanley et al., 2006). It has been previously reported, however, that some

PPTases found outside secondary metabolite clusters can be ambiguously involved in multiple biosynthetic pathways (Bunet et al., 2014). In *S. tropica*, due to its location outside any BGCs, we hypothesize that the PPTase 0777 may play this pleiotropic role and act as a functionally redundant PPTase compensating the absence of the PPTase 2496 in the mutant strain *S. tropica* ∆2496 (**Fig. 23, B**). In order to successfully implement our desired approach for the broad inactivation of diverse BGCs by single PPTase-gene deletion, future work will therefore depend upon the prior knock-out of this putative pleiotropic PPTase 0777. The resulting *S. tropica* ∆0777 mutant could then be used as a starter strain for further genome editing steps, which the marker-less deletions created by CRISPR/Cas9 would facilitate.

Lastly, a comparative analysis of the proteome of the *S. tropica* wild-type and ΔPPTase 2496 strains indicated that several enzymes encoded within the *pks3* gene cluster were significantly downregulated in the mutant (**Fig. 31**). We were unable to verify whether these variations were caused by a polar effect of the PPTase 2496 deletion and complementation experiments should be carried out to confirm this. Interestingly, the difference in abundance of those core biosynthetic enzymes was not reflected in the metabolome or antimicrobial profile of the strains (**Fig. 27**). This observation suggests that the product of the *pks3* BGC is not detected in our experimental setup. It also supports our hypothesis that the cryptic compounds and antimicrobial activity reported in Chapter 2 are not related to *pks3* but rather the *nrps1* cluster.

Additional research efforts will focus on optimizing the conjugal transfer of plasmids in *S. tropica* to obtain better yields. These would involve, for instance, testing different ratios of donor and recipient cells, as well as reducing *Salinispora* clumping for better spore isolation. Also, conjugations of the retargeted pCRISPomyces-2 plasmids will be repeated to delete the PPTases 0685, 0777 and 2822, as well as the two *nrps1* and *nrps2* gene clusters. Analysis of the mutants metabolic and antimicrobial profiles should allow to link the production of the cryptic metabolites with a specific orphan BGC. Ultimately, our study pioneers the application of the CRISPR/Cas9 technology in the genus *Salinispora* and lays the foundation for its use as a potentially faster, marker-less and multiplex genome editing method. This new tool should facilitate and accelerate the study of *Salinispora* for the discovery of novel natural products.

CHAPTER 5 |

FINAL CONCLUSIONS AND FUTURE PERSPECTIVES

The AMR crisis has prompted a tremendous and renewed interest in the discovery of microbially-derived novel bioactive compounds. Exploring the world's oceans has revealed this vast ecosystem as a trove of unique bacterial taxa with promising biosynthetic potential. While they collectively represent a remarkable resource to unearth new natural products, the actual discovery of novel molecules from these microorganisms is limited because most of the BGCs they encode are not expressed under typical laboratory settings. This is certainly true for the marine actinobacterium *Salinispora*, as an astonishing 80% of its BGCs are still orphan.

In Chapter two, we addressed this issue by examining how co-cultivation of *S. tropica* with marine phototrophs could be used to stimulate its biosynthetic activity and impact its metabolome for novel natural product discovery. In Chapter three, we used high-throughput proteomics to provide a better understanding of these co-cultures by identifying candidate BGCs that were up-regulated in response to phytoplankton. Finally, in Chapter four we implemented for the first time the CRISPR/Cas9 system in *S. tropica*, as a promising tool to link specific BGCs to detected molecules and/or observed bioactivity. The main findings and hypotheses resulting from these chapters are depicted in Figure 32.

1. EXPLOITING PHYTOPLANKTON TO AWAKEN SILENT BGCS

Historically, natural product research has heavily relied on growing actinomycetes in monoculture and in nutrient-rich broth. Although fruitful for decades, this approach rapidly showed its limitation as the post-genomic era revealed that the pool of secondary metabolites isolated from actinomycetes represented only a small fraction of the actual biosynthetic capability encoded in their genomes. This derives, in part, from the fact that cultivating microbes in typical laboratory conditions is fundamentally a poor proxy for their natural environments, lacking the myriad of molecular cues required for the induction of their secondary pathways. As most of those signals come from the interactions with other microorganisms, simulating small-scale communities by co-

cultivation of secondary metabolite producers has proven an efficient method to awaken silent BGCs (Abdalla et al., 2017; Bertrand et al., 2014; Yu et al., 2019).

For instance, co-cultivation of the marine-derived fungal *Aspergillus fumigatus* with *Streptomyces leeuwenhoekii* lead to the characterization of the lasso peptide chaxapeptin from the latter species (Wakefield et al., 2017). The BGC encoding the compound had been previously identified by genomic analysis two years prior but its product was not detected when *S. leeuwenhoekii* was grown in monoculture (Gomez-Escribano et al., 2015). In another study, production of the antibiotics istamycin from the marine bacterium *Streptomyces tenjimariensis* was shown to increase upon exposure to twelve different bacterial species, which were sensitive to the antimicrobial compound (Slattery et al., 2001). This observation interestingly suggested the ecological role of istamycin as a mean to subdue competitive species.

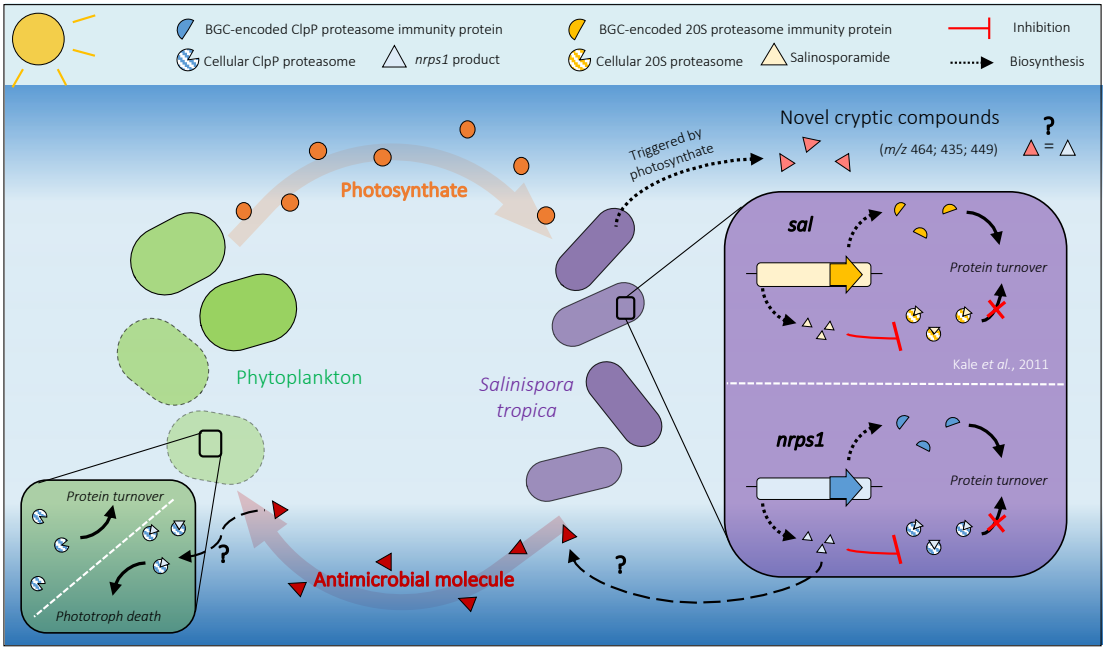

Figure 32 | Interaction of *Salinispora tropica* with phytoplankton. Marine phototrophs release photosynthate that triggers the biosynthesis of novel cryptic metabolites in *S. tropica*. *S. tropica* produces an unknown antimicrobial molecule that kills phytoplankton. The proposed mechanism of the antimicrobial metabolite as well as the activity of the *nrps1* product are depicted (green and purple boxes, respectively). We hypothesize that the BGC *nrps1* may produce a ClpP-proteasome inhibitor, to which *S. tropica* would be resistant because of an immunity protein encoded within the BGC, similarly to what is known for *sal*/salinosporamide. The *nrps1*-encoded proteasome inhibitor could kill the phototrophs by preventing protein turnover, leading to cell death.

In *Salinispora*, co-culture has been employed but failed so far to result in the discovery of novel natural products from the genus. Co-inoculation of *S. arenicola* with the marine fungus *Emericella* sp. induced production of the emericellamide compound in the latter species only (Oh et al., 2007). More recently, Patin and colleagues showed that *S. arenicola* and *S. tropica* strains exhibited antimicrobial activities against various marine heterotrophs (Patin et al., 2018, 2016, 2017). Although some of these interactions were found to be caused by already known bioactive compounds (*e.g.* siderophores), several of those were mediated by an uncharacterized mechanism and overall no new natural product was identified (Patin et al., 2016). In a following manuscript, the interactions between *S. tropica* CNY-681 and several heterotrophs were further explored by MS/MS networking analysis (Patin et al., 2018). The networks generated revealed unknown molecular families unique to the co-cultures but they were either (i) not proven to be produced by *S. tropica* rather than the co-inoculated heterotroph or (ii) related to the already characterized siderophore desferrioxamine E (Patin et al., 2018). These studies, however, provided a valuable insight on the ecological significance of the genus *Salinispora* and of its role within benthic microbial communities (Patin et al., 2017).

The work presented in Chapter two expands our understanding of the impact that the *Salinispora* genus has on the complex microbial communities inhabiting the seas. Using metabolomics, we characterized the production of cryptic metabolites in the type strain *Salinispora tropica* CNB-440^{T} in response to the presence of a range of prokaryotic and eukaryotic phytoplankton species. Molecules with identical *m/z* were never reported in the literature and they were also distinct from the molecular families described by Patin et al. when *S. tropica* was grown with marine heterotrophs (Patin et al., 2018). This finding confirms the overlooked potential of co-culturing *Salinispora* specifically with phytoplankton to elicit the production of novel secondary metabolites. We also showed that *S. tropica* intriguingly inhibits the growth of these marine phototrophs *via* a mechanism we could not link to the cryptic compounds (**Fig. 32**). This observation is of significance as a growing body of evidence suggests that members of the genus *Salinispora* may be more exposed to phytoplankton than what was previously thought, whether because they sediment out of the water column, grow in sunlit coastal sediments or belong to the same coral-associated microbiota (Guidi et al., 2016; Ocampo-Alvarez et al., 2020; Patin et al., 2017).

Understanding the ecological context of the producer organisms is becoming crucial for natural product discovery, as improving our knowledge of the interactions occurring in their environments allows to uncover the specific cues that trigger the expression of silent BGCs (Adnani et al., 2017; Behie et al., 2017; van der Meij et al., 2017). For instance, work by Onaka et al. demonstrated that the mycolic acid contained in the outer cell layer of different bacteria induced production of a red pigment in various *Streptomyces* species (Onaka et al., 2011). Such examples were also reported from the seas, as a study led by Seyedsayamdost et al. showed that the marine proteobacterium *Phaeobacter gallaeciensis* inhibits the growth of the microalgae *E. huxleyi* in co-culture by producing the algaecidal molecule roseobacticide (Seyedsayamdost et al., 2011). Interestingly, they were able to demonstrate that the production of this bioactive secondary metabolite was dependent on p-coumaric acid, a compound characteristic of aging algae that accumulates when they reach stationary phase. P-coumaric acid acted as a chemical cues that specifically triggered the otherwise silent biosynthetic pathway of roseobacticide, therefore controlling the dynamics of *P. gallaeciensis*-*E. huxleyi* interactions (Seyedsayamdost et al., 2011).

In our study, the requirement of photosynthate for the detection of the cryptic molecules comes with a set of challenges that future work should address. First, the vast diversity of phototrophic microbes found in the world's oceans should be explored and tested in co-culture with marine actinobacteria to investigate the extent of their potential to induce silent BGCs. Second, most of those phytoplankton can be arduous to grow in the laboratory and as such, efforts should be directed toward the improvement of cultivation media and techniques for marine phototrophs. For example, supporting the growth of the cyanobacteria *Synechococcus* in large volumes turned out to be one of the major limitations in our attempt to elucidate the structure of our cryptic compounds by NMR. Concurrently, future research should focus on identifying the exact chemical signals of photosynthate that prompt the production of the cryptic compounds in our co-culture system. If the specific compounds were to be identified, it could facilitate the isolation and characterization of novel natural products, as exemplified by the discovery of the algaecidal roseobacticide molecule linked to p-coumaric acid (Seyedsayamdost et al., 2011). One could, for instance, extract or chemically synthesize versions of the inducing compounds to elicit the expression of silent BGCs in *Salinispora,* or other marine

actinobacteria, grown in large scales without the need of phototrophs. Finally, our data warrants a broader investigation of the true ecological niches of members of the genus *Salinispora* and of their study *in situ* as a mean to harvest new bioactive secondary metabolites.

2. EXPLOITING -OMICS TO GAIN INSIGHT ON BIOSYNTHETIC ACTIVITY

The advent of next-generation sequencing technologies, coupled with bioinformatics pipelines such as antiSMASH, have propelled the use of genome mining of BGCs for natural product discovery. The amount of data that has resulted from these extensive mining efforts is colossal, as they have, to date, led to the identification of more than 300,000 putative BGCs, of which less than 0.5% are experimentally verified (Blin et al., 2019; Medema et al., 2011; Palaniappan et al., 2020). The overwhelming wealth of available genomic data at our disposal requires to establish methods to prioritize the study of orphan BGCs. One way consists of identifying the BGCs that are effectively silent (due to a poor or conditional level of expression or inactivation of their biosynthetic genes) from those simply producing compounds that are difficult to detect and isolate (due to compound instability, limited sensitivity of detection methods or absence of bioactivity to screen for). As genomic-based approaches alone do not allow such discernment, other -omics technologies are instrumental for the discovery of novel natural products (Palazzotto & Weber, 2018).

In *Salinispora*, bioinformatic analysis of the draft genomes of 119 strains predicted 176 distinct BGCs, of which 80% are still orphan (Letzel et al., 2017). This is exemplified in the type strain *S. tropica* CNB-440^{T}, which encodes in its genome at least twenty putative BGCs and only nine have been assigned to a natural product so far. Based on the sequences of these orphan BGCs alone, it is difficult to prioritize and identify promising clusters for natural product discovery. A recent work led by Amos and colleagues used comparative transcriptomics of different *Salinispora* species to isolate the molecule salinipostin, as well as identify seven transcriptionally silent BGCs (Amos et al., 2017). This study was the first to investigate the transcriptome of *Salinispora* to obtain information on the genus clusters beyond genomic approaches. It was done, however, solely on strains of *Salinispora* growing axenically in rich broth, therefore providing

limited information on the actual biosynthetic activity profile that the actinobacterium may have in its natural environment. Additionally, transcriptomics typically depicts an imprecise vision of an organism metabolism, because the level of transcription of a given gene is an approximate estimate of its protein expression level (*i.e.* mRNA degradation, poor translation efficiency, post-translational modifications etc.). Meanwhile, proteomics approaches have proven successful to discover new secondary metabolites and link them to their corresponding BGCs (Du & van Wezel, 2018). For instance, a proteomining concept based on quantitative proteomics used the correlations between abundance of natural products or antimicrobial activity and concurrent variations in the bacterium proteome to identify the matching gene cluster (Gubbens et al., 2014).

In Chapter three, we employed for the first time a proteomic-based approach in the genus *Salinispora* to identify candidate biosynthetic pathways that could be responsible for the production of the cryptic compounds and/or the antimicrobial activity described in our co-culture study. By using state-of-the-art high-throughput proteomics, we reported the activity of orphan BGCs that were previously thought to be silent in *S. tropica*. In particular, we provided evidence suggesting that the *nrps1* BGC is upregulated when this actinobacterium is exposed to phytoplankton and discussed a potential mechanism for the antimicrobial effect of *S. tropica* upon marine phototrophs (**Fig. 29**). Our proteomic analysis generated promising hypotheses that further experimental work will confirm, such as inactivation of the candidate BGCs. Also, as our data suggested several orphans BGCs to be expressed (*e.g. pks3*, *nrps1* and *nrps2*) that may be producing secondary metabolites undetected in our experimental setup, different analytical chemistry methods must be explored in order to characterize the products of these potentially active BGCs. Additional research efforts should extend our study to other species of the genus *Salinispora*, as well as testing various growth conditions and media. Looking into the proteomes of the phytoplankton we co-inoculated with *S. tropica* could also be of interest as it could reveal important clues to understand the nature of their interactions. Overall, employing proteomics in a more systematic way when examining marine actinobacteria should dramatically improve our understanding of their biosynthetic potential to uncover novel natural products.

3. BETTER TOOLS TO ENGINEER MARINE ACTINOBACTERIA

As mentioned above, genome- or proteome-based approaches alone do not always allow the isolation of new compounds. Whether it is because identified orphans BGCs are silent or encoding undetectable molecules, altering the genome of producing strains can be crucial for natural products discovery and is widely used in *Streptomyces* species. For instance, inactivating a transcriptional repressor encoded within a silent gene cluster using CRISPR/Cas9 resulted in the production of scleric acid in *Streptomyces albus* (Alberti et al., 2019). In *Salinispora*, however, very few examples of genetic engineering have been reported in the literature, but they are all based upon integrative vectors and PCR-targeted mutagenesis. In order to investigate the salt requirement of the genus, the integrative plasmid pSET152 was used to introduce the *mscL* gene at the pseudo-attB phage attachment sites present in the genome of *S. tropica* (Bucarey et al., 2012). The λ-Red-mediated recombination method was also employed to chromosomally replace the *salL* chlorinase gene of the *sal* BGC with a fluorinase gene *flA,* leading to the production of fluorosalinosporamide (Eustáquio et al., 2011). In all cases, generation of the recombinant strains of *Salinispora* suffered from several disadvantages. It either relied on a single cross-over event that lacks stability, integrated selectable markers that limits the number of genomic modifications possible or required relatively time-consuming additional steps to obtain marker-free mutants (Datsenko & Wanner, 2000; Gust et al., 2003; Kieser et al., 2000). Conversely, the CRISPR/Cas9 technology has been applied successfully in soil actinobacteria for rapid generation of marker-less and stable double cross-over mutants but has yet to be used in *Salinispora* (Alberti et al., 2019; Jinek et al., 2012).

In Chapter four, we implemented for the first time the marker-less and multiplex genome editing method CRISPR/Cas9 in *S. tropica*, deleting successfully the entire *nrps2* BGC, as well as the PPTase 2496. The analysis by proteomics of the post-translational modifications of the ACPs/PCPs in the *S. tropica* PPTase-deficient strain suggested the functional redundancy of the PPTase 0777, providing a clear indication of the next steps to be carried out to test our strategy. Future work should, indeed, delete the PPTase 0777 in order to use the resulting recombinant cell as a starter strain for further genome editing of the remaining PPTases. Ultimately, we believe that disruption of these broad-specificity enzymes represents a promising way to inactivate multiple BGCs *via* single

gene deletion. Focussing on groups of BGCs, rather than working at the individual BGC scale, when using genetic engineering could greatly facilitate the prioritization and screening of orphan BGCs.

The many challenges we have faced while attempting the different genetic modifications of *S. tropica* highlighted the urgency with which we need to develop better genome engineering tools for marine actinobacteria. Most of these microbes are currently difficult to cultivate in the laboratory or genetically intractable, which hampers our ability to exploit efficiently their biosynthetic potential for natural product discovery. For instance, key factors for the efficient transfer of DNA in marine actinobacteria should be identified for the establishment of robust and reproducible methods. More globally, sets of molecular biology tools must be created for these marine bacteria (*e.g.* inducible promoters, regulators etc.). For instance, no replicative plasmids have been formally reported to function in the genus *Salinispora*, although we believe the pCRISPomyces-2 vector was able to propagate in our cells based on the isolation of apramycin-resistant exconjugants. Collectively, the development of these currently lacking means to manipulate and interrogate the biosynthetic ability of these rare actinomycetes that are found in the oceans could lead to boundless improvements in our search for novel natural product.

REFERENCES

Abdalla, M. A., Sulieman, S., & McGaw, L. J. (2017). **Microbial communication: A significant approach for new leads**. *South African Journal of Botany*, *113*, 461–470. https://doi.org/10.1016/j.sajb.2017.10.001

Abdelmohsen, U. R., Grkovic, T., Balasubramanian, S., Kamel, M. S., Quinn, R. J., & Hentschel, U. (2015). **Elicitation of secondary metabolism in actinomycetes**. *Biotechnology Advances*, *33*(6), 798–811. https://doi.org/10.1016/j.biotechadv.2015.06.003

Adnani, N., Rajski, S. R., & Bugni, T. S. (2017). **Symbiosis-inspired approaches to antibiotic discovery**. *Natural Product Reports*, *34*(7), 784–814. https://doi.org/10.1039/c7np00009j

Ahmed, L., Jensen, P. R., Freel, K. C., Brown, R., Jones, A. L., Kim, B. Y., & Goodfellow, M. (2013). **Salinispora pacifica sp. nov., an actinomycete from marine sediments**. *Antonie van Leeuwenhoek, International Journal of General and Molecular Microbiology*, *103*(5), 1069–1078. https://doi.org/10.1007/s10482-013-9886-4

Alberti, F., Leng, D. J., Wilkening, I., Song, L., Tosin, M., & Corre, C. (2019). **Triggering the expression of a silent gene cluster from genetically intractable bacteria results in scleric acid discovery**. *Chemical Science*, *10*(2), 453–463. https://doi.org/10.1039/c8sc03814g

Allard, N., Garneau, D., Poulin-Laprade, D., Burrus, V., Brzezinski, R., & Roy, S. (2015). **A diaminopimelic acid auxotrophic *Escherichia coli* donor provides improved counterselection following intergeneric conjugation with actinomycetes**. *Canadian Journal of Microbiology*, *61*(8), 565–574. https://doi.org/10.1139/cjm-2015-0041

Aminov, R. I. (2010). **A brief history of the antibiotic era: Lessons learned and challenges for the future**. *Frontiers in Microbiology*, *1*, 1–7. https://doi.org/10.3389/fmicb.2010.00134

Amos, G. C. A., Awakawa, T., Tuttle, R. N., Letzel, A. C., Kim, M. C., Kudo, Y., Fenical, W., Moore, B. S., & Jensen, P. R. (2017). **Comparative transcriptomics as a guide to natural product discovery and biosynthetic gene cluster functionality**. *Proceedings of the National Academy of Sciences of the United States of America*, *114*(52), E11121–E11130. https://doi.org/10.1073/pnas.1714381115

Andersson, F. I., Tryggvesson, A., Sharon, M., Diemand, A. V., Classen, M., Best, C., Schmidt, R., Schelin, J., Stanne, T. M., Bukau, B., Robinson, C. V., Witt, S., Mogk, A., & Clarke, A. K. (2009). **Structure and function of a novel type of ATP-dependent Clp protease**. *Journal of Biological Chemistry*, *284*(20), 13519–13532. https://doi.org/10.1074/jbc.M809588200

Asolkar, R., Freel, K., Jensen, P., Fenical, W., Kondratyuk, T., Park, E.-J., & Pezzuto JM. (2009). **Arenamides A - C , Cytotoxic NF K B Inhibitors from the Marine Actinomycete Salinispora.** *72*, 396–402. https://doi.org/10.1021/np800617a

Asolkar, R., Kirkland, T. N., Jensen, P. R., & Fenical, W. (2010). **Arenimycin, an antibiotic effective against rifampin- and methicillin-resistant Staphylococcus aureus from the marine actinomycete Salinispora arenicola**. *The Journal of Antibiotics*, *63*(1), 37–39. https://doi.org/10.1038/ja.2009.114

Awakawa, T., Crüsemann, M., Munguia, J., Ziemert, N., Nizet, V., Fenical, W., & Moore,

B. S. (2015). **Salinipyrone and Pacificanone Are Biosynthetic By-products of the Rosamicin Polyketide Synthase**. *ChemBioChem*, *16*(10), 1443–1447. https://doi.org/10.1002/cbic.201500177

Baltz, R. H. (2008). **Renaissance in antibacterial discovery from actinomycetes**. *Current Opinion in Pharmacology*, *8*(5), 557–563. https://doi.org/10.1016/j.coph.2008.04.008

Baltz, R. H. (2019). **Natural product drug discovery in the genomic era: realities, conjectures, misconceptions, and opportunities**. *Journal of Industrial Microbiology and Biotechnology*, *46*(3–4), 281–299. https://doi.org/10.1007/s10295-018-2115-4

Bauermeister, A., Velasco-alzate, K., Dias, T., Macedo, H., Walsh, D. A., & Findlay, B. (2018). **Metabolomic Fingerprinting of Salinispora From Atlantic Oceanic Islands.** *9*(December), 1–13. https://doi.org/10.3389/fmicb.2018.03021

Becker, S. H., & Darwin, K. H. (2017). **Bacterial Proteasomes: Mechanistic and Functional Insights.** *81*(1), 1–20. https://doi.org/https://doi.org/10.1128/MMBR.00036-16

Behie, S. W., Bonet, B., Zacharia, V. M., McClung, D. J., & Traxler, M. F. (2017). **Molecules to ecosystems: Actinomycete natural products in situ**. *Frontiers in Microbiology*, *7*(2149), 1–11. https://doi.org/10.3389/fmicb.2016.02149

Beld, J., Sonnenschein, E. C., Vickery, C. R., Noel, J. P., & Burkart, M. D. (2014). **The phosphopantetheinyl transferases: Catalysis of a post-translational modification crucial for life**. *Natural Product Reports*, *31*(1), 61–108. https://doi.org/10.1039/c3np70054b

Bentley, S. D., Chater, K. F., Cerdeño-Tárraga, A. M., Challis, G. L., Thomson, N. R., James, K. D., Harris, D. E., Quail, M. A., Kieser, H., Harper, D., Bateman, A., Brown, S., Chandra, G., Chen, C. W., Collins, M., Cronin, A., Fraser, A., Goble, A., Hidalgo, J., … Hopwood, D. A. (2002). **Complete genome sequence of the model actinomycete Streptomyces coelicolor A3(2)**. *Nature*, *417*(6885), 141–147. https://doi.org/10.1038/417141a

Bérdy, J. (2005). **Bioactive Microbial Metabolites**. *The Journal of Antibiotics*, *58*(1), 1–26. https://doi.org/10.1038/ja.2005.1.

Bérdy, J. (2012). **Thoughts and facts about antibiotics: Where we are now and where we are heading**. *Journal of Antibiotics*, *65*(8), 385–395. https://doi.org/10.1038/ja.2012.27

Bertrand, S., Bohni, N., Schnee, S., Schumpp, O., Gindro, K., & Wolfender, J. L. (2014). **Metabolite induction via microorganism co-culture: A potential way to enhance chemical diversity for drug discovery**. *Biotechnology Advances*, *32*(6), 1180–1204. https://doi.org/10.1016/j.biotechadv.2014.03.001

Blin, K., Pedersen, L. E., Weber, T., & Lee, S. Y. (2016). **CRISPy-web: An online resource to design sgRNAs for CRISPR applications**. *Synthetic and Systems Biotechnology*, *1*(2), 118–121. https://doi.org/10.1016/j.synbio.2016.01.003

Blin, K., Shaw, S., Steinke, K., Villebro, R., Ziemert, N., Lee, S. Y., Medema, M. H., & Weber, T. (2019). **AntiSMASH 5.0: Updates to the secondary metabolite genome mining pipeline**. *Nucleic Acids Research*, *47*(W1), W81–W87. https://doi.org/10.1093/nar/gkz310

Bonet, B., Teufel, R., Crüsemann, M., Ziemert, N., & Moore, B. S. (2015). **Direct capture and heterologous expression of salinispora natural product genes for the biosynthesis of enterocin**. *Journal of Natural Products*, *78*(3), 539–542. https://doi.org/10.1021/np500664q

Bose, U., Hodson, M. P., Shaw, P. N., Fuerst, J. A., & Hewavitharana, A. K. (2014). **Bacterial production of the fungus-derived cholesterol-lowering agent mevinolin**. *Biomedical Chromatography*, *28*(9), 1163–1166. https://doi.org/10.1002/bmc.3138

Bose, U., Ortori, C. A., Sarmad, S., Barrett, D. A., Hewavitharana, A. K., Hodson, M. P., Fuerst, J. A., & Shaw, P. N. (2017). **Production of N-acyl homoserine lactones by the sponge-associated marine actinobacteria Salinispora arenicola and Salinispora pacifica**. *FEMS Microbiology Letters*, *364*(2), 1–7. https://doi.org/10.1093/femsle/fnx002

Brown, E. D., & Wright, G. D. (2016). **Antibacterial drug discovery in the resistance era**. *Nature*, *529*(7586), 336–343. https://doi.org/10.1038/nature17042

Bruns, H., Crüsemann, M., Letzel, A. C., Alanjary, M., McInerney, J. O., Jensen, P. R., Schulz, S., Moore, B. S., & Ziemert, N. (2018). **Function-related replacement of bacterial siderophore pathways**. *ISME Journal*, *12*(2), 320–329. https://doi.org/10.1038/ismej.2017.137

Bucarey, S. A., Penn, K., Paul, L., Fenical, W., & Jensen, P. R. (2012). **Genetic complementation of the obligate marine actinobacterium Salinispora tropica with the large mechanosensitive channel gene mscl rescues cells from osmotic downshock**. *Applied and Environmental Microbiology*, *78*(12), 4175–4182. https://doi.org/10.1128/AEM.00577-12

Buchanan, G. O., Williams, P. G., Feling, R. H., Kauffman, C. A., Jensen, P. R., & Fenical, W. (2005). **Sporolides A and B: Structurally unprecedented halogenated macrolides from the marine actinomycete Salinispora tropica**. *Organic Letters*, *7*(13), 2731–2734. https://doi.org/10.1021/ol050901i

Bull, A. T., & Goodfellow, M. (2019). **Dark, rare and inspirational microbial matter in the extremobiosphere: 16 000 m of bioprospecting campaigns**. *Microbiology (United Kingdom)*, *165*(12), 1252–1264. https://doi.org/10.1099/mic.0.000822

Bumpus, S. B., Evans, B. S., Thomas, P. M., Ntai, I., & Kelleher, N. L. (2009). **A proteomics approach to discovering natural products and their biosynthetic pathways**. *Nature Biotechnology*, *27*(10), 951–956. https://doi.org/10.1038/nbt.1565

Bunet, R., Riclea, R., Laureti, L., Hôtel, L., Paris, C., Girardet, J. M., Spiteller, D., Dickschat, J. S., Leblond, P., & Aigle, B. (2014). **A single Sfp-type phosphopantetheinyl transferase plays a major role in the biosynthesis of PKS and NRPS derived metabolites in Streptomyces ambofaciens ATCC23877**. *PLoS ONE*, *9*(1), 1–12. https://doi.org/10.1371/journal.pone.0087607

Carlet, J., Collignon, P., Goldmann, D., Goossens, H., Gyssens, I. C., Harbarth, S., Jarlier, V., Levy, S. B., N'Doye, B., Pittet, D., Richtmann, R., Seto, W. H., Van Der Meer, J. W., & Voss, A. (2011). **Society's failure to protect a precious resource: Antibiotics**. *The Lancet*, *378*(9788), 369–371. https://doi.org/10.1016/S0140-6736(11)60401-7

Castro-Falcón, G., Hahn, D., Reimer, D., & Hughes, C. C. (2016). **Thiol Probes to Detect Electrophilic Natural Products Based on Their Mechanism of Action**. *ACS Chemical Biology*, *11*(8), 2328–2336. https://doi.org/10.1021/acschembio.5b00924

Chen, Y., Unger, M., Ntai, I., McClure, R. A., Albright, J. C., Thomson, R. J., & Kelleher, N. L. (2013). **Gobichelin A and B: Mixed-ligand siderophores discovered using proteomics**. *MedChemComm*, *4*(1), 233–238. https://doi.org/10.1039/c2md20232h

Christie-Oleza, J. A., & Armengaud, J. (2010). **In-depth analysis of exoproteomes from marine bacteria by shotgun liquid chromatography-tandem mass spectrometry:**

The Ruegeria pomeroyi DSS-3 case-study. *Marine Drugs*, *8*(8), 2223–2239. https://doi.org/10.3390/md8082223

Christie-Oleza, J. A., Armengaud, J., Guerin, P., & Scanlan, D. J. (2015). **Functional distinctness in the exoproteomes of marine Synechococcus**. *Environmental Microbiology*, *17*(10), 3781–3794. https://doi.org/10.1111/1462-2920.12822

Christie-Oleza, J. A., Sousoni, D., Lloyd, M., Armengaud, J., & Scanlan, D. J. (2017). **Nutrient recycling facilitates long-term stability of marine microbial phototroph-heterotroph interactions**. *Nature Microbiology*, *2*(June), 17100. https://doi.org/10.1038/nmicrobiol.2017.100

Chua, K., Laurent, F., Coombs, G., Grayson, M. L., & Howden, B. P. (2011). **Not community-associated methicillin-resistant Staphylococcus aureus (CA-MRSA)! A clinician's guide to community MRSA - Its evolving antimicrobial resistance and implications for therapy**. *Clinical Infectious Diseases*, *52*(1), 99–114. https://doi.org/10.1093/cid/ciq067

Coates, A. R., Halls, G., & Hu, Y. (2011). **Novel classes of antibiotics or more of the same?** *British Journal of Pharmacology*, *163*(1), 184–194. https://doi.org/10.1111/j.1476-5381.2011.01250.x

Cobb, R. E., Wang, Y., & Zhao, H. (2015). **High-Efficiency Multiplex Genome Editing of Streptomyces Species Using an Engineered CRISPR/Cas System**. *ACS Synthetic Biology*, *4*(6), 723–728. https://doi.org/10.1021/sb500351f

Colomb-Cotinat, M., Lacoste, J., Brun-Buisson, C., Jarlier, V., Coignard, B., & Vaux, S. (2016). **Estimating the morbidity and mortality associated with infections due to multidrug-resistant bacteria (MDRB), France, 2012**. *Antimicrobial Resistance and Infection Control*, *5*(1). https://doi.org/10.1186/s13756-016-0154-z

Corre, C., Song, L., O'Rourke, S., Chater, K. F., & Challis, G. L. (2008). **2-Alkyl-4-hydroxymethylfuran-3-carboxylic acids, antibiotic production inducers discovered by Streptomyces coelicolor genome mining**. *Proceedings of the National Academy of Sciences of the United States of America*, *105*(45), 17510–17515. https://doi.org/10.1073/pnas.0805530105

Cox, J., Hein, M. Y., Luber, C. A., Paron, I., Nagaraj, N., & Mann, M. (2014). **Accurate proteome-wide label-free quantification by delayed normalization and maximal peptide ratio extraction, termed MaxLFQ**. *Molecular and Cellular Proteomics*, *13*(9), 2513–2526. https://doi.org/10.1074/mcp.M113.031591

Cox, J., & Mann, M. (2008). **MaxQuant enables high peptide identification rates, individualized p.p.b.-range mass accuracies and proteome-wide protein quantification**. *Nature Biotechnology*, *26*(12), 1367–1372. https://doi.org/10.1038/nbt.1511

Crawford, L. J., Walker, B., & Irvine, A. E. (2011). **Proteasome inhibitors in cancer therapy**. *Journal of Cell Communication and Signaling*, *5*(2), 101–110. https://doi.org/10.1007/s12079-011-0121-7

Cross, T. (1981). **Aquatic Actinomycetes: A Critical Survey of the Occurrence, Growth and Role of Actinomycetes in Aquatic Habitats**. *Journal of Applied Bacteriology*, *50*(3), 397–423. https://doi.org/10.1111/j.1365-2672.1981.tb04245.x

Cui, L., & Su, X. Z. (2009). **Discovery, mechanisms of action and combination therapy of artemisinin**. *Expert Review of Anti-Infective Therapy*, *7*(8), 999–1013. https://doi.org/10.1586/ERI.09.68

Culp, E., & Wright, G. D. (2017). **Bacterial proteases, untapped antimicrobial drug**

targets. *Journal of Antibiotics*, *70*(4), 366–377. https://doi.org/10.1038/ja.2016.138

da Silva, A. B., Pinto, F. C. L., Silveira, E. R., Costa-Lotufo, L. V., Costa, W. S., Ayala, A. P., Canuto, K. M., Barros, A. B., Araújo, A. J., Marinho Filho, J. D. B., & Pessoa, O. D. L. (2019). **4-Hydroxy-pyran-2-one and 3-hydroxy-N-methyl-2-oxindole derivatives of Salinispora arenicola from Brazilian marine sediments**. *Fitoterapia*, *138*(August), 104357. https://doi.org/10.1016/j.fitote.2019.104357

Da Silva, A. B., Silveira, E. R., Wilke, D. V., Ferreira, E. G., Costa-Lotufo, L. V., Torres, M. C. M., Ayala, A. P., Costa, W. S., Canuto, K. M., De Araújo-Nobre, A. R., Araújo, A. J., Filho, J. D. B. M., & Pessoa, O. D. L. (2019). **Antibacterial Salinaphthoquinones from a Strain of the Bacterium Salinispora arenicola Recovered from the Marine Sediments of St. Peter and St. Paul Archipelago, Brazil**. *Journal of Natural Products*, *82*(7), 1831–1838. https://doi.org/10.1021/acs.jnatprod.9b00062

Darken, M. A., Berenson, H., Shirk, R. J., & Sjolander, N. O. (1960). **Production of tetracycline by Streptomyces aureofaciens in synthetic media.** *Applied Microbiology*, *8*(1954), 46–51. https://doi.org/10.1128/aem.8.1.46-51.1960

Datsenko, K. A., & Wanner, B. L. (2000). **One-step inactivation of chromosomal genes in Escherichia coli K-12 using PCR products.** *Proceedings of the National Academy of Sciences of the United States of America*, *97*(12), 6640–6645. https://doi.org/10.1073/pnas.120163297

de Kraker, M. E. A., Stewardson, A. J., & Harbarth, S. (2016). **Will 10 Million People Die a Year due to Antimicrobial Resistance by 2050?** *PLoS Medicine*, *13*(11), 1–6. https://doi.org/10.1371/journal.pmed.1002184

De Oliveira, D. M. P., Forde, B. M., Kidd, T. J., Harris, P. N. A., Schembri, M. A., Beatson, S. A., Paterson, D. L., & Walker, M. J. (2020). **Antimicrobial Resistance in ESKAPE Pathogens**. *Clinical Microbiology Reviews*, *33*(3), 1–49. https://doi.org/10.1128/CMR.00181-19

Demain, A. L., & Sanchez, S. (2009). **Microbial drug discovery: 80 Years of progress**. *Journal of Antibiotics*, *62*(1), 5–16. https://doi.org/10.1038/ja.2008.16

Denora, N., Potts, B., & Stella, V. (2007). **A Mechanistic and Kinetic Study of the b-Lactone Hydrolysis of Salinosporamide A (NPI-0052), A Novel Proteasome Inhibitor**. *Journal of Pharmaceutical Sciences*, *96*(8), 2037–2047. https://doi.org/10.1002/jps

Dias, D. A., Urban, S., & Roessner, U. (2012). **A Historical overview of natural products in drug discovery**. *Metabolites*, *2*(2), 303–336. https://doi.org/10.3390/metabo2020303

Du, C., & van Wezel, G. P. (2018). **Mining for Microbial Gems: Integrating Proteomics in the Postgenomic Natural Product Discovery Pipeline**. *Proteomics*, *18*(18), 1–10. https://doi.org/10.1002/pmic.201700332

Dulmage, H. T. (1953). **The production of neomycin by Streptomyces fradiae in synthetic media.** *Applied Microbiology*, *1*(2), 103–106. https://doi.org/10.1128/aem.1.2.103-106.1953

Duncan, K. R., Crüsemann, M., Lechner, A., Sarkar, A., Li, J., Ziemert, N., Wang, M., Bandeira, N., Moore, B. S., Dorrestein, P. C., & Jensen, P. R. (2015). **Molecular networking and pattern-based genome mining improves discovery of biosynthetic gene clusters and their products from salinispora species**. *Chemistry and Biology*, *22*(4), 460–471. https://doi.org/10.1016/j.chembiol.2015.03.010

Eustáquio, A. S., McGlinchey, R. P., Liu, Y., Hazzard, C., Beer, L. L., Florova, G.,

Alhamadsheh, M. M., Lechnera, A., Kale, A. J., Kobayashi, Y., Reynolds, K. A., & Moore, B. S. (2009). **Biosynthesis of the salinosporamide A polyketide synthase substrate chloroethylmalonyl-coenzyme A from S-adenosyl- L -methionine**. *Proceedings of the National Academy of Sciences*, *106*(12). https://doi.org/https://doi.org/10.1073/pnas.0901237106

Eustáquio, S., & Moore, B. S. (2008). **Mutasynthesis of fluorosalinosporamide, a potent and reversible inhibitor of the proteasome**. *Angewandte Chemie - International Edition*, *47*(21), 3936–3938. https://doi.org/10.1002/anie.200800177

Eustáquio, S., Nam, S. J., Penn, K., Lechner, A., Wilson, M. C., Fenical, W., Jensen, P. R., & Moore, B. S. (2011). **The discovery of salinosporamide K from the marine bacterium "Salinispora pacifica" by Genome mining gives insight into pathway evolution**. *ChemBioChem*, *12*(1), 61–64. https://doi.org/10.1002/cbic.201000564

Eustáquio, S., O'Hagan, D., & Moore, B. S. (2010). **Engineering fluorometabolite production: Fluorinase expression in salinispora tropica yields fluorosalinosporamide**. *Journal of Natural Products*, *73*(3), 378–382. https://doi.org/10.1021/np900719u

Feling, R. H., Buchanan, G. O., Mincer, T. J., Kauffman, C. A., Jensen, P. R., Fenical, W., & John, D. (2003). **Salinosporamide A: A highly cytotoxic proteasome inhibitor from a novel microbial source, a marine bacterium of the new genus Salinospora**. *Angewandte Chemie - International Edition*, *42*(3), 355–357. https://doi.org/10.1002/anie.200390115

Fenical, W., & Jensen, P. R. (2006). **Developing a new resource for drug discovery : marine actinomycete bacteria.** *2*(12), 666–673. https://doi.org/10.1038/nchembio841

Fischbach, M. A., & Walsh, C. T. (2006). **Assembly-line enzymology for polyketide and nonribosomal peptide antibiotics: Logic machinery, and mechanisms**. *Chemical Reviews*, *106*(8), 3468–3496. https://doi.org/10.1021/cr0503097

Fleming, A. (1929). **On the antibacterial action of cultures of a penicillium, with special reference to their use in the isolation of B. influenzae.** *The British Journal of Experimental Pathology*, *10*(3), 226–236.

Fu, Y., Sander, J. D., Reyon, D., Cascio, V. M., & Joung, J. K. (2014). **Improving CRISPR-Cas nuclease specificity using truncated guide RNAs**. *Nature Biotechnology*, *32*(3), 279–284. https://doi.org/10.1038/nbt.2808

Genilloud, O. (2017). **Actinomycetes: Still a source of novel antibiotics**. *Natural Product Reports*, *34*(10), 1203–1232. https://doi.org/10.1039/c7np00026j

Gomez-Escribano, J. P., Castro, J. F., Razmilic, V., Chandra, G., Andrews, B., Asenjo, J. A., & Bibb, M. J. (2015). **The Streptomyces leeuwenhoekii genome: De novo sequencing and assembly in single contigs of the chromosome, circular plasmid pSLE1 and linear plasmid pSLE2**. *BMC Genomics*, *16*(1), 1–11. https://doi.org/10.1186/s12864-015-1652-8

Graf, R., Li, X., Chu, V. T., & Rajewsky, K. (2019). **sgRNA Sequence Motifs Blocking Efficient CRISPR/Cas9-Mediated Gene Editing**. *Cell Reports*, *26*(5), 1098-1103.e3. https://doi.org/10.1016/j.celrep.2019.01.024

Greunke, C., Glöckle, A., Antosch, J., & Gulder, T. A. M. (2017). **Biocatalytic Total Synthesis of Ikarugamycin**. *Angewandte Chemie - International Edition*, *56*(15), 4351–4355. https://doi.org/10.1002/anie.201611063

Gubbens, J., Zhu, H., Girard, G., Song, L., Florea, B. I., Aston, P., Ichinose, K., Filippov, D.

V., Choi, Y. H., Overkleeft, H. S., Challis, G. L., & Van Wezel, G. P. (2014). **Natural product proteomining, a quantitative proteomics platform, allows rapid discovery of biosynthetic gene clusters for different classes of natural products**. *Chemistry and Biology*, *21*(6), 707–718. https://doi.org/10.1016/j.chembiol.2014.03.011

Guidi, L., Chaffron, S., Bittner, L., Eveillard, D., Larhlimi, A., Roux, S., Darzi, Y., Audic, S., Berline, L., Brum, J. R., Coelho, L. P., Espinoza, J. C. I., Malviya, S., Sunagawa, S., Dimier, C., Kandels-Lewis, S., Picheral, M., Poulain, J., Searson, S., … Gorsky, G. (2016). **Plankton networks driving carbon export in the oligotrophic ocean**. *Nature*, *532*(7600), 465–470. https://doi.org/10.1038/nature16942

Guillard, R. (1975). **Culture of phytoplankton for feeding marine invertebrates**. *Culture of Marine Invertebrate Animals*, 29–60.

Gulder, T. A. M., & Moore, B. S. (2010). **Salinosporamide natural products: Potent 20 S proteasome inhibitors as promising cancer chemotherapeutics**. *Angewandte Chemie - International Edition*, *49*(49), 9346–9367. https://doi.org/10.1002/anie.201000728

Gust, B., Challis, G. L., Fowler, K., Kieser, T., & Chater, K. F. (2003). **PCR-targeted Streptomyces gene replacement identifies a protein domain needed for biosynthesis of the sesquiterpene soil odor geosmin**. *Proceedings of the National Academy of Sciences*, *100*(4). https://doi.org/https://doi.org/10.1073/pnas.0337542100

Harrison, S. J., Mainwaring, P., Price, T., Millward, M. J., Padrik, P., Underhill, C. R., Cannell, P. K., Reich, S. D., Trikha, M., & Spencer, A. (2016). **Phase i clinical trial of marizomib (NPI-0052) in patients with advanced malignancies including multiple myeloma: Study NPI-0052-102 final results**. *Clinical Cancer Research*, *22*(18), 4559–4566. https://doi.org/10.1158/1078-0432.CCR-15-2616

He, H., Ding, W. D., Bernan, V. S., Richardson, A. D., Ireland, C. M., Greenstein, M., Ellestad, G. A., & Carter, G. T. (2001). **Lomaiviticins A and B, potent antitumor antibiotics from Micromonospora lomaivitiensis [8]**. *Journal of the American Chemical Society*, *123*(22), 5362–5363. https://doi.org/10.1021/ja010129o

Janso, J. E., Haltli, B. A., Eustáquio, A. S., Kulowski, K., Waldman, A. J., Zha, L., Nakamura, H., Bernan, V. S., He, H., Carter, G. T., Koehn, F. E., & Balskus, E. P. (2014). **Discovery of the lomaiviticin biosynthetic gene cluster in Salinispora pacifica**. *Tetrahedron*, *70*(27–28), 4156–4164. https://doi.org/10.1016/j.tet.2014.03.009

Jensen, P. R., Dwight, R., & Fenical, W. (1991). **Distribution of actinomycetes in near-shore tropical marine sediments**. *Applied and Environmental Microbiology*, *57*(4), 1102–1108. https://doi.org/10.1128/aem.57.4.1102-1108.1991

Jensen, P. R., Gontang, E., Mafnas, C., Mincer, T. J., & Fenical, W. (2005). **Culturable marine actinomycete diversity from tropical Pacific Ocean sediments**. *Environmental Microbiology*, *7*(7), 1039–1048. https://doi.org/10.1111/j.1462-2920.2005.00785.x

Jensen, P. R., & Mafnas, C. (2006). **Biogeography of the marine actinomycete Salinispora.** *Environmental Microbiology*, *8*(11), 1881–1888. https://doi.org/10.1111/j.1462-2920.2006.01093.x

Jensen, P. R., Williams, P. G., Oh, D. C., Zeigler, L., & Fenical, W. (2007). **Species-specific secondary metabolite production in marine actinomycetes of the genus Salinispora**. *Applied and Environmental Microbiology*, *73*(4), 1146–1152. https://doi.org/10.1128/AEM.01891-06

Jensen, P. R, Moore, B. S., & Fenical, W. (2015). **The marine actinomycete genus Salinispora : a model organism for secondary metabolite discovery**. *Natural Product Reports*, *32*, 738–751. https://doi.org/10.1039/C4NP00167B

Jinek, M., Chylinski, K., Fonfara, I., Hauer, M., Doudna, J. A., & Charpentier, E. (2012). **A Programmable Dual-RNA–Guided DNA Endonuclease in Adaptive Bacterial Immunity.** *337*(August), 816–822. https://doi.org/10.1126/science.1225829

Jones, B. M., Iglesias-Rodriguez, M. D., Skipp, P. J., Edwards, R. J., Greaves, M. J., Young, J. R., Elderfield, H., & O'Connor, C. D. (2013). **Responses of the Emiliania huxleyi Proteome to Ocean Acidification**. *PLoS ONE*, *8*(4). https://doi.org/10.1371/journal.pone.0061868

Kale, A. J., McGlinchey, R. P., Lechner, A., & Moore, B. S. (2011). **Bacterial self-resistance to the natural proteasome inhibitor salinosporamide A**. *ACS Chemical Biology*, *6*(11), 1257–1264. https://doi.org/10.1021/cb2002544

Kersten, R. D., Lane, A. L., Nett, M., Richter, T. K. S., Duggan, B. M., Dorrestein, P. C., & Moore, B. S. (2013). **Bioactivity-Guided Genome Mining Reveals the Lomaiviticin Biosynthetic Gene Cluster in Salinispora tropica**. *ChemBioChem*, *14*(8), 955–962. https://doi.org/10.1002/cbic.201300147

Khayatt, B. I., Overmars, L., Siezen, R. J., & Francke, C. (2013). **Classification of the Adenylation and Acyl-Transferase Activity of NRPS and PKS Systems Using Ensembles of Substrate Specific Hidden Markov Models**. *PLoS ONE*, *8*(4). https://doi.org/10.1371/journal.pone.0062136

Kim, J. H., Komatsu, M., Shin-ya, K., Omura, S., & Ikeda, H. (2018). **Distribution and functional analysis of the phosphopantetheinyl transferase superfamily in *Actinomycetales* microorganisms**. *Proceedings of the National Academy of Sciences*, *115*(26), 6828–6833. https://doi.org/10.1073/pnas.1800715115

Kim, T. K., Hewavitharana, A. K., Shaw, P. N., & Fuerst, J. A. (2006). **Discovery of a New Source of Rifamycin Antibiotics in Marine Sponge Actinobacteria by Phylogenetic Prediction**. *Applied and Environmental Microbiology*, *72*(3), 2118–2125. https://doi.org/10.1128/AEM.72.3.2118

Kirstein, J., Hoffmann, A., Lilie, H., Schmidt, R., Helga, R. W., Heike, B. O., Mogk, A., & Turgay, K. (2009). **The antibiotic ADEP reprogrammes CIP, switching it from a regulated to an uncontrolled protease**. *EMBO Molecular Medicine*, *1*(1), 37–49. https://doi.org/10.1002/emmm.200900002

Lambalot, R. H., Gehring, A. M., Flugel, R. S., Zuber, P., LaCelle, M., Marahiel, M. A., Reid, R., Khosla, C., & Walsh, C. T. (1996). **A new enzyme superfamily - The phosphopantetheinyl transferases**. *Chemistry and Biology*, *3*(11), 923–936. https://doi.org/10.1016/S1074-5521(96)90181-7

Letzel, A. C., Li, J., Amos, G. C. A., Millán-Aguiñaga, N., Ginigini, J., Abdelmohsen, U. R., Gaudêncio, S. P., Ziemert, N., Moore, B. S., & Jensen, P. R. (2017). **Genomic insights into specialized metabolism in the marine actinomycete Salinispora**. *Environmental Microbiology*, *19*(9), 3660–3673. https://doi.org/10.1111/1462-2920.13867

Macherla, V. R., Mitchell, S. S., Manam, R. R., Reed, K. A., Chao, T. H., Nicholson, B., Deyanat-Yazdi, G., Mai, B., Jensen, P. R., Fenical, W. F., Neuteboom, S. T. C., Lam, K. S., Palladino, M. A., & Potts, B. C. M. (2005). **Structure-activity relationship studies of salinosporamide A (NPI-0052), a novel marine derived proteasome inhibitor**. *Journal of Medicinal Chemistry*, *48*(11), 3684–3687.

https://doi.org/10.1021/jm048995+

Madeira, F., Park, Y. M., Lee, J., Buso, N., Gur, T., Madhusoodanan, N., Basutkar, P., Tivey, A. R. N., Potter, S. C., Finn, R. D., & Lopez, R. (2019). **The EMBL-EBI search and sequence analysis tools APIs in 2019**. *Nucleic Acids Research*, *47*(W1), W636–W641. https://doi.org/10.1093/nar/gkz268

Maldonado, L. A., Fenical, W., Jensen, P. R., Kauffman, C. A., Mincer, T. J., Ward, A. C., Bull, A. T., & Goodfellow, M. (2005). **Salinispora arenicola gen. nov., sp. nov. and Salinispora tropica sp. nov., obligate marine actinomycetes belonging to the family Micromonosporaceae**. *International Journal of Systematic and Evolutionary Microbiology*, *55*(5), 1759–1766. https://doi.org/10.1099/ijs.0.63625-0

Manivasagan, P., Kang, K. H., Sivakumar, K., Li-Chan, E. C. Y., Oh, H. M., & Kim, S. K. (2014). **Marine actinobacteria: An important source of bioactive natural products**. *Environmental Toxicology and Pharmacology*, *38*(1), 172–188. https://doi.org/10.1016/j.etap.2014.05.014

Manivasagan, P., Venkatesan, J., Sivakumar, K., & Kim, S. K. (2014). **Pharmaceutically active secondary metabolites of marine actinobacteria**. *Microbiological Research*, *169*(4), 262–278. https://doi.org/10.1016/j.micres.2013.07.014

McMurry, J. E. (2009). **Secondary Metabolites:An Introduction To Natural Product Chemistry**. *Organic Chemistry: With Biological Applications*, 1016–1046.

Medema, M. H., Blin, K., Cimermancic, P., De Jager, V., Zakrzewski, P., Fischbach, M. A., Weber, T., Takano, E., & Breitling, R. (2011). **AntiSMASH: Rapid identification, annotation and analysis of secondary metabolite biosynthesis gene clusters in bacterial and fungal genome sequences**. *Nucleic Acids Research*, *39*(SUPPL. 2), 339–346. https://doi.org/10.1093/nar/gkr466

Medema, M. H., Kottmann, R., Yilmaz, P., Cummings, M., Biggins, J. B., Blin, K., De Bruijn, I., Chooi, Y. H., Claesen, J., Coates, R. C., Cruz-Morales, P., Duddela, S., Düsterhus, S., Edwards, D. J., Fewer, D. P., Garg, N., Geiger, C., Gomez-Escribano, J. P., Greule, A., … Glöckner, F. O. (2015). **Minimum Information about a Biosynthetic Gene cluster**. *Nature Chemical Biology*, *11*(9), 625–631. https://doi.org/10.1038/nchembio.1890

Millan-Aguinaga, N., Chavarria, K. L., Ugalde, J. A., Letzel, A.-C., Rouse, G. W., & Jensen, P. R. (2017). **Phylogenomic Insight into Salinispora (Bacteria, Actinobacteria) Species Designations**. *Scientific Reports*, *7*(1), 3564. https://doi.org/10.1038/s41598-017-02845-3

Mincer, T. J., Jensen, P. R., Kauffman, C. a, & Fenical, W. (2002). **Widespread and Persistent Populations of a Major New Marine Actinomycete Taxon in Ocean Sediments Widespread and Persistent Populations of a Major New Marine Actinomycete Taxon in Ocean Sediments**. *Applied and Environmental Microbiology*, *68*(10), 5005–5011. https://doi.org/10.1128/AEM.68.10.5005

Miyanaga, A., Janso, J. E., McDonald, L., He, M., Liu, H., Barbieri, L., Eustáquio, A. S., Fielding, E. N., Carter, G. T., Jensen, P. R., Feng, X., Leighton, M., Koehn, F. E., & Moore, B. S. (2011). **Discovery and assembly-line biosynthesis of the lymphostin pyrroloquinoline alkaloid family of mtor inhibitors in salinispora bacteria**. *Journal of the American Chemical Society*, *133*(34), 13311–13313. https://doi.org/10.1021/ja205655w

Molinski, T. F., Dalisay, D. S., Lievens, S. L., & Saludes, J. P. (2009). **Drug development from marine natural products**. *Nature Reviews Drug Discovery*, *8*(1), 69–85.

https://doi.org/10.1038/nrd2487

Momose, I., & Kawada, M. (2016). **The therapeutic potential of microbial proteasome inhibitors**. *International Immunopharmacology*, *37*, 23–30. https://doi.org/10.1016/j.intimp.2015.11.013

Mootz, H. D., Schwarzer, D., & Marahiel, M. A. (2000). **Construction of hybrid peptide synthetases by module and domain fusions**. *Proceedings of the National Academy of Sciences of the United States of America*, *97*(11), 5848–5853. https://doi.org/10.1073/pnas.100075897

Moreno-Cinos, C., Goossens, K., Salado, I. G., Van Der Veken, P., De Winter, H., & Augustyns, K. (2019). **ClpP protease, a promising antimicrobial target**. *International Journal of Molecular Sciences*, *20*(9). https://doi.org/10.3390/ijms20092232

Mungan, M. D., Alanjary, M., Blin, K., Weber, T., Medema, M. H., & Ziemert, N. (2020). **ARTS 2.0: feature updates and expansion of the Antibiotic Resistant Target Seeker for comparative genome mining**. *Nucleic Acids Research*, *48*(May), 546–552. https://doi.org/10.1093/nar/gkaa374

Murphy, B. T., Narender, A. T., Kauffman, A. C. A., Woolery, M., Jensen, A. P. R., & A, W. F. (2010). **Saliniquinones A – F , New Members of the Highly Cytotoxic Anthraquinone-γ-Pyrones from the Marine Actinomycete Salinispora arenicola.** *63*(6), 929–934. https://doi.org/10.1071/CH10068

Navarro-Muñoz, J. C., Selem-Mojica, N., Mullowney, M. W., Kautsar, S. A., Tryon, J. H., Parkinson, E. I., De Los Santos, E. L. C., Yeong, M., Cruz-Morales, P., Abubucker, S., Roeters, A., Lokhorst, W., Fernandez-Guerra, A., Cappelini, L. T. D., Goering, A. W., Thomson, R. J., Metcalf, W. W., Kelleher, N. L., Barona-Gomez, F., & Medema, M. H. (2020). **A computational framework to explore large-scale biosynthetic diversity**. *Nature Chemical Biology*, *16*(1), 60–68. https://doi.org/10.1038/s41589-019-0400-9

Nett, M., & Moore, B. S. (2009). **Exploration and engineering of biosynthetic pathways in the marine actinomycete Salinispora tropica**. *Pure and Applied Chemistry*, *81*(6), 1075–1084. https://doi.org/10.1351/PAC-CON-08-08-08

Netzker, T., Schroeckh, V., Gregory, M. A., Flak, M., Krespack, M. K. C., Leadlay, P. F., & Brakhage, A. A. (2016). **An Efficient Method To Generate Gene Deletion Mutants of the**. *Applied and Environmental Microbiology*, *82*(12), 3481–3492. https://doi.org/10.1128/AEM.00371-16.Editor

Newman, D. J., & Cragg, G. M. (2016). **Natural Products as Sources of New Drugs from 1981 to 2014**. *Journal of Natural Products*, *79*(3), 629–661. https://doi.org/10.1021/acs.jnatprod.5b01055

Ng, Y. K., Hewavitharana, A. K., Webb, R., Shaw, P. N., & Fuerst, J. A. (2013). **Developmental cycle and pharmaceutically relevant compounds of Salinispora actinobacteria isolated from Great Barrier Reef marine sponges**. *Applied Microbiology and Biotechnology*, *97*(7), 3097–3108. https://doi.org/10.1007/s00253-012-4479-0

O'Neill, J. (2014). **Antimicrobial Resistance: Tackling a crisis for the health and wealth of nations** *The Review on Antimicrobial Resistance Chaired*. *December*.

Ocampo-Alvarez, H., Meza-Canales, I. D., Mateos-Salmón, C., Rios-Jara, E., Rodríguez-Zaragoza, F. A., Robles-Murguía, C., Muñoz-Urias, A., Hernández-Herrera, R. M., Choix-Ley, F. J., & Becerril-Espinosa, A. (2020). **Diving Into Reef Ecosystems for Land-Agriculture Solutions: Coral Microbiota Can Alleviate Salt Stress During**

Germination and Photosynthesis in Terrestrial Plants. *Frontiers in Plant Science*, *11*(May), 1–14. https://doi.org/10.3389/fpls.2020.00648

Oh, D. C., Gontang, E. A., Kauffman, C. A., Jensen, P. R., & Fenical, W. (2008). **Salinipyrones and pacificanones, mixed-precursor polyketides from the marine actinomycete Salinispora pacifica**. *Journal of Natural Products*, *71*(4), 570–575. https://doi.org/10.1021/np0705155

Oh, D. C., Kauffman, C. A., Jensen, P. R., & Fenical, W. (2007). **Induced production of emericellamides A and B from the marine-derived fungus Emericella sp. in competing co-culture**. *Journal of Natural Products*, *70*(4), 515–520. https://doi.org/10.1021/np060381f

Oh, D. C., Williams, P. G., Kauffman, C. A., Jensen, P. R., & Fenical, W. (2006). **Cyanosporasides A and B, chloro- and cyano-cyclopenta[a]indene glycosides from the marine actinomycete "Salinispora pacifica."** *Organic Letters*, *8*(6), 1021–1024. https://doi.org/10.1021/ol052686b

Onaka, H. (2017). **Novel antibiotic screening methods to awaken silent or cryptic secondary metabolic pathways in actinomycetes**. *The Journal of Antibiotics*, *70*(8), 865–870. https://doi.org/10.1038/ja.2017.51

Onaka, H., Mori, Y., Igarashi, Y., & Furumai, T. (2011). **Mycolic acid-containing bacteria induce natural-product biosynthesis in Streptomyces species**. *Applied and Environmental Microbiology*, *77*(2), 400–406. https://doi.org/10.1128/AEM.01337-10

Owens, R. A., Hammel, S., Sheridan, K. J., Jones, G. W., & Doyle, S. (2014). **A proteomic approach to investigating gene cluster expression and secondary metabolite functionality in Aspergillus fumigatus**. *PLoS ONE*, *9*(9). https://doi.org/10.1371/journal.pone.0106942

Palaniappan, K., Chen, I. M. A., Chu, K., Ratner, A., Seshadri, R., Kyrpides, N. C., Ivanova, N. N., & Mouncey, N. J. (2020). **IMG-ABC v.5.0: An update to the IMG/Atlas of Biosynthetic Gene Clusters Knowledgebase**. *Nucleic Acids Research*, *48*(D1), D422–D430. https://doi.org/10.1093/nar/gkz932

Palazzotto, E., & Weber, T. (2018). **Omics and multi-omics approaches to study the biosynthesis of secondary metabolites in microorganisms**. *Current Opinion in Microbiology*, *45*, 109–116. https://doi.org/10.1016/j.mib.2018.03.004

Patin, N., Floros, D., Hughes, C. C., Dorrestein, P., & Jensen, P. (2018). **The role of inter-species interactions in Salinispora specialized metabolism**. *Microbiology*, *164*(7), 946–955. https://doi.org/10.1099/mic.0.000679

Patin, N. V., Duncan, K. R., Dorrestein, P. C., & Jensen, P. R. (2016). **Competitive strategies differentiate closely related species of marine actinobacteria**. *The ISME Journal*, *10*(2), 478–490. https://doi.org/10.1038/ismej.2015.128

Patin, N. V., Schorn, M., Aguinaldo, K., Lincecum, T., Moore, B. S., & Jensen, P. R. (2017). **Effects of actinomycete secondary metabolites on sediment microbial communities**. *Applied and Environmental Microbiology*, *83*(4), 1–16. https://doi.org/10.1128/AEM.02676-16

Penn, K., Jenkins, C., Nett, M., Udwary, D. W., Gontang, E. A., McGlinchey, R. P., Foster, B., Lapidus, A., Podell, S., Allen, E. E., Moore, B. S., & Jensen, P. R. (2009). **Genomic islands link secondary metabolism to functional adaptation in marine Actinobacteria**. *ISME Journal*, *3*(10), 1193–1203. https://doi.org/10.1038/ismej.2009.58

Penn, K., & Jensen, P. R. (2012). **Comparative genomics reveals evidence of marine adaptation in Salinispora species**. *BMC Genomics*, *13*(1), 1–12. https://doi.org/10.1186/1471-2164-13-86

Pereira, F. (2019). **Have marine natural product drug discovery efforts been productive and how can we improve their efficiency?** *Expert Opinion on Drug Discovery*, *14*(8), 717–722. https://doi.org/10.1080/17460441.2019.1604675

Pham, J. V., Yilma, M. A., Feliz, A., Majid, M. T., Maffetone, N., Walker, J. R., Kim, E., Cho, H. J., Reynolds, J. M., Song, M. C., Park, S. R., & Yoon, Y. J. (2019). **A review of the microbial production of bioactive natural products and biologics**. *Frontiers in Microbiology*, *10*, 1–27. https://doi.org/10.3389/fmicb.2019.01404

Probert, I., & Houdan, A. (2004). **The Laboratory Culture of Coccolithophores**. *Coccolithophores*, 217–249. https://doi.org/10.1007/978-3-662-06278-4_9

Reed, K. A., Manam, R. R., Mitchell, S. S., Xu, J., Teisan, S., Chao, T. H., Deyanat-Yazdi, G., Neuteboom, S. T. C., Lam, K. S., & Potts, B. C. M. (2007). **Salinosporamides D-J from the marine actinomycete Salinispora tropica, bromosalinosporamide, and thioester derivatives are potent inhibitors of the 20S proteasome**. *Journal of Natural Products*, *70*(2), 269–276. https://doi.org/10.1021/np0603471

Reen, F. J., Romano, S., Dobson, A. D. W., & O'Gara, F. (2015). **The sound of silence: Activating silent biosynthetic gene clusters in marine microorganisms**. *Marine Drugs*, *13*(8), 4754–4783. https://doi.org/10.3390/md13084754

Ren, H., Wang, B., & Zhao, H. (2017). **Breaking the silence: new strategies for discovering novel natural products**. *Current Opinion in Biotechnology*, *48*, 21–27. https://doi.org/10.1016/j.copbio.2017.02.008

Rice, L. B. (2008). **Federal Funding for the Study of Antimicrobial Resistance in Nosocomial Pathogens: No ESKAPE**. *The Journal of Infectious Diseases*, *197*(8), 1079–1081. https://doi.org/10.1086/533452

Richter, T. K. S., Hughes, C. C., & Moore, B. S. (2015). **Sioxanthin, a novel glycosylated carotenoid, reveals an unusual subclustered biosynthetic pathway**. *Environmental Microbiology*, *17*(6), 2158–2171. https://doi.org/10.1111/1462-2920.12669

Robert, X., & Gouet, P. (2014). **Deciphering key features in protein structures with the new ENDscript server**. *Nucleic Acids Research*, *42*(W1), 320–324. https://doi.org/10.1093/nar/gku316

Roberts, A. A., Schultz, A. W., Kersten, R. D., Dorrestein, P. C., & Moore, B. S. (2012). **Iron acquisition in the marine actinomycete genus Salinispora is controlled by the desferrioxamine family of siderophores**. *FEMS Microbiology Letters*, *335*(2), 95–103. https://doi.org/10.1111/j.1574-6968.2012.02641.x

Rutledge, P. J., & Challis, G. L. (2015). **Discovery of microbial natural products by activation of silent biosynthetic gene clusters**. *Nature Reviews Microbiology*, *13*(8), 509–523. https://doi.org/10.1038/nrmicro3496

Schlawis, C., Kern, S., Kudo, Y., Grunenberg, J., Moore, B. S., & Schulz, S. (2018). **Structural Elucidation of Trace Components Combining GC/MS, GC/IR, DFT-Calculation and Synthesis—Salinilactones, Unprecedented Bicyclic Lactones from Salinispora Bacteria**. *Angewandte Chemie - International Edition*, *57*(45), 14921–14925. https://doi.org/10.1002/anie.201807923

Schley, C., Altmeyer, M. O., Swart, R., Müller, R., & Huber, C. G. (2006). **Proteome analysis of Myxococcus xanthus by off-line two-dimensional chromatographic separation using monolithic poly-(styrene-divinylbenzene) columns combined**

with ion-trap tandem mass spectrometry. *Journal of Proteome Research*, *5*(10), 2760–2768. https://doi.org/10.1021/pr0602489

Schultz, A. W., Lewis, C. A., Luzung, M. R., Baran, P. S., & Moore, B. S. (2010). **Functional characterization of the cyclomarin/cyclomarazine prenyltransferase cymd directs the biosynthesis of unnatural cyclic peptides**. *Journal of Natural Products*, *73*(3), 373–377. https://doi.org/10.1021/np9006876

Schultz, A. W., Oh, D. C., Carney, J. R., Williamson, R. T., Udwary, D. W., Jensen, P. R., Gould, S. J., Fenical, W., & Moore, B. S. (2008). **Biosynthesis and structures of cyclomarins and cyclomarazines, prenylated cyclic peptides of marine actinobacterial origin**. *Journal of the American Chemical Society*, *130*(13), 4507–4516. https://doi.org/10.1021/ja711188x

Schulze, C. J., Navarro, G., Ebert, D., Derisi, J., & Linington, R. G. (2015). **Salinipostins A-K, long-chain bicyclic phosphotriesters as a potent and selective antimalarial chemotype**. *Journal of Organic Chemistry*, *80*(3), 1312–1320. https://doi.org/10.1021/jo5024409

Scott, T. A., & Piel, J. (2019). **The hidden enzymology of bacterial natural product biosynthesis**. *Nature Reviews Chemistry*, *3*(7), 404–425. https://doi.org/10.1038/s41570-019-0107-1

Seyedsayamdost, M. R., Case, R. J., Kolter, R., & Clardy, J. (2011). **The Jekyll-and-Hyde chemistry of phaeobacter gallaeciensis**. *Nature Chemistry*, *3*(4), 331–335. https://doi.org/10.1038/nchem.1002

Shen, B. (2015). **A New Golden Age of Natural Products Drug Discovery**. *Cell*, *163*(6), 1297–1300. https://doi.org/10.1016/j.cell.2015.11.031

Shepherd, M. D., Kharel, M. K., Bosserman, M. A., & Rohr, J. (2010). **Laboratory maintenance of streptomyces species**. *Current Protocols in Microbiology*, *SUPP.18*, 1–10. https://doi.org/10.1002/9780471729259.mc10e01s18

Sher, D., Thompson, J. W., Kashtan, N., Croal, L., & Chisholm, S. W. (2011). **Response of Prochlorococcus ecotypes to co-culture with diverse marine bacteria**. *ISME Journal*, *5*(7), 1125–1132. https://doi.org/10.1038/ismej.2011.1

Silver, L. L. (2011). **Challenges of antibacterial discovery**. *Clinical Microbiology Reviews*, *24*(1), 71–109. https://doi.org/10.1128/CMR.00030-10

Singh, S., Prasad, P., Subramani, R., & Aalbersberg, W. (2014). **Production and purification of a bioactive substance against multi-drug resistant human pathogens from the marine-sponge-derived Salinispora sp.** *Asian Pacific Journal of Tropical Biomedicine*, *4*(10), 825–831. https://doi.org/10.12980/APJTB.4.2014C1154

Slattery, M., Rajbhandari, I., & Wesson, K. (2001). **Competition-Mediated Antibiotic Induction in the Marine Bacterium Streptomyces tenjimariensis**. *Microbial Ecology*, *41*(2), 90–96. https://doi.org/10. 1007/s002480000084 ?

Snoberger, A., Anderson, R. T., & Smith, D. M. (2017). **The proteasomal ATPases use a slow but highly processive strategy to unfold proteins**. *Frontiers in Molecular Biosciences*, *4*(APR). https://doi.org/10.3389/fmolb.2017.00018

Stanley, A. E., Walton, L. J., Kourdi Zerikly, M., Corre, C., & Challis, G. L. (2006). **Elucidation of the Streptomyces coelicolor pathway to 4-methoxy-2,2'- bipyrrole-5-carboxaldehyde, an intermediate in prodiginine biosynthesis**. *Chemical Communications*, *38*, 3981–3983. https://doi.org/10.1039/b609556a

Süssmuth, R. D., & Mainz, A. (2017). **Nonribosomal Peptide Synthesis—Principles and**

Prospects. *Angewandte Chemie - International Edition*, *56*(14), 3770–3821. https://doi.org/10.1002/anie.201609079

Takahashi, Y., & Nakashima, T. (2018). **Actinomycetes, an inexhaustible source of naturally occurring antibiotics**. *Antibiotics*, *7*(2). https://doi.org/10.3390/antibiotics7020045

Tang, X., Li, J., Millán-Aguiñaga, N., Zhang, J. J., O'Neill, E. C., Ugalde, J. A., Jensen, P. R., Mantovani, S. M., & Moore, B. S. (2015). **Identification of Thiotetronic Acid Antibiotic Biosynthetic Pathways by Target-directed Genome Mining**. *ACS Chemical Biology*, *10*(12), 2841–2849. https://doi.org/10.1021/acschembio.5b00658

Tenconi, E., & Rigali, S. (2018). **Self-resistance mechanisms to DNA-damaging antitumor antibiotics in actinobacteria**. *Current Opinion in Microbiology*, *45*(Figure 2), 100–108. https://doi.org/10.1016/j.mib.2018.03.003

Thomy, D., Culp, E., Adamek, M., Cheng, E. Y., Ziemert, N., Wright, G. D., Sass, P., & Brötz-Oesterhelt, H. (2019). **The ADEP biosynthetic gene cluster in Streptomyces hawaiiensis NRRL 15010 reveals an accessory clpP gene as a novel antibiotic resistance factor**. *Applied and Environmental Microbiology*, *85*(20). https://doi.org/10.1128/AEM.01292-19

Tibrewal, N., & Tang, Y. (2014). **Biocatalysts for Natural Product Biosynthesis**. *Annual Review of Chemical and Biomolecular Engineering*, *5*(1), 347–366. https://doi.org/10.1146/annurev-chembioeng-060713-040008

Tsueng, G., & Lam, K. S. (2008). **Growth of Salinispora tropica strains CNB440, CNB476, and NPS21184 in nonsaline, low-sodium media**. *Applied Microbiology and Biotechnology*, *80*(5), 873–880. https://doi.org/10.1007/s00253-008-1614-z

Tuttle, R. N., Demko, A. M., Patin, N. V, Kapono, C. A., Donia, M. S., Dorrestein, P., & Jensen, P. R. (2019). **Detection of natural products and their producers in ocean sediments**. *Applied and Environmental Microbiology*, *85*(8), 1–15. https://doi.org/10.1128/AEM.02830-18

Udwary, D. W., Zeigler, L., Asolkar, R. N., Singan, V., Lapidus, A., Fenical, W., Jensen, P. R., & Moore, B. S. (2007). **Genome sequencing reveals complex secondary metabolome in the marine actinomycete Salinispora tropica**. *Proceedings of the National Academy of Sciences*, *104*(25), 10376–10381. https://doi.org/10.1073/pnas.0700962104

van der Meij, A., Worsley, S. F., Hutchings, M. I., & van Wezel, G. P. (2017). **Chemical ecology of antibiotic production by actinomycetes**. *FEMS Microbiology Reviews*, *41*(3), 392–416. https://doi.org/10.1093/femsre/fux005

Villadsen, N. L., Jacobsen, K. M., Keiding, U. B., Weibel, E. T., Christiansen, B., Vosegaard, T., Bjerring, M., Jensen, F., Johannsen, M., Tørring, T., & Poulsen, T. B. (2017). **Synthesis of ent-BE-43547A 1 reveals a potent hypoxia-selective anticancer agent and uncovers the biosynthetic origin of the APD-CLD natural products**. *Nature Chemistry*, *9*(3), 264–272. https://doi.org/10.1038/nchem.2657

Wakefield, J., Hassan, H. M., Jaspars, M., Ebel, R., & Rateb, M. E. (2017). **Dual induction of new microbial secondary metabolites by fungal bacterial co-cultivation**. *Frontiers in Microbiology*, *8*(JUL), 1–10. https://doi.org/10.3389/fmicb.2017.01284

Walsh, C. T., & Fischbach, M. A. (2010). **Natural products version 2.0: Connecting genes to molecules**. *Journal of the American Chemical Society*, *132*(8), 2469–2493. https://doi.org/10.1021/ja909118a

Walsh, Christopher. (2017). **Where will new antibiotics come from?** *Pharmaceutical Engineering*, *37*(1), 72. https://doi.org/10.1038/nrmicro727

Walsh, CT. (2008). **The chemical versatility of natural-product assembly lines**. *Accounts of Chemical Research*, *41*(1), 4–10. https://doi.org/10.1021/ar7000414

Ward, J. M., & Hodgson, J. E. (1993). **The biosynthetic genes for clavulanic acid and cephamycin production occur as a 'super-cluster' in three Streptomyces**. *FEMS Microbiology Letters*, *110*(2), 239–242. https://doi.org/10.1111/j.1574-6968.1993.tb06326.x

Weber, J. M., Wierman, C. K., & Hutchinson, C. R. (1985). **Genetic analysis of erythromycin production in Streptomyces erythreus**. *Journal of Bacteriology*, *164*(1), 425–433. https://doi.org/10.1128/jb.164.1.425-433.1985

Whitman, W. B., Coleman, D. C., & Wiebe, W. J. (1998). **Prokaryotes: The unseen majority**. *Proceedings of the National Academy of Sciences*, *95*(12), 6578–6583. https://doi.org/10.1073/pnas.95.12.6578

Williams, P. G., Miller, E. D., Asolkar, R. N., Jensen, P. R., & Fenical, W. (2007). **Arenicolides A-C, 26-membered ring macrolides from the marine actinomycete Salinispora arenicola**. *Journal of Organic Chemistry*, *72*(14), 5025–5034. https://doi.org/10.1021/jo061878x

Wilson, W. H., Carr, N. G., & Mann, N. H. (1996). **The effect of phosphate status on the kinetics of cyanophage infection in the oceanic cyanobacterium Synechococcus sp. WH7803. 32**, 506–516.

Wilson, Z. E., & Brimble, M. A. (2009). **Molecules derived from the extremes of life**. *Natural Product Reports*, *26*(1), 44–71. https://doi.org/10.1039/b800164m

Xu, M., Hillwig, M. L., Lane, A. L., Tiernan, M. S., Moore, B. S., & Peters, R. J. (2014). **Characterization of an orphan diterpenoid biosynthetic operon from salinispora arenicola**. *Journal of Natural Products*, *77*(9), 2144–2147. https://doi.org/10.1021/np500422d

Yamanaka, K., Reynolds, K. A., Kersten, R. D., Ryan, K. S., Gonzalez, D. J., Nizet, V., Dorrestein, P. C., & Moore, B. S. (2014). **Direct cloning and refactoring of a silent lipopeptide biosynthetic gene cluster yields the antibiotic taromycin A**. *Proceedings of the National Academy of Sciences of the United States of America*, *111*(5), 1957–1962. https://doi.org/10.1073/pnas.1319584111

Yu, M., Li, Y., Banakar, S. P., Liu, L., Shao, C., Li, Z., & Wang, C. (2019). **New metabolites from the Co-culture of marine-derived actinomycete streptomyces rochei MB037 and fungus rhinocladiella similis 35**. *Frontiers in Microbiology*, *10*, 1–11. https://doi.org/10.3389/fmicb.2019.00915

Zhang, B., Tian, W., Wang, S., Yan, X., Jia, X., Pierens, G. K., Chen, W., Ma, H., Deng, Z., & Qu, X. (2017). **Activation of Natural Products Biosynthetic Pathways via a Protein Modification Level Regulation**. *ACS Chemical Biology*, *12*(7), 1732–1736. https://doi.org/10.1021/acschembio.7b00225

Zhao, P., Gu, W., Huang, A., Wu, S., Liu, C., Huan, L., Gao, S., Xie, X., & Wang, G. (2018). **Effect of iron on the growth of Phaeodactylum tricornutum via photosynthesis**. *Journal of Phycology*, *54*(1), 34–43. https://doi.org/10.1111/jpy.12607

APPENDIX 1

Phytoplankton trigger the production of cryptic metabolites in the marine actinobacteria *Salinispora tropica*.

Audam Chhun[1,#], Despoina Sousoni[1], Maria del Mar Aguiló-Ferretjans[2], Lijiang Song[3], Christophe Corre[1,3,#], Joseph A. Christie-Oleza[1,2,4,#]

[1] School of Life Sciences, University of Warwick, Coventry, UK
[2] University of the Balearic Islands, Palma, Spain
[3] Department of Chemistry, University of Warwick, Coventry, UK
[4] IMEDEA (CSIC-UIB), Esporles, Spain

[#]Corresponding authors: a.chhun@warwick.ac.uk, c.corre@warwick.ac.uk and joseph.christie@uib.eu

Abstract

Bacteria from the Actinomycete family are a remarkable source of natural products with pharmaceutical potential. The discovery of novel molecules from these organisms is, however, hindered because most of the biosynthetic gene clusters (BGCs) encoding these secondary metabolites are cryptic or silent and are referred to as orphan BGCs. While co-culture has proven to be a promising approach to unlock the biosynthetic potential of many microorganisms by activating the expression of these orphan BGCs, it still remains an underexplored technique. The marine actinobacteria *Salinispora tropica*, for instance, produces valuable compounds such as the anti-cancer molecule salinosporamide A but half of its putative BGCs are still orphan. Although previous studies have looked into using marine heterotrophs to induce orphan BGCs in *Salinispora*, the potential impact of co-culturing marine phototrophs with *Salinispora* has yet to be investigated. Following the observation of clear antimicrobial phenotype of the actinobacterium on a range of phytoplanktonic organisms, we here report the discovery of novel cryptic secondary metabolites produced by *S. tropica* in response to its co-culture with photosynthetic primary producers. An approach combining metabolomics and proteomics revealed that the photosynthate released by phytoplankton influences the biosynthetic capacities of *S. tropica* with both production of new molecules and the activation of orphan BGCs. Our work pioneers the use of phototrophs as a promising strategy to accelerate the discovery of novel natural products from actinobacteria.

Importance

The alarming increase of antimicrobial resistance has generated an enormous interest in the discovery of novel active compounds. The isolation of new microbes to untap novel natural products is currently hampered because most biosynthetic gene clusters (BGC) encoded by these microorganisms are not expressed under standard laboratory conditions, *i.e.* mono-cultures. Here we show that co-culturing can be an easy way for triggering silent BGC. By combining state-of-the-art metabolomics and high-throughput proteomics, we characterized the activation of cryptic metabolites and silent biosynthetic gene clusters in the marine actinobacteria *Salinispora tropica* by the presence of phytoplankton photosynthate. We further suggest a mechanistic understanding of the antimicrobial effect this actinobacterium has on a broad range of prokaryotic and eukaryotic phytoplankton species and reveal a promising candidate for antibiotic production.

Introduction

Soil actinomycetes are a rich source of drug-like natural products, to which we owe up to 70% of all microbial antibiotics used today (Bérdy, 2005). Identification of novel secondary metabolites from this extensively studied family has, however, stalled over the last few decades as a result of the recurring rediscovery of already known compounds. This has led in recent years to a thriving interest for the study of new microorganisms, with the rational that ecologically distinct microorganisms produce equally distinct secondary metabolites (Molinski et *al.*, 2009; Wilson and Brimble, 2009). For instance, the heterotrophic bacteria *Salinispora* drew particular attention when discovered, as it was the first obligate marine actinomycete described (Jensen *et al*., 1991; Mincer *et al*., 2002, Jensen & Mafnas, 2006) and has since proven to be an important source of new natural products for the pharmaceutical industry (Maldonado *et al.*, 2005; Feling *et al.*, 2003; Buchanan *et al*., 2005; Asolkar *et al*., 2010). Despite the increasing number of novel strains identified with promising biosynthetic capacities, many hurdles in natural product discovery remain. Most of these microbial secondary metabolites are encoded by groups of colocalized genes, called biosynthetic gene clusters (BGCs), which are now more easily identified because of the improvement in sequencing technologies and bioinformatic tools (Medema *et al*., 2011). The majority of these discovered BGCs, however, have yet to be linked to their products and are called orphan BGCs. They are generally considered to be either silent - because of a low level of expression or inactivation of their biosynthetic genes - or the metabolites they produce are cryptic - difficult to detect and isolate (Reen *et al*., 2015; Rutledge and Challis, 2015). The observation of numerous orphan BGCs in genome-sequenced microorganisms has resulted in a growing interest in developing biological or chemical means to activate such clusters (Abdelmohsen *et al*., 2015; Onaka, 2017). One of the simplest and most efficient methods described in the literature relies on co-cultivation of different microbes to elicit novel natural product biosynthesis (Slattery *et al*., 2001; Bertrand *et al*., 2014).

The genome of the marine actinomycete *Salinispora tropica* comprises at least 20 putative BGCs of which 11 are orphan (**Table 1**, Penn *et al.*, 2009, Udwary *et al*., 2007). Recent studies have shown that *Salinispora* co-inoculated with various marine heterotrophs could produce one or several antimicrobial compounds, which remain uncharacterized as traditional analytical chemistry methods did not allow their identification and no candidate BGC was proposed (Patin *et al*., 2016; Patin *et al*., 2018). While co-culturing appears to be a promising mean to activate orphan BGCs in *Salinispora*, it remains an underexplored technique to unravel the biosynthetic potential of this genus. Additionally, little has been done to establish the BGCs that are activated under such culturing conditions. Combining metabolomics with proteomics analyses has proven successful in linking novel compounds to active orphan BGCs in several *Streptomyces* species, but has not yet been applied to the genus *Salinispora* (Schley *et al*., 2006; Gubbens *et al*., 2014; Owens *et al.*, 2014).

Here we report the discovery of novel cryptic secondary metabolites produced by *S. tropica* CNB-440. By using an approach combining metabolomics and proteomics, we investigated how marine microbial phototrophs, and their photosynthate, induce the production of new metabolites and activate the expression of orphan BGCs in *S. tropica*. This strategy confirms microbial interactions as a promising and simple approach for future discovery of novel natural products.

Material and methods

1. Culture conditions and cell abundance monitoring

1.1. Strains and growth media

Axenic marine phototrophs *Synechococcus sp.* WH7803, *Emiliania huxleyi* RCC1242 and *Phaeodactylum tricornutum* CCAP1055/1 were routinely grown in Artificial Seawater (ASW, Wilson *et al*., 1996), K-media (Probert and Houdan, 2004), and F/2 media (Guillard *et al*., 1975), respectively. Cultures were set-up in Falcon 25 cm^2 rectangular culture flasks with vented caps containing 20 ml of media and incubated at a constant light intensity of 10 µmol photons m^{-2} s^{-1}, at 22 °C with orbital shaking (140 rpm). *Salinispora tropica* CNB-440 was grown in marine broth (MB, Difco), and incubated at 30 °C with orbital shaking (220 rpm). The *S. tropica* mutants *salA*$^-$ and *salL*$^-$ were generously provided by the Moore Laboratory, USA (Eustáquio *et al.*, 2008; Eustáquio *et al.*, 2009).

1.2. Co-culture setup

Salinispora cells were grown to late exponential phase in 10 ml of MB before washing them three times with sterile mineral media, as appropriate for each phototroph, and finally resuspending the washed cell pellet in 10 ml of mineral media. Exponentially growing axenic phototroph cells and the washed *Salinispora* were co-inoculated in fresh media to a concentration of 10% (v/v) and 20% (v/v), respectively. *Salinispora* cells were also washed and resuspended in a conditioned *Synechococcus* supernatant (SUPSYN), when required for the metabolomic and proteomic analyses. To obtain the conditioned supernatant, *Synechococcus* cultures were incubated for 35 days as described above before centrifugation (4000 x *g* for 10 min at room temperature) and further filtration through 0.22 µm pore size filters to remove cells and particulate organic matter. Washed *Salinispora* cells were used to inoculate SUPSYN and MB, and cultures were incubated at 22°C with shaking (140 rpm) and a light intensity of 10 µmol photons m^{-2} s^{-1}. For the physically separated *Synechococcus-Salinispora* co-cultures using the porous filters, cells were grown in 24 mm transwell with 0.4 µm pore polycarbonate membrane inserts (Corning). *Synechococcus* cells were inoculated in the well to a concentration of 20% (v/v) and *Salinispora* in the insert to a concentration of 55% (v/v).

1.3. Flow cytometry

Phototroph cell abundance was monitored using their autofluorescence by flow cytometry using a LSR Fortessa Flow Cytometer (BD) instrument, and the BD FACSDiva acquisition software (BD). Cells were detected and gated using ex. 488 nm – em. 710/50 nm at voltage 370 V, and ex. 640 nm – em. filter 670/14 nm at voltage 480 V. To remove any *Salinispora* cell aggregates that would block the flow cell, samples were pre-filtered through a sterile mesh with pore size of 35 µm (Corning) prior to analysis.

2. Metabolomic analysis

2.1. Sample preparation

The culture supernatants were analyzed by non-targeted metabolomic using either raw or concentrated supernatants. Raw supernatants were collected by sampling 200 µl of 0.22 µm-filtered culture milieu, prior to being mixed with an equal volume of HPLC-grade methanol. For concentrating the supernatant, cells from 10 to 100 mL of cultures were removed by centrifugation (4,000 x *g* for 15 min) followed by a filtering step using 0.22 µm vacuum filter bottle system (Corning). Pre-purification of the compounds of interest from the supernatants was carried out by solid phase extraction using C18-silica. Using a 90:10 A/B mobile phase

(where A is water with 0.1% formic acid and B is methanol with 0.1% formic acid) the undesired polar molecules and salts passed through the silica while the compounds of interest were retained and later collected following elution with a 10:90 A/B mobile phase. The obtained fractions were dried under reduced pressure at 40 °C (in a speed-vac) and resuspended in 1-3 mL of 50:50 HPLC-grade methanol/water solution. All samples were stored in snap-seal amber glass vials (Thames Restek) and kept at -20 °C until analysis.

2.2. Low-resolution LC-MS

Metabolites present in the cultures were routinely analyzed by reversed-phase liquid chromatography. A Dionex UltiMate 3000 HPLC (ThermoScientific) coupled with an amaZon SL Ion Trap MS (Bruker) was used. A Zorbax Eclipse Plus C18 column with dimensions 4.6 mm x 150 mm, 5 µm particle size (Agilent Technologies) was employed for metabolite separation with a linear gradient of 95:5 A/B to 30:70 A/B over 5 minutes, followed by second linear gradient to 20:80 A/B over 10 minutes with a flow rate of 1 ml min^{-1} (Mobile phase A: water with 0.1% formic acid, B: methanol with 0.1% formic acid). The mass spectrometer was operated in positive ion mode with a 100-1000 *m/z* scan range. The injected volume was 10 µL at a temperature of 25 °C. Data was processed with the Bruker Compass DataAnalysis software version 4.2 (Bruker).

2.3. High-resolution LC-MS

To acquire molecular formulae information, samples were analyzed using an Ultra-high resolution MaXis II Q-TOF mass spectrometer equipped with electrospray source coupled with Dionex 3000RS UHPLC was employed (Bruker). A reverse phase C18 column (Agilent Zorbax, 100x2.1 mm, 1.8 µm) and a guard column (Agilent C18, 10x2.1 mm, 1.8 µm) were used for separation applying a linear gradient of 95:5 A/B to 0:100 A/B over 20 minutes (Mobile phase A: water with 0.1% formic acid, B: acetonitrile with 0.1% formic acid). The injected volume was 2 µL, and the flow rate was 0.2 ml min^{-1}. At the beginning of each run, 7.5 µl of 10 mM of sodium formate solution was injected for internal calibration. The mass spectrometer was operated in positive ion mode with a 50-2500 *m/z* scan range. MS/MS data was acquired for the three most intense peaks in each scan.

3. Proteomic analysis

3.1. Preparation of cellular proteome samples

Cultures were set up as described above and incubated for 5 days after which cells were collected by centrifuging 10 mL of culture at 4,000 x *g* for 10 min at 4 °C. Cell pellets were placed on dry ice before storing at -20 °C until further processing. The cell pellets were resuspended in 200 µL 1x NuPAGE lithium dodecyl sulfate (LDS) sample buffer (ThermoFischer Scientific), supplemented with 1% ß-mercaptoethanol. Cell pellets were lysed by bead beating (2x45 sec and 1x30 sec at 6.0 m/s) and sonication (5 min), followed by three successive 5-min incubations at 95 °C with short vortex steps in between. Cell lysates containing all proteins were loaded on an SDS-PAGE precast Tris-Bis NuPAGE gel (Invitrogen), using MOPS solution (Invitrogen) as the running buffer. Protein migration in the SDS-PAGE gel was performed for 5 min at 200 V, to allow removal of contaminants and purification of the polypeptides. The resulting gel was stained using SimplyBlue SafeStain (Invitrogen) to visualize the cellular proteome. The gel bands containing the cellular proteome were excised and stored at -20 °C until further processing.

3.2. Trypsin in-gel digestion and nano LC-MS/MS analysis

Polyacrylamide gel bands were destained and standard in-gel reduction and alkylation were performed using dithiothreitol and iodoacetamide, respectively, after which proteins were in-gel digested overnight with 2.5 ng μL^{-1} trypsin (Christie-Oleza and Armengaud, 2010). The resulting peptide mixture was extracted by sonication of the gel slices in a solution of 5% formic acid in 25% acetonitrile, and finally concentrated at 40 °C in a speed-vac. For mass spectrometry analysis, peptides were resuspended in a solution of 0.05% trifluoroacetic acid in 2.5% acetonitrile prior to filtering using a 0.22 µm cellulose acetate spin column. Samples were analyzed by nanoLC-ESI-MS/MS with an Ultimate 3000 LC system (Dionex-LC Packings) coupled to an Orbitrap Fusion mass spectrometer (Thermo Scientific) using a 60 min LC separation on a 25 cm column and settings as previously specified (Christie-Oleza *et al.*, 2015).

3.3. Proteomic data analysis

Raw mass spectral files were processed for protein identification and quantification using the software MaxQuant (version 1.5.5.1; Cox and Mann, 2008) and the UniProt database of *S. tropica* CNB-440 (UP000000235). Quantification and normalization of spectral counts was done using the Label-Free Quantification (LFQ) method (Cox *et al.*, 2014). Samples were matched between runs for peptide identification and other parameters were set by default. Data processing was completed using the software Perseus (version 1.5.5.3). Proteins were filtered by removing decoy and contaminants and were considered valid when present in at least two replicates for one condition. The relative abundance of each protein was calculated using protein intensities transformed to a logarithmic scale with base 2 and normalized to protein size. Variations in protein expression were assessed with a two-sample T-test, with a false discovery rate (FDR) *q* below 0.05 and a log(2) fold change above 2 (**Supplementary File S1**).

Results

Salinispora tropica has antimicrobial activity on a diverse range of marine phototrophs

Unlike other heterotrophs, which usually enhance the growth of phototrophic organisms when in co-culture (*e.g.* Christie-Oleza *et al.*, 2017; Sher *et al.*, 2011), *S. tropica* showed a clear antimicrobial activity on marine phytoplankton (**Fig. 1, A**). All three phototrophic model species tested, namely the cyanobacteria *Synechococcus* sp. WH7803, the coccolithophore *Emiliana huxleyi* and the diatom *Phaeodactylum tricornutum*, showed a strong decline in the presence of *S. tropica*, being especially remarkable for the two former species (**Fig. 1, A**). While also affected, the diatom *P. tricornutum* was not killed by *S. tropica* but, instead, its cells densities were significantly maintained one order of magnitude lower than when incubated axenically.

We were therefore interested in characterizing the nature of this inhibition. While other *Salinispora* species, such as *Salinispora arenicola*, are known to biosynthesize antibiotic molecules (Asolkar *et al.*, 2010), no antimicrobial compound has yet been characterized in *S. tropica* CNB-440. Previous studies have shown, however, that *S. tropica* is able to outcompete other heterotrophs in co-culture by secreting siderophores leading to iron depletion (Patin *et al.*, 2016). To evaluate whether iron sequestration could explain the negative interactions observed in the present phototroph-*Salinispora* system, we supplemented the co-cultures with increasing concentrations of iron (**Supplementary Fig. S1**). The results obtained suggest

that the antimicrobial phenotype was not due to siderophore activity, as saturating amount of iron could not rescue the growth of the phototrophs.

We then hypothesized that a yet unknown antimicrobial compound, to which our photosynthetic microorganisms are sensitive to, could be produced by *S. tropica.* To test this assumption, we setup co-cultures in which *S. tropica* and *Synechococcus* were physically separated by a porous filter, preventing direct cell-to-cell interactions while allowing the diffusion of small molecules (**Fig. 1, B**). *S. tropica* was still able to impair *Synechococcus* proliferation in these experimental conditions, confirming that a secreted molecule was causing the death of the phototroph.

Phototrophs elicit the production of novel cryptic metabolites in *S. tropica*

We analyzed the co-culture supernatants using non-targeted metabolomics to identify the pool of secondary metabolites secreted by *S. tropica* in response to the different phototrophs. The *Synechococcus*-*S. tropica* co-culture revealed eight molecular ions that were not present in the respective axenic cultures (**Fig. 2, A**). These molecules were further characterized by high-resolution MS/MS analysis, from which we generated empirical chemical formulae, allowing us to assign most of them to two subgroups of related compounds being: (i) ions **1**, **2**, **5** and **8**; and (ii) ions **4**, **6** and **7** (**Fig. 2, A** and **Supplementary Table S1**).

Ions **1**, **2**, **5** and **8** were derivatives of salinosporamide; a well-characterized molecule produced by *S. tropica* that presents a unique fused γ-lactam-β-lactone bicyclic ring structure (Feling *et al*., 2003), and that is now being tested as a drug because of its anti-cancer properties. Molecules **5** and **8** are consistent with known degradation products of salinosporamide A and B, respectively (Denora *et al*., 2007; **Supplementary Fig. S2**), while molecules **1** and **2** are proposed to result from the nucleophilic addition of Tris (the buffering agent used in the ASW culture medium) to the lactone ring of salinosporamide A and B, respectively (**Supplementary Fig. S2**). These salinosporamide sub-products were further confirmed by their absence when i) Tris was not added (**Supplementary Fig. S3**), or ii) salinosporamide mutants that no longer produced these metabolites, *i.e.* salA$^-$ and salL$^-$ (Eustáquio *et al*., 2009), were used (**Supplementary Fig. S4**). In order to test the activity of salinosporamide and its derivatives on the phototrophs, we co-cultured *Synechococcus* with both salinosporamide mutants. Salinosporamide and its derivatives were not responsible for the antimicrobial activity as both deficient mutants were still able to inhibit the phototroph (**Supplementary Fig. S5**).

The second group of ions, *i.e.* peaks **4**, **6** and **7**, were also related. Molecule **6** gave a *m/z* value of 435.2609 $[M+H]^+$; based on the accuracy of this value and the isotopic pattern the empirical chemical formula $C_{22}H_{35}N_4O_5$ was predicted by the DataAnalysis software (**Table 2**). The predicted formula for molecule **4** suggests that, with a 28.9900 Da mass difference when compared to **6**, the compound had lost one hydrogen and gained an atom of nitrogen and oxygen. MS/MS analyses confirmed that both molecules **4** and **6** had an identical molecular fragment (*i.e. m/z* 276.1600 ± 0.0001 $[M+H]^+$, with the empirical chemical formula $C_{16}H_{22}NO_3$), indicating that the two molecules share a core backbone (**Table 2**). Similarly, molecule **7** had the same chemical formula than **6** but with the addition of a methyl group (14.0155 Da mass difference; **Table 2**). Molecule **3** did not share an obvious link to any other metabolites and, therefore, was considered a new biosynthesized product of *Salinispora*

(**Table 2**). Most interestingly, the search for compounds with the same molecular formulae as **3**, **4**, **6** or **7** in multiple databases (*e.g.* Reaxys, SciFinder, Dictionary of NP) returned no known natural product, suggesting that they are novel compounds. Unfortunately, despite multiple attempts, the isolation of these molecules has so far proven too challenging for their structural elucidation.

The production of these novel compounds was only triggered by the presence of the phototrophs as they were only detected in the co-cultures of all three phototrophs (**Fig. 2, A and B**), but not when grown in mono culture – as shown by the absence of these metabolites when *S. tropica* was grown alone in mineral ASW or nutrient rich media MB (**Fig. 2, C and D**). Furthermore, we confirmed that the supernatant of a phototroph culture – containing the photosynthate – was enough to induce such metabolite production (**Fig. 2, D**).

Photosynthate triggers the expression of orphan gene clusters in *S. tropica*

Having detected novel secondary metabolites produced by *S. tropica* in response to phototroph-released photosynthate, we set out to investigate how it affected the induction of its BGCs. To this end, we analyzed and compared the proteome of *S. tropica* when grown in presence of the phytoplankton's photosynthate – *i.e.* in conditioned *Synechococcus* supernatant – and in nutrient rich broth – *i.e.* marine broth. Surprisingly, we were able to detect proteins encoded by almost all of *S. tropica*'s BGCs, including 10 of its 11 orphans BGCs (**Fig. 3, A**).

Of particular interest were the orphan BGCs *pks3* and *nrps1*, for which we detected 72% (18/25) and 42% (14/33) of their encoded proteins, respectively (**Fig. 3, A**). Moreover, the *pks3* BGC was noticeably highly detected as eight of its detected proteins showed a relative abundance above 0.1% (**Supplementary Table S2**). While it has been previously suggested that *pks3* may produce a spore pigment polyketide, very little experimental evidence is available in the literature, and the product of *pks3* had not been confirmed (Kersten *et al*., 2013). On the other hand, the non-ribosomal peptide synthetase (NRPS) gene cluster *nrps1* has only been predicted to produce a non-ribosomal dipeptide (Penn *et al*., 2009). Intriguingly, the most abundant proteins detected from this *nrps1* BGC were the non-ribosomal peptide synthetase (A4X2Q0), the condensation domain-containing protein (A4X2R5) and an ATP-dependent Clp protease subunit (A4X2S2), with a relative abundance of 0.004%, 0.001% and 0.121%, respectively (**Table 3**). While the two former are thought to direct the biosynthesis of the non-ribosomal peptide, the later may be involved in conferring resistance to the synthesized antimicrobial compound (Kirstein *et al.*, 2009), as further discussed below.

The already characterized *lom* and *sal* BGCs were also abundantly detected with 81% (47/58) and 77% (23/30) of their encoded proteins detected, respectively, some representing high relative abundances within the proteome (**Fig. 3, A**). The BGC *lom* is linked to the cytotoxic glycoside lomaiviticin molecule (Kersten *et al*., 2013). However, this metabolite previously showed no antimicrobial activity on co-cultured heterotrophic organisms (Patin *et al.*, 2018) and, hence, it is unlikely to cause the antimicrobial phenotype observed on the phototrophs in this study. The high abundance of the *sal* cluster, producing the salinosporamide compound, is not surprising given the high detection of this metabolite by LC-MS (**Fig. 2, A**).

Interestingly, the comparative proteomic analysis of *S. tropica* grown in photosynthate *versus* marine broth confirmed that the detection of several BGCs rose in response to phototroph-released nutrients, being *lom* and *pks3* the most remarkable ones (**Fig. 3, B-C**). For instance, the *lom* cluster had 77% (36/47) of its detected proteins overexpressed in the presence of the photosynthate (**Fig. 3, B**). The orphan *pks3* BGC was also triggered by the photosynthate, as the pivotal biosynthetic enzymes for polyketide biosynthesis, *i.e.* acyl-CoA ligase (A4X7T8), 3-ketoacyl-ACP synthase (A4X7U0) and long-chain fatty acid-CoA ligase (A4X7U3), were up-regulated (3.1, 2.6 and 4.1-fold change, respectively; **Fig. 3, C** and **Supplementary Table S2**).

Discussion

We show that *S. tropica* is able to inhibit the growth of both marine cyanobacteria and eukaryotic phototrophs by some, yet, unidentified mechanism (**Fig. 1**). This observation broadens the potential role and impact that the *Salinispora* genus has on marine microbial communities. *Salinispora* is a widely-distributed bacterium found in all tropical and subtropical oceans (Mincer *et al*., 2002; Bauermeister *et al*., 2018). While mostly inhabiting marine sediments, bacteria from this genus were also isolated from marine sponges where it is suggested they influence the sponge microbiota through the production of acyl homoserine lactone molecules and antibiotics (Singh *et al*., 2014; Bose *et al*., 2017). Similarly, different species of *Salinispora* were shown to possess distinct mechanisms to outcompete co-occurring marine heterotrophs in sediments, *i.e.* through the production of siderophores to deplete iron or antimicrobial molecules (Patin *et al*., 2017; Tuttle *et al*., 2019), although no antimicrobial compound has yet been identified for *S. tropica* (Patin *et al.*, 2018). We herein provide the first evidence that *Salinispora* might not only directly influence heterotrophic communities, but also kill both prokaryotic and eukaryotic phytoplankton to which they are exposed, *e.g.* when these sediment out of the water column or phototrophs able to grow in sunlit coastal sediments.

While we were successful in identifying and obtaining the molecular formulae of novel cryptic metabolites produced in response to phytoplanktonic photosynthate (**Fig. 2**, **Table 2**), we were unable to isolate and identify the compound responsible for the antimicrobial effect on the marine phototrophs by using traditional bioactivity-guided assays with HPLC fractionation of crude extracts (data not shown). This mechanism proved similarly elusive in previous studies, where *S. tropica* showed an antimicrobial activity on marine heterotrophs, but the molecule responsible was not identified (Patin *et al*., 2016; Patin *et al*., 2018). The parallelism between our observations and those described in the literature suggests that the active compound(s) may be the same. We reason that the compound's instability, and/or synergic effect of several molecules required for activity, could explain the difficulty in identifying the antimicrobial agent. For instance, the large number of structurally-related metabolites resulting from the chemical reaction of salinosporamide with various compounds (*i.e*. water, Tris) may support this hypothesis, as the antimicrobial molecule may be similarly unstable. The diversity of products arising from a single BGC may also be due to the promiscuity of the biosynthetic enzymes utilizing structurally related primary precursors. This results in a range of compounds, each produced at lower titers than a single natural product, and ultimately hamper the isolation of sufficient amounts of the compounds of interest. Whichever the case, we show that *Salinispora* can produce a broad-range antibiotic able to affect both unicellular prokaryotes and eukaryotes alike, such as the marine diatom and coccolithophore tested in our study. Such a broad-range antimicrobial could suggest a mode of action affecting a

common target present in both types of cells such as the proteasome, a proteolytic complex present in the three domains of life (Becker and Darwin, 2016).

Exploring the proteome of *S. tropica* exposed to photosynthate, we detected proteins encoded by almost all its BGCs, including most of its orphan BGCs (**Fig. 3**). Notably, the *sal* BGC, producing the salinosporamide compound, was one of the most highly expressed BGC as most of its proteins were detected with high relative abundance. This finding is in agreement with previous studies that have shown by transcriptomics that the BGC *sal* is highly and constitutively expressed when grown in nutrient rich A1 medium (Amos *et al*., 2017). Also, the high expression of this BGC correlated with a noticeable detection of salinosporamide derivatives by LC-MS. The agreement between the metabolomic and proteomic data suggests that it is possible to correlate activated BGCs with the actual biosynthesis of their corresponding natural product. Therefore, the abundant detection of several orphans BGC proteins, including those from *pks3* and *nrps1* BGCs, may be promising candidates responsible for the biosynthesis of the cryptic metabolites detected by LC-MS and, potentially, the antimicrobial activity observed on co-cultured phototrophs.

The proteins detected from the BGC *nrps1* are essential enzymes involved in non-ribosomal peptide biosynthesis, *i.e.* A4X2Q0, a non-ribosomal peptide synthetase (NRPS) made of a C-A-PCP domain, and A4X2RS, a condensation domain-containing protein made of C-PCP-TE domain. The detection of these proteins therefore strongly suggests the actual synthesis of the non-ribosomal peptide and could well be the novel metabolites detected by LC-MS, which include four nitrogen atoms in their predicted molecular formulae (**Table 2**). Interestingly, the substrate specificity of A4X2Q0's A-domain is alanine and another three A-domains are encoded in the *nrps1* BGC. Further work is required to elucidate the structure of this series of cryptic metabolites. From this same BGC we also detected a highly abundant ATP-dependent Clp protease proteolytic subunit (ClpP, A4X2S2) that may be providing *Salinispora* with self-resistance against the *nrps1* peptides. Virtually all organisms across the tree of life have a system for targeted proteolysis for protein turnover, with most bacteria, mitochondria and chloroplasts relying on a ClpP-type proteasome while eukaryotes, archaea and some actinobacteria typically possess the homologous 20S proteasome structure (Becker and Darwin, 2016; Snoberger *et al*., 2017). The ClpP proteasome is known to be the target for certain antibiotics, including the novel acyldepsipeptide (ADEP) class (Kirstein *et al.*, 2009), and it is common to find alternative ClpP proteasomes encoded nearby the antibiotic-producing BGC to confer resistance to the host cell (Thomy *et al*., 2019). In a similar fashion, salinosporamide A is a 20S proteasome inhibitor, to which *Salinispora* is resistant because of an extra copy of the proteasome beta subunit gene within the salinosporamide-producing cluster (Kale *et al*., 2011). We can thus reasonably infer from the presence of *clpP* in the *nrps1* BGC that it is likely to produce an antibiotic targeting the ClpP proteasome, a class of antimicrobial compounds that has recently gained considerable attention as an attractive option to tackle multidrug resistant pathogens (**Fig. 4**; Momose and Kawada, 2016; Culp and Wright, 2017; Moreno-Cinos *et al.*, 2019). We here provide the first proteomic evidence that *S. tropica*'s *nrps1* is active and may produce a promising antimicrobial compound acting as a ClpP proteasome inhibitor. The synthesis of such antibiotic would explain the antimicrobial effect of *Salinispora* on all marine phototrophs tested in our study as they all rely on the ClpP proteolytic machinery (Andersson *et al.*, 2009; Jones *et al.*, 2013; Zhao *et al.*, 2018). Additional evidence, such as genetic inactivation of the *nrps1* BGC, will confirm this mechanism.

We show that the photosynthate released by primary producers influences the biosynthetic capacities of *Salinispora*, activating the expression of several orphan BGCs and inducing the production of novel metabolites. Our metabolomics analysis further confirmed the potential of co-culturing for natural product discovery as we identified novel cryptic secondary metabolites, although future work is required to elucidate the structure of the new molecules. Finally, our study extends the pool of known compounds produced by the genus *Salinispora* and pioneers the use of phototrophs as a promising strategy to trigger novel natural products from marine actinobacteria. We also provide a valuable insight into the biosynthetic potential of *S. tropica* with our proteomic dataset, which reveals the *nrps1* BGC as a promising candidate for antibiotic production.

Conflicts of interest

The authors declare that they have no conflicts of interest.

Acknowledgments

We thank Vinko Zadjelovic, Linda Westermann and Fabrizio Alberti for helpful discussions throughout the project. We also acknowledge technical support from Cleidiane Zampronio of the WPH Proteomic Facility at the University of Warwick. In addition, we thank the BBSRC/EPSRC Synthetic Biology Research Centre WISB BB/M017982/1 for access to the flow cytometer and Yin Chen for access to the LC-MS.
A.C. was supported by an MIBTP PhD scholarship (BB/M01116X/1) and D.S. by a NERC CENTA DTP studentship (NE/L002493/1). J.A.C.-O was funded by a NERC Independent Research Fellowship NE/K009044/1 and Ramón y Cajal contract RYC-2017-22452 (funded by the Ministry of Science, Innovation and Universities, the National Agency of Research, and the European Social Fund). C.C. thanks BBSRC (grant BB/M022765/1) and European Union's Horizon 2020 research No. 765147 for support. L.S. would like to acknowledge BBSRC (BB/M017982/1 and BB/R000689/1) and EPSRC (EP/P0305721/1) for financial support.

References

Abdelmohsen UR, Grkoviv T, Balasubramanian S, Kamel MS, Quinn RJ, Hentschel U: **Elicitation of secondary metabolism in actinomycetes.** *Biotechnol Adv* (2015), 33(6 Pt 1):798-811. doi: 10.1016/j.biotechadv.2015.06.003.

Andersson FI, Tryggvesson A, Sharon M, Diemand AV, Classen M, Best C, Schmidt R, Schelin J, Stanne TM, Bukau B, Robinson CV, Witt S, Mogk A, Clarke AK: **Structure and function of a novel type of ATP-dependent Clp protease.** *J Biol Chem* (2009), 284(20):13519-32. doi: 10.1074/jbc.M809588200.

Asolkar RN, Kirkland TN, Jensen PR, Fenical W: **Arenimycin, an antibiotic effective again rifampin- and methicillin-resistant *Staphylococcus aureus* from the marine actinomycete *Salinispora arenicola***. *J Antibio* (2010), 63(1):37-0. doi: 10.1038/ja.2009.114.

469 Bauermeister A, Velasco-Alzate K, Dias T, Macedo H, Ferreira EG, Jimenez PC, Lotufo TMC,
470 Lopes NP, Gaudêncio SP, Costa-Lotufo LV: **Metabolomic fingerprinting of Salinispora from**
471 **Atlantic oceanic islands**. *Front Microbiol* (2018), 9:3021. doi: 10.3389/fmicb.2018.03021.
472
473 Becker SH, Darwin KH: **Bacterial proteasomes: mechanistic and functional insights.** *Microbiol*
474 *Mol Biol Rev* (2016), 81(1). doi: 10.1128/MMBR.00036-16.
475
476 Bérdy J: **Bioactive microbial metabolites**. *J Antibiot* (2005), 58(1):1-26. doi:
477 10.1038/ja.2005.1.
478
479 Bertrand S, Bohni N, Schnee S, Schumpp O, Gindro K, Wolfender JL: **Metabolite induction via**
480 **microorganism co-culture: a potential way to enhance chemical diversity for drug discovery**.
481 *Biotechnol Adv* (2014), 32(6):1180-204. doi: 10.1016/j.biotechadv.2014.03.001.
482
483 Bose U, Ortori CA, Sarmad S, Barrett DA, Hewavitharana AK, Hodson MP, Fuerst JA, Shaw PN,
484 Boden R: **Production of N-acyl homoserine lactones by the sponge-associated marine**
485 **actinobacteria *Salinispora arenicola* and *Salinispora pacifica*.** FEMS Microbiol Lett (2017),
486 364(2). doi: 10.1093/femsle/fnx002.
487
488 Buchanan GO, Williams PG, Feling RH, Kauffman CA, Jensen PR, Fenical W: **Sporolides A and**
489 **B: structurally unprecedented halogenated macrolides from the marine actinomycete**
490 ***Salinispora tropica*.** *Org Lett* (2005), 7(13):2731-4. doi: 10.1021/ol050901i.
491
492 Christie-Oleza JA, Armengaud J: **In-depth analysis of exoproteomes from marine bacteria by**
493 **shotgun liquid chromatography-tandem mass spectrometry: the *Ruegeria pomeroyi* DSS-3**
494 **case-study.** *Mar Drugs* (2010), 8(8):2223-39. doi: 10.3390/md8082223.
495
496 Christie-Oleza JA, Scanlan DJ, Armengaud J: **"You produce while I clean up", a strategy**
497 **revealed by exoproteomics during Synechococcus-Roseobacter interactions.** *Proteomics*
498 (2015), 15(20):3454-62. doi: 10.1002/pmic.201400562.
499
500 Christie-Oleza JA, Sousoni D, Lloyd M, Armengaud J, Scanlan DJ: **Nutrient recycling facilitates**
501 **long-term stability of marine microbial phototroph-heterotroph interactions.** *Nat Microbiol*
502 (2017), 2:17100. doi: 10.1038/nmicrobiol.2017.100.
503
504 Cox J, Hein MY, Luber CA, Paron I, Nagaraj N, Mann M: **Accurate proteome-wide label-free**
505 **quantification by delayed normalization and maximal peptide ratio extraction, termed**
506 **MaxLFQ.** *Mol Cell Proteomics* (2014), 13(9):2513-26. doi: 10.1074/mcp.M113.031591.
507
508 Cox J, Mann M: **MaxQuant enables high peptide identification rates, individualized p.p.b.-**
509 **range mass accuracies and proteome-wide protein quantification.** *Nat Biotechnol* (2008),
510 26(12):1367-72. doi: 10.1038/nbt.1511.
511
512 Culp E, Wright GD: **Bacterial proteases, untapped antimicrobial drug targets.** *J Antibiot*
513 *(Tokyo)* (2017), 70(4):366-377. doi: 10.1038/ja.2016.138.
514

515 Denora N, Potts BC, Stella VJ: **A mechanistic and kinetic study of the beta-lactone hydrolysis**
516 **of Salinosporamide A (NPI-0052), a novel proteasome inhibitor.** *J Pharm Sci* (2007),
517 96(8):2037-47. doi: 10.1002/jps.20835.
518
519 Dineshkumar K, Aparna V, Madhuri KZ, Hopper W: **Biological activity of sporolides A and B**
520 **from Salinispora tropica: in silico target prediction using ligand-based pharmacophore**
521 **mapping and in vitro activity validation on HIV-1 reverse transcriptase.** *Chem Biol Drug Des*
522 (2014), 83(3):350-61. doi: 10.1111/cbdd.12252.
523
524 Eustáquio AS, McGlinchey RP, Liu Y, Hazzard C, Beer LL, Florova G, Alhamadsheh MM, Lechner
525 A, Kale AJ, Kobayashi Y, Reynolds KA, Moore BS: **Biosynthesis of the salinosporamide A**
526 **polyketide synthase substrate chloroethylmalonyl-coenzyme A from S-adenosyl-L-**
527 **methionine**. *Proc Natl Acad Sci USA* (2009), 106(30):12295-300. doi:
528 10.1073/pnas.0901237106.
529
530 Eustáquio AS, Pojer F, Noel JP, Moore BS: **Discovery and characterization of a marine**
531 **bacterial SAM-dependent chlorinase**. *Nat Chem Biol* (2008), 4(1):69-74. doi:
532 10.1038/nchembio.2007.56.
533
534 Feling RH, Buchanan GO, Mincer TJ, Kauffman CA, Jensen PR, Fenical W: **Salinosporamide A:**
535 **a highly cytotoxic proteasome inhibitor from a novel microbial source, a marine bacterium**
536 **of the new genus Salinospora**. *Angew Chem Int Ed Engl* (2003), 42(3):355-7. doi:
537 10.1002/anie.200390115.
538
539 Guillard RRL: **Culture of phytoplankton for feeding marine invertebrates.** In: Smith W.L.,
540 Chanley M.H. (eds) *Culture of Marine Invertebrate Animals. Springer, Boston, MA* (1975), 29-
541 60. doi: https://doi.org/10.1007/978-1-4615-8714-9_3.
542
543 Gubbens J, Zhu H, Girard G, Song L, Florea BI, Aston P, Ichinose K, Filippov DV, Choi YH,
544 Overkleeft HS, Challis GL, van Wezel GP: **Natural product proteomining, a quantitative**
545 **proteomics platform, allows rapid discovery of biosynthetic gene clusters for different**
546 **classes of natural products**. *Chem Biol* (2014). 21(6):707-18. doi:
547 10.1016/j.chembiol.2014.03.011.
548
549 Jensen PR, Dwight R, Fenical W: **Distribution of actinomycetes in near-shore tropical marine**
550 **sediments.** *Appl Environ Microbiol* (1991), 57(4):1102-8
551
552 Jensen PR, Mafnas C: **Biogeography of the marine actinomycete Salinispora.** *Environ*
553 *Microbiol* (2006), 8(11):1881-8. doi: 10.1111/j.1462-2920.2006.01093.x.
554
555 Jones BM, Iglesias-Rodriguez MD, Skipp PJ, Edwards RJ, Greaves MJ, Young JR, Elderfield H,
556 O'Connor CD: **Responses of the Emiliania huxleyi proteome to ocean acidification.** *PLoS One*
557 (2013), 8(4). doi: 10.1371/journal.pone.0061868.
558
559 Kale AJ, McGlinchey RP, Lechner A, Moore BS: **Bacterial self-resistance to the natural**
560 **proteasome inhibitor salinosporamide A.** *ACS Chem Biol* (2011), 6(11):1257-64. doi:
561 10.1021/cb2002544.

562
563 Kersten RD, Lane AL, Nett M, Richter TKS, Duggan BM, Dorrestein PC, Moore BS: **Bioactivity-**
564 **guided genome mining reveals the lomaiviticin biosynthetic gene cluster in *Salinispora***
565 ***tropica*.** *ChemBioChem* (2013). 14:955-962. doi: 10.1002/cbic.201300147.
566
567 Kirstein J, Hoffmann A, Lilie H, Schmidt R, Rübsamen-Waigmann H, Brötz-Oesterhelt H, Mogk
568 A, Turgay K: **The antibiotic ADEP reprogrammes ClpP, switching it from a regulated to an**
569 **uncontrolled protease.** *EMBO Mol Med* (2009), 1(1):37-49. doi: 10.1002/emmm.200900002.
570
571 Maldonado LA, Fenical W, Jensen PR, Kauffman CA, Mincer TJ, Ward AC, Bull AT, Goodfellow
572 M: ***Salinispora arenicola* gen. nov., sp. nov. and *Salinispora tropica* sp. nov., obligate marine**
573 **actinomycetes belonging to the family Micromonosporaceae**. *Int J Syst Evol Microbiol*
574 (2005), 55(Pt 5):1759-66. doi: 10.1099/ijs.0.63625-0.
575
576 Medema MH, Blin K, Cimermancic P, de Jager V, Zakrzewski P, Fischbach MA, Weber T, Takano
577 E, Breitling R: **antiSMASH: rapid identification, annotation and analysis of secondary**
578 **metabolite biosynthesis gene clusters in bacterial and fungal genome sequences.** *Nucleic*
579 *Acids Res* (2011). 39:W339-46. doi: 10.1093/nar/gkr466.
580
581 Miyanaga A, Janso JE, McDonarld L, He M, Liu H, Barbieri L, Eustáquio AS, Fielding EN, Carter
582 GT, Jensen PR, Feng X, Leighton M, Koehn FE, Moore BS: **Discovery and Assembly Line**
583 **Biosynthesis of the Lymphostin Pyrroloquinoline Alkaloid Family of mTOR Inhibitors in**
584 **Salinispora Bacteria.** *J Am Chem Soc* (2011), 133(34):13311-13313. doi: 10.1021/ja205655w.
585
586 Mincer TJ, Jensen PR, Kauffman CA, Fenical W: **Widespread and persistent populations of a**
587 **major new marine actinomycete taxon in ocean sediments.** *Appl Environ Microbiol* (2002),
588 68(10):5005-11. doi: 10.1128/aem.68.10.5005-5011.2002.
589
590 Molinski TF, Dalisay DS, Lievens SL, Saludes JP: **Drug development from marine natural**
591 **products.** *Nat Rev Drug Discov* (2009), 8(1):69:85. doi: 10.1038/nrd2487.
592
593 Momose I, Kawada M: **The therapeutic potential of microbial proteasome inhibitors.** *Int*
594 *Immunopharmacol* (2016), 37:23-30. doi: 10.1016/j.intimp.2015.11.013.
595
596 Moreno-Cinos C, Goossens K, Salado IG, Van Der Veken P, De Winter H, Augustyns K: **ClpP**
597 **protease, a promising antimicrobial target.** *Int J Mol Sci* (2019), 20(9). doi:
598 10.3390/ijms20092232.
599
600 Onaka H: **Novel antibiotic screening methods to awaken silent or cryptic secondary**
601 **metabolic pathways in actinomycetes.** *J Antibio* (2017), 70(8):865-870. doi:
602 10.1038/ja.2017.51.
603
604 Owens RA, Hammel S, Sheridan KJ, Jones GW, Doyle S: **A proteomic approach to investigating**
605 **gene cluster expression and secondary metabolite functionality in *Aspergillus fumigatus***.
606 *PLoS One* (2014), 9(9):e106942. doi: 10.1371/journal.pone.0106942.
607

608 Patin NV, Duncan KR, Dorrestein PC, Jensen PR: **Competitive strategies differentiate closely**
609 **related species of marine actinobacteria.** *ISME J* (2016), 10(2):478-90. doi:
610 10.1038/ismej.2015.128.
611
612 Patin NV, Floros DJ, Hughes CC, Dorrestein PC, Jensen PR: **The role of inter-species**
613 **interactions in Salinispora specialized metabolism.** *Microbiology* (2018), 164(7):946-955.
614 doi: 10.1099/mic.0.000679.
615
616 Patin NV, Schorn M, Aguinaldo K, Lincecum T, Moore BS, Jensen PR: **Effects of Actinomycetes**
617 **secondary metabolites on sediment microbial communities.** *Appl Environ Microbiol* (2017),
618 83(4). doi: 10.1128/AEM.02676-16.
619
620 Penn K, Jenkins C, Nett M, Udwary DW, Gontang EA, McGlinchey Rp, Foster B, Lapidus A,
621 Podell S, Allen EE, Moore BS, Jensen PR: **Genomic islands link secondary metabolism to**
622 **functional adaptation in marine Actinobacteria**. *ISME J* (2009), 3(10):1193-203. doi:
623 10.1038/ismej.2009.58.
624
625 Probert I, Houdan A: **The Laboratory Culture of Coccolithophores.** In: Thierstein H.R., Young
626 J.R. (eds) *Coccolithophores. Springer, Berlin, Heidelberg* (2004). doi:
627 https://doi.org/10.1007/978-3-662-06278-4_9.
628
629 Reen FJ, Romano S, Dobson ADW, O'Gara F: **The sound of silence: activating silent**
630 **biosynthetic gene clusters in marine microorganisms**. *Mar Drugs* (2015), 13(8):4754-4783.
631 10.3390/md13084754.
632
633 Richter TKS, Hughes CC, Moore BS: **Sioxanthin, a novel glycosylated carotenoid reveals an**
634 **unusual subclustered biosynthetic pathway.** *Environ Microbiol* (2015), 17(6):2158-2171. doi:
635 10.1111/1462-2920.12669.
636
637 Roberts AA, Schultz AW, Kersten RD, Dorrestein PC, Moore BS: **Iron acquisition in the marine**
638 **actinomycete genus Salinispora is controlled by the desferrioxamine family of**
639 **siderophores.** *FEMS Microbiol Lett* (2012), 335(2):95-103. doi: 10.1111/j.1574-
640 6968.2012.02641.x.
641
642 Rutledge PJ, Challis GL: **Discovery of microbial natural products by activation of silent**
643 **biosynthetic gene clusters**. *Nat Rev Microbiol* (2015), 13(8):509-23. doi:
644 10.1038/nrmicro3496.
645
646 Schley C, Altmeyer MO, Swart R, Müller R, Huber CG: **Proteome analysis of *Myxococcus***
647 ***xanthus* by off-line two-dimensional chromatographic separation using monolithic poly-**
648 **(styrene-divinylbenzene) columns combined with ion-trap tandem mass spectrometry**. *J*
649 *Proteome Res* (2006), 5(10):2760-8. doi: 10.1021/pr0602489.
650
651 Sher D, Thompson JW, Kashtan N, Croal L, Chisholm SW: **Response of *Prochlorococcus***
652 **ecotypes to co-culture with diverse marine bacteria.** *ISME J* (2011), 5(7):1125-32. doi:
653 10.1038/ismej.2011.1.
654

655 Singh S, Prasad P, Subramani R, Aalbersberg W: **Production and purification of a bioactive**
656 **substance against multi-drug resistant human pathogens from the marine-sponge-derived**
657 ***Salinispora* sp.** *Asian Pac J Trop Biomed* (2014), 4(10):825-831. doi:
658 10.12980/APJTB.4.2014C1154.
659
660 Slattery M, Rajbhandari I, Wesson K: **Competition-mediated antibiotic induction in the**
661 **marine bacterium *Streptomyces tenjimariensis*.** *Microb Ecol* (2001), 41(2);90-96. doi:
662 10.1007/s002480000084.
663
664 Snoberger A, Anderson RT, Smith DM: **The proteasomal ATPases use a slow but highly**
665 **processive strategy to unfold proteins.** *Front Mol Biosci* (2017). 4:18. doi:
666 10.3389/fmolb.2017.00018.
667
668 Süssmuth RD, Mainz A: **Nonribosomal peptide synthesis-principles and prospects.** *Angew*
669 *Chem Int Ed Engl* (2017), 56(14):3770-3821. doi: 10.1002/anie.201609079.
670
671 Thomy D, Culp E, Adamek M, Cheng EY, Ziemert N, Wright GD, Sass P, Brötz-Oesterhelt H: **The**
672 **ADEP biosynthetic gene cluster in *Streptomyces hawaiiensis* NRRL 15010 reveals an**
673 **accessory *ClpP* gene as a novel antibiotic resistance factor.** *Appl Environ Microbiol* (2019),
674 85(20). doi: 10.1128/AEM.01292-19.
675
676 Tuttle NR, Demko AM, Patin NV, Kapono CA, Donia MS, Dorrestein P, Jensen PR: **Detection of**
677 **natural products and their producers in ocean sediments.** *Appl Environ Microbiol* (2019),
678 85(8). doi: 10.1128/AEM.02830-18.
679
680 Udwary DW, Zeigler L, Asolkar RN, Singan V, Lapidus A, Fenical W, Jensen PR, Moore BS:
681 **Genome sequencing reveals complex secondary metabolome in the marine actinomycete**
682 ***Salinispora tropica***. *Proc Natl Acad Sci USA* (2007), 104(25);10376-81. doi:
683 10.1073/pnas.0700962104.
684
685 Wilson WH, Carr NG, Mann NH: **The effect of phosphate status on the kinetics of cyanophage**
686 **infection in the oceanic cyanobacterium *Synechococcus* sp. WH7803**. *J Phycol* (1996), 32(4).
687 doi: 10.1111/j.0022-3646.1996.00506.x.
688
689 Wilson ZE, Brimble MA: **Molecules derived from the extremes of life.** *Nat Prod Rep* (2009),
690 26(1):44-71. doi: 10.1039/b800164m.
691
692 Zhao P, Gu W, Huang A, Wu S, Liu C, Huan L, Gao S, Xie X, Wang G: **Effect of iron on the growth**
693 **of *Phaeodactylum tricornutum* via photosynthesis.** *J phycol* (2018), 54(1):34-43. doi:
694 10.1111/jpy.12607.
695

Table 1 | Biosynthetic gene clusters of *Salinispora tropica* CNB-440. Table shows the characterized (in orange) and orphan (in green) BGCs of *S. tropica* CNB-440.

BGC name	Biosynthetic class	Product	Genetic location (strop_)	Size (kb)	Reference
sal	polyketide/non-ribosomal peptide	salinosporamide	RS05130-RS05275	41.8	Feling *et al.*, 2003
lom	polyketide	lomaiviticin	RS10930-RS11215	62.2	Kersten *et al.*, 2013
des	hydroxamate	desferrioxamine	RS12775-RS12855	19.2	Roberts *et al.*, 2012
spo	polyketide	sporolide	RS13560-RS13730	49.2	Dineshkumar *et al.*, 2014
slm	polyketide	salinilactam	RS13850-RS13965	82.0	Udwary *et al.*, 2007
lym	polyketide/non-ribosomal peptide	lymphostin	RS15295-RS15350	25.0	Miyanaga *et al.*, 2011
terp1	terpenoid	sioxanthin	RS16250-RS16295	10.4	Richter *et al.*, 2015
spt	butyrolactone	salinipostin	RS20900-RS20940	11.1	Amos *et al.*, 2017
terp2	terpenoid	sioxanthin	RS22405-RS22445	11.7	Richter *et al.*, 2015
pks1	polyketide	*NA*	RS02980-RS03095	30.9	*NA*
nrps1	non-ribosomal peptide	*NA*	RS03375-RS03535	37.5	*NA*
amc	carbohydrate	*NA*	RS11765-RS11795	6.6	*NA*
bac1	ribosomal peptide	*NA*	RS11800-RS12275	19.2	*NA*
pks3	polyketide	*NA*	RS12510-RS12630	23.3	*NA*
sid2	non-ribosomal peptide	*NA*	RS13260-RS13385	40.7	*NA*
sid3	non-ribosomal peptide	*NA*	RS13985-RS14120	29.2	*NA*
sid4	non-ribosomal peptide	*NA*	RS14125-RS14260	40.8	*NA*
bac2	ribosomal peptide	*NA*	RS14265-RS15290	19.0	*NA*
pks4	polyketide	*NA*	RS21120-RS21540	10.0	*NA*
nrps2	non-ribosomal peptide	*NA*	RS22250-RS22350	34.7	*NA*

696

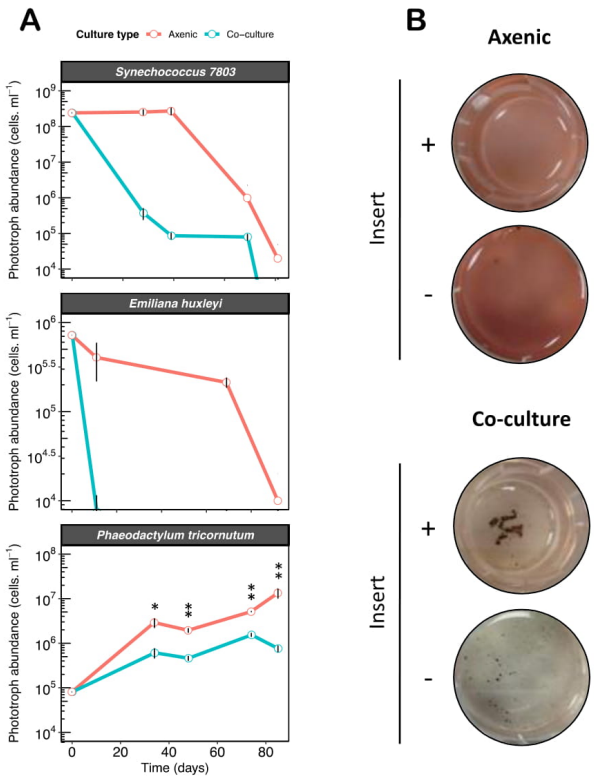

Figure 1 | *Salinispora tropica* inhibits the growth of marine phototrophs *via* the secretion of an antimicrobial molecule (A) *S. tropica* inhibits marine phototrophs growth in co-culture. Cultures of three marine phototrophs grown axenically (red lines) and in co-culture with *Salinispora tropica* (blue lines). Graph shows mean ± standard deviation of three biological replicates. Statistically significant cell abundances are indicated (T-test, significant * at *p*-value < 0.05 and ** at *p*-value < 0.01). **(B)** *Synechococcus* growth inhibition by *S. tropica* mediated by a diffusible molecule. The cyanobacterium was grown axenically and in co-culture with *S. tropica,* separated by a 0.4 µm pore membrane insert. Photographs of representative cultures of three biological replicates are shown, 7 days after inoculation. Red pigmentation is characteristic of healthy *Synechococcus* cells, while cell bleaching indicates cell death.

697

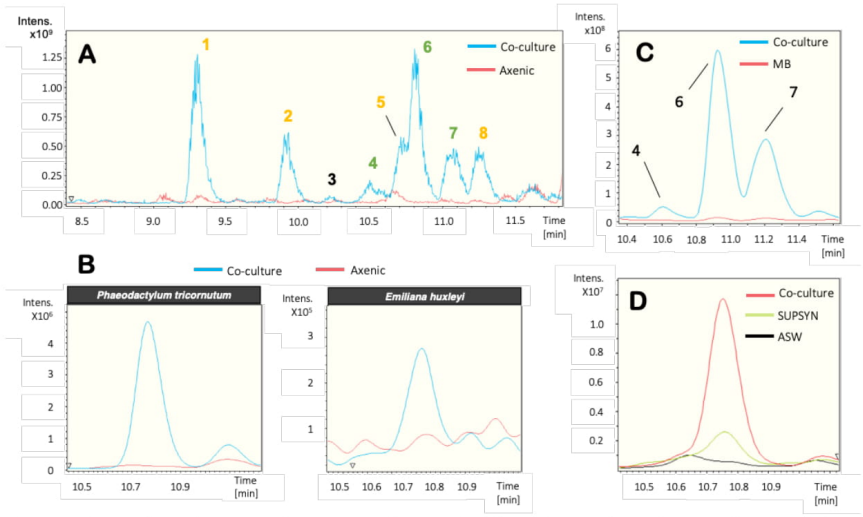

Figure 2 | Marine phototrophs trigger the production of cryptic molecules in *S. tropica*
(A) *S. tropica* produces detectable small molecules in co-culture with *Synechococcus*. Overlaid base peak chromatograms (BPCs) of *Synechococcus* culture concentrated supernatants, when grown in artificial sea water (ASW) either axenically (red) or in co-culture with *S. tropica* (blue). Peaks characteristic of the co-culture condition are labelled from **1** to **8**. Color of the labels indicate groups of related compounds. **(B)** Other marine phototrophs also trigger the production of metabolite **6** by *S. tropica* as observed in panel A. Figure shows extracted ion chromatograms for the molecule **6** EIC 435.2 ± 0.1 in the supernatants of the phototrophs grown axenically (red) and in co-culture with *S. tropica* (blue). **(C)** The production of the related molecules **4**, **6** and **7** is dependent on the presence of photosynthate rather than high-nutrient availability. Graph shows extracted ion chromatograms for all three cryptic molecules EIC (464.2; 435.2; 449.2) ± 0.5 in the concentrated supernatants of *S. tropica* grown axenically in marine broth (MB, red) or in co-culture with *Synechococcus* in ASW (Co-culture, blue). **(D)** Cryptic molecule production is triggered by nutrients released by *Synechococcus* rather than cell-to-cell interactions. Graph shows extracted ion chromatograms for the cryptic molecule **6** (EIC 435.2 ± 0.5) in the supernatant of *S. tropica* grown axenically either in artificial sea water (ASW, black line) or in a conditioned *Synechococcus* supernatant (SUPSYN, green line); and in co-culture with *Synechococcus* (Co-culture, red line).

Table 2 | Characteristics of the cryptic molecules. MS Peak numbering is based on HPLC retention time. High-resolution LC-(+)ESI-MS *m/z* values and predicted chemical formulae for $[M+H]^+$ are provided.

MS Peak	Observed *m/z*	Chemical formulae for $[M+H]^+$ (calculated *m/z*; err [ppm])	MS/MS
3	438.1701	$[C_{28}\ H_{24}\ N\ O_4]^+$ (438.1700; -0.3)	194.0817 177.1279
4	464.2509	$[C_{22}\ H_{34}\ N_5\ O_6]^+$ (464.2504; -1.2)	**276.1600** 171.0880 154.0615
6	435.2609	$[C_{22}\ H_{35}\ N_4\ O_5]^+$ (435.2602; -1.7)	372.2290 **276.1599** 142.0979
7	449.2764	$[C_{23}\ H_{37}\ N_4\ O_5]^+$ (449.2758; -1.3)	156.1135

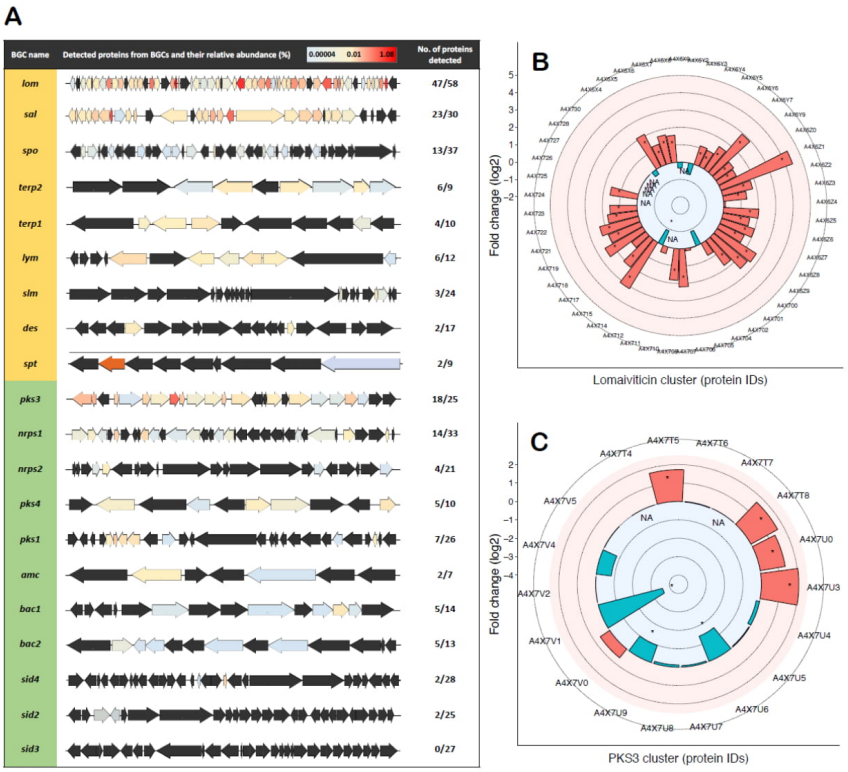

Figure 3 | Photosynthate activates orphan biosynthetic gene clusters in *S. tropica*. (A) Characterized (orange) and orphan BGCs (green) in *S. tropica* CNB-440 detected by high-throughput proteomics when grown with photosynthate (SUPSYN). Genes are colored according to the relative abundance of their corresponding proteins. Those that were not detected are represented in black. Photosynthate increased the detection of proteins involved in the production of lomaiviticin **(B)** and the orphan PKS3 **(C)** in comparison with cells grown in MB. Up- (red) and down-regulated (blue) proteins in the presence of the photosynthate is shown. Statistically significant fold changes are indicated by an asterisk (T-test, significant at *q*-value < 0.05). *NA* indicate proteins for which the T-test and fold change could not be estimated because of missing values within a set of replicates.

Table 3 | Detected proteins from the *nrps1* orphan BGC in *S. tropica* CNB-440 grown with photosynthate. Proteins involved in non-ribosomal peptide biosynthesis and antibiotic self-resistance are highlighted in bold.

Protein ID	Annotation	Relative abundance (%; n = 3)
A4X2P5	RidA family protein	0.014
A4X2P8	MFS transporter	0.011
A4X2Q0	**non-ribosomal peptide synthetase**	**0.004**
A4X2Q2	SDR family oxidoreductase	0.002
A4X2R0	acyl-CoA dehydrogenase	0.005
A4X2R1	acyl-CoA dehydrogenase	0.001
A4X2R4	D-alanine--poly(phosphoribitol) ligase	0.004
A4X2R5	**condensation domain-containing protein**	**0.001**
A4X2R7	argininosuccinate synthase	0.001
A4X2R8	methionyl-tRNA formyltransferase	0.087
A4X2S2	**ATP-dependent Clp protease proteolytic subunit**	**0.121**
A4X2S4	potassium channel family protein	0.002
A4X2S5	2-oxoacid:ferredoxin oxidoreductase subunit beta	0.006
A4X2S6	2-oxoacid:acceptor oxidoreductase subunit alpha	0.004

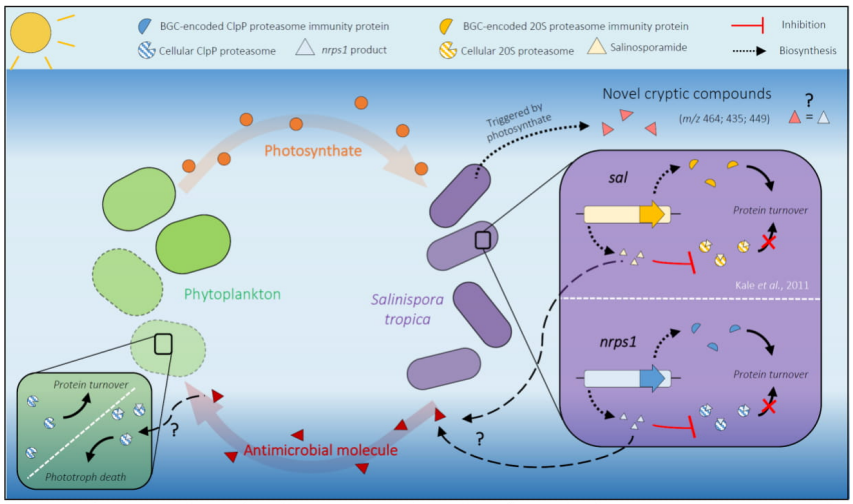

Figure 4 | Interaction of *Salinispora tropica* with phytoplankton. Marine phototrophs release photosynthate that triggers the biosynthesis of novel cryptic metabolites in *S. tropica*. *S. tropica* produces an unknown antimicrobial molecule that kills phytoplankton. The proposed mechanism of the antimicrobial metabolite as well as the activity of the *nrps1* product are depicted (green and purple boxes, respectively). The BGC *nrps1* would produce a ClpP-proteasome inhibitor, to which *S. tropica* would be resistant because of an immunity protein encoded within the BGC, similarly to what is known for *sal*/salinosporamide. The *nrps1*-encoded proteasome inhibitor could kill the phototrophs by preventing protein turnover, leading to cell death.

727

APPENDIX 2

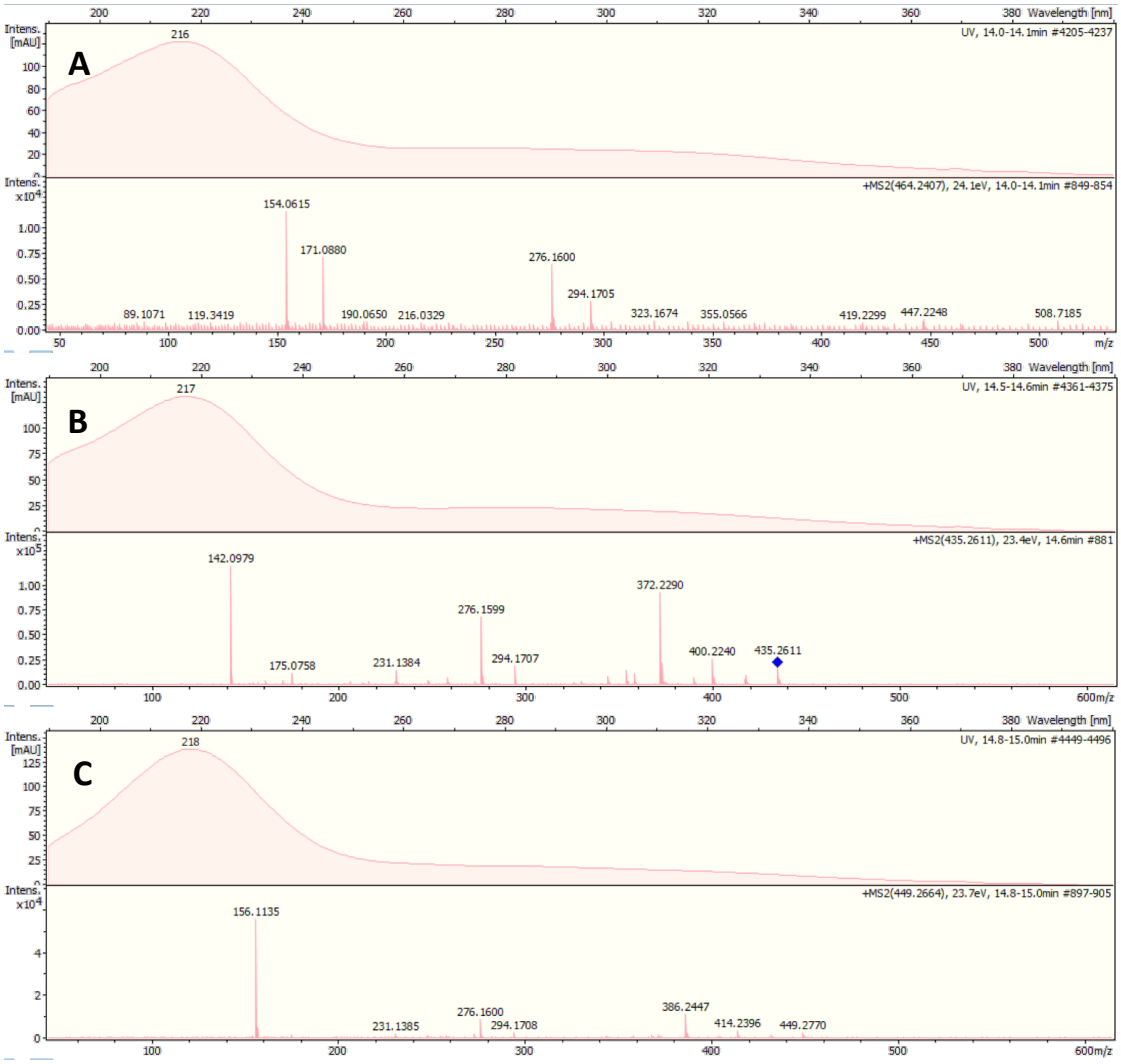

Appendix 2 | MS/MS fragmentation spectra of the cryptic molecules. High-resolution LC/(+)ESI-MS/MS spectra obtained for molecule **4** (**A**), **6** (**B**), and **7** (**C**).

APPENDIX 3

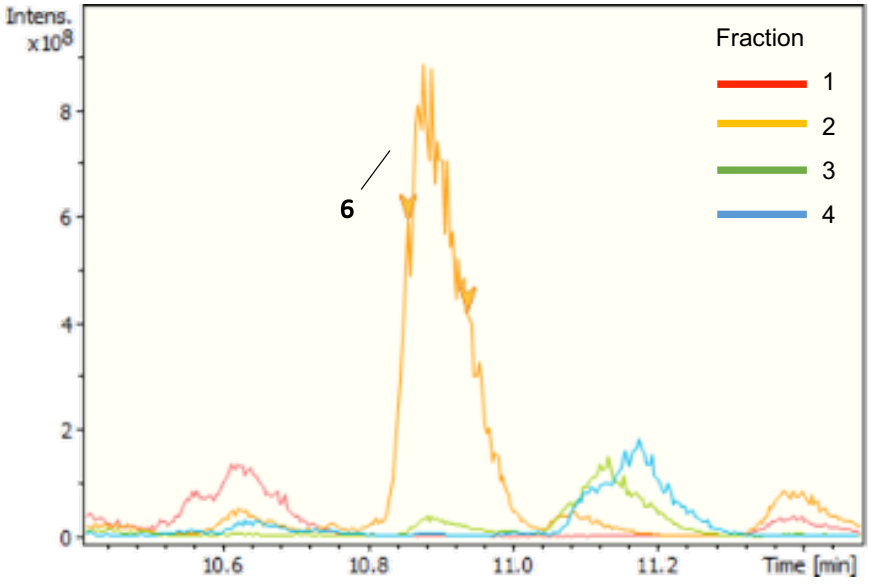

Appendix 3 | Graph shows overlaid base peak chromatograms issued from the LC-MS analysis of the HPLC-collected fractions 1 (red), 2 (orange), 3 (green) and 4 (blue), resuspended in ASW.

APPENDIX 4

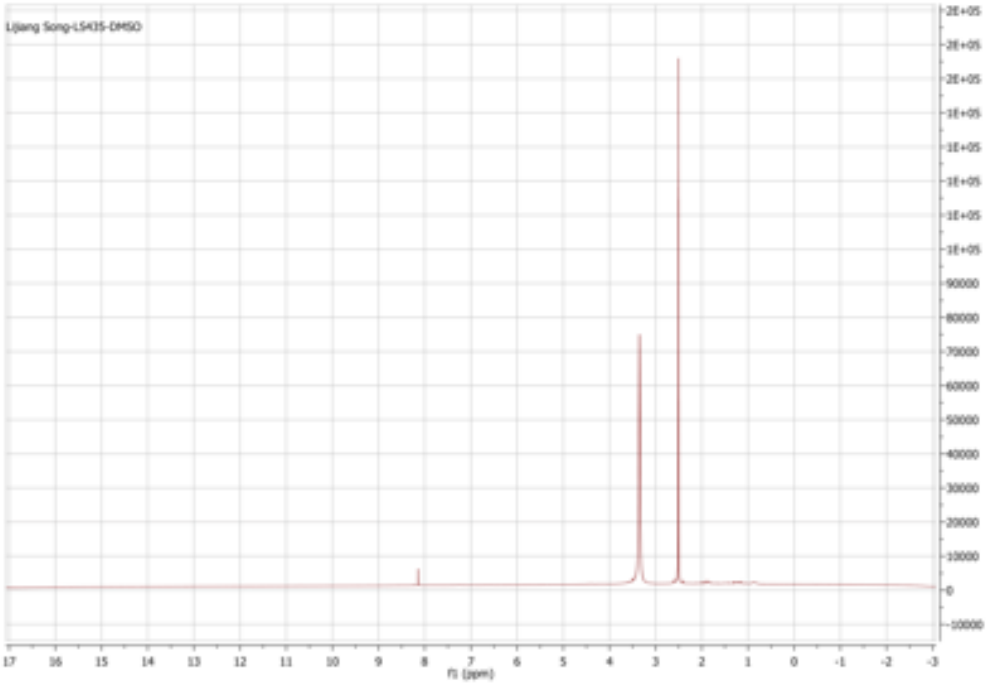

Appendix 4 | ^{1}H-NMR spectrum (700 MHz, (d_6DMSO) of the HPLC fraction containing the cryptic compound **6**.

APPENDIX 5

Appendix 5 | List of primers used to retarget the pCRISPomyces-2 plasmid.

Name	Sequence 5'—3'	Description
AC_025	ACGCcctccggcaggcagattgcc	Protospacer for PPtase 0777 (STROP_RS03935)
AC_026	AAACggcaatctgcctgccggagg	
AC_029	ACGCctccggccactcaggcaggt	Protospacer for PPTase 685 (STROP_RS03465)
AC_030	AAACacctgcctgagtggccggag	
AC_037	ACGCcttgaggagtgcttccttcc	Protospacer for PPTase 2822 (STROP_RS14165)
AC_038	AAACggaaggaagcactcctcaag	
AC_041	ACGCccaaccgatccacacataca	Protospacer for PPTase 2496 (STROP_RS12565)
AC_042	AAACtgtatgtgtggatcggttgg	
AC_047	tcggttgccgccgggcgtttttttatAACCTCATCGAGTACCACC	Amplify homology arms A for PPTase777 - Fwd
AC_048	gccctccgatgacagggtggCAGTCCAGAGTCTGCGTG	Amplify homology arms A for PPTase777 - Rvs
AC_049	gtcacgcagactctggactgCCACCCTGTCATCGGAG	Amplify homology arms B for PPTase777 - Fwd
AC_050	gcggccttttacggttcctggcctCAGGGATCGTCGGTCTG	Amplify homology arms B for PPTase777- Rvs
AC_051	tcggttgccgccgggcgtttttttatGCACATCCTTCACATCG	Amplify homology arms A for PPTase685 - Fwd
AC_052	gggggcagccatggtgacagATGACCGTTCCGGATTC	Amplify homology arms A for PPTase685 - Rvs
AC_053	cgggaatccggaacggtcatCTGTCACCATGGCTGCC	Amplify homology arms B for PPTase685 - Fwd
AC_054	gcggccttttacggttcctggcctGAACAGGTTGACGGCCAG	Amplify homology arms B for PPTase685 - Rvs
AC_059	tcggttgccgccgggcgtttttttatTGTATCCCACCCCGATCTG	Amplify homology arms A for PPTase2822 - Fwd
AC_060	gacggaaaggtggcaccaccACCGCTCCTCCATAGCCA	Amplify homology arms A for PPTase2822 - Rvs
AC_061	ggtggctatggaggagcggtGGTGGTGCCACCTTTCC	Amplify homology arms B for PPTase2822 - Fwd
AC_062	gcggccttttacggttcctggcctCCAGGTATCCAGGGTAGGTG	Amplify homology arms B for PPTase2822 - Rvs
AC_063	tcggttgccgccgggcgtttttttatATCCTGCTTCCGTCCATG	Amplify homology arms A for PPTase2496 - Fwd
AC_064	gttaacctctctccgtgaacGATGTCGCCGATGTGTG	Amplify homology arms A for PPTase2496 - Rvs
AC_065	acccacacatcggcgacatcGTTCACGGAGAGAGGTTAACC	Amplify homology arms B for PPTase2496 - Fwd
AC_066	gcggccttttacggttcctggcctGTTGGTTCCCGAGACACAC	Amplify homology arms B for PPTase2496 - Rvs
AC_069	tcggttgccgccgggcgtttttttatGGCTTCTTCTCCTCCTTCTCC	Amplify homology arms A for NRPS2 - Fwd
AC_070	cggctgagcacctggtccacCTTGCTGAGATGTCGGTAAGG	Amplify homology arms A for NRPS2 - Rvs
AC_071	cttaccgacatctcagcaagGTGGACCAGGTGCTCAGC	Amplify homology arms B for NRPS2 - Fwd
AC_072	gcggccttttacggttcctggcctAGAACCTCGGTAGCGTACTCC	Amplify homology arms B for NRPS2 - Rvs
AC_089	tcggttgccgccgggcgtttttttatGTCACGGTGGCTCAGACTAC	Amplify homology arms A for NRPS1 - Fwd
AC_090	tcgggtgggtgggttggttccTGCTGTCGTTTCTCACCTG	Amplify homology arms A for NRPS1 - Rvs
AC_091	caggtgagaaacgacagcagGAACCAACCCACCCACCC	Amplify homology arms B for NRPS1 - Fwd
AC_092	gcggccttttacggttcctggcctGACAGACCGGATTCATGCAC	Amplify homology arms B for NRPS1 - Rvs
gAC_073	GAGACATCTTTGAAGACAAacgcatccgaccctgacagtcactgttttaga gctagaaatagcaagttaaaataaggctagtccgttatcaacttgaaaaagtggca ccgagtcggtgctttttttagcataaccccttggggcctctaaacgggtcttgaggggt tttttggctgctccttcggtcggacgtgcgtctacgggcaccttaccgcagccgtcgg ctgtgcgacacggacggatcgggcgaactggccgatgctgggagaagcgcgctgc tgtacggcgcgcaccgggtgcggagcccctcggcgagcggtgtgaaacttctgtga atggcctgttcggttgctttttttatacggctgccagataaggcttgcagcatctggg cggctaccgctatgatcggggcgttcctgcaattcttagtgcgagtatctgaaaggg gatacgcctccgacatgatgagcccctgtttAAGTCTTCTTTCACGTGGC	gBlock for *nrps2* guide RNAs such as BbsI-spacer1-gRNAtail-T7term-gapdhp(EL)-spacer2-BbsI
gAC_088	GAGACATCTTTGAAGACAAacgcgggcggtttcggaggtgaatgttttaga gctagaaatagcaagttaaaataaggctagtccgttatcaacttgaaaaagtggca ccgagtcggtgctttttttagcataaccccttggggcctctaaacgggtcttgaggggt tttttggctgctccttcggtcggacgtgcgtctacgggcaccttaccgcagccgtcgg ctgtgcgacacggacggatcgggcgaactggccgatgctgggagaagcgcgctgc tgtacggcgcgcaccgggtgcggagcccctcggcgagcggtgtgaaacttctgtga atggcctgttcggttgctttttttatacggctgccagataaggcttgcagcatctggg cggctaccgctatgatcggggcgttcctgcaattcttagtgcgagtatctgaaaggg gatacgctgggccgatacctgggcggcgtttAAGTCTTCTTTCACGTGGC	gBlock for *nrps1* guide RNAs such as BbsI-spacer1-gRNAtail-T7term-gapdhp(EL)-spacer2-BbsI

APPENDIX 6

Appendix 6 | List of primers used for PCR-verification of the *S. tropica* exconjugants.

Name	Sequence 5'—3'	Description	Expected size
AC_099	CTCGATCGCCACGTTATCTG	Check knock-out of PPTase 685 outside homology arms - Fwd	2,622 bp if WT 1,940 bp if KO
AC_100	CGTGGTGCTGTCGGTCTG	Check knock-out of PPTase 685 outside homology arms - Rvs	
AC_101	CTGGTGGTCTTCTGGGAGG	Check knock-out of PPTase 777 outside homology arms - Fwd	2,784 bp if WT 2,050 bp if KO
AC_102	CTGCCAGAGGTGAACAGCA	Check knock-out of PPTase 777 outside homology arms - Rvs	
AC_084c	GGGTCTTCGTCGATGTCACT	Check knock-out of PPTase2496 outside homology arms - Fwd	2,642 bp if WT 2,142 bp if KO
AC_085c	GAAGAGGGCGTACTGGTCG	Check knock-out of PPTase2496 outside homology arms - Rvs	
AC_095	gacgggcatgatgggatcta	Check knock-out *nrps1* - amplify within the BGC *nrps1* - Fwd	892 bp if WT No amplicon if KO
AC_096	caaagatctggtcgccgaag	Check knock-out *nrps1* - amplify within the BGC *nrps1* - Rvs	
AC_097	AAGATCACAGCCCAGGGAAA	Check knock-out of *nrps1* outside homology arms - Fwd	40,700 bp if WT 571 bp if KO
AC_098	ACCTGGAGCATGATCTACCG	Check knock-out of *nrps1* outside homology arms - Rvs	
AC_086b	GCCACCATAGAACGTTGC	Check knock-out of NRPS2 outside homology arms - Fwd	37,143 bp if WT 2,448 bp if KO
AC_087b	CCACCGCCAGATCTAAAGG	Check knock-out of NRPS2 outside homology arms - Rvs	

APPENDIX 7

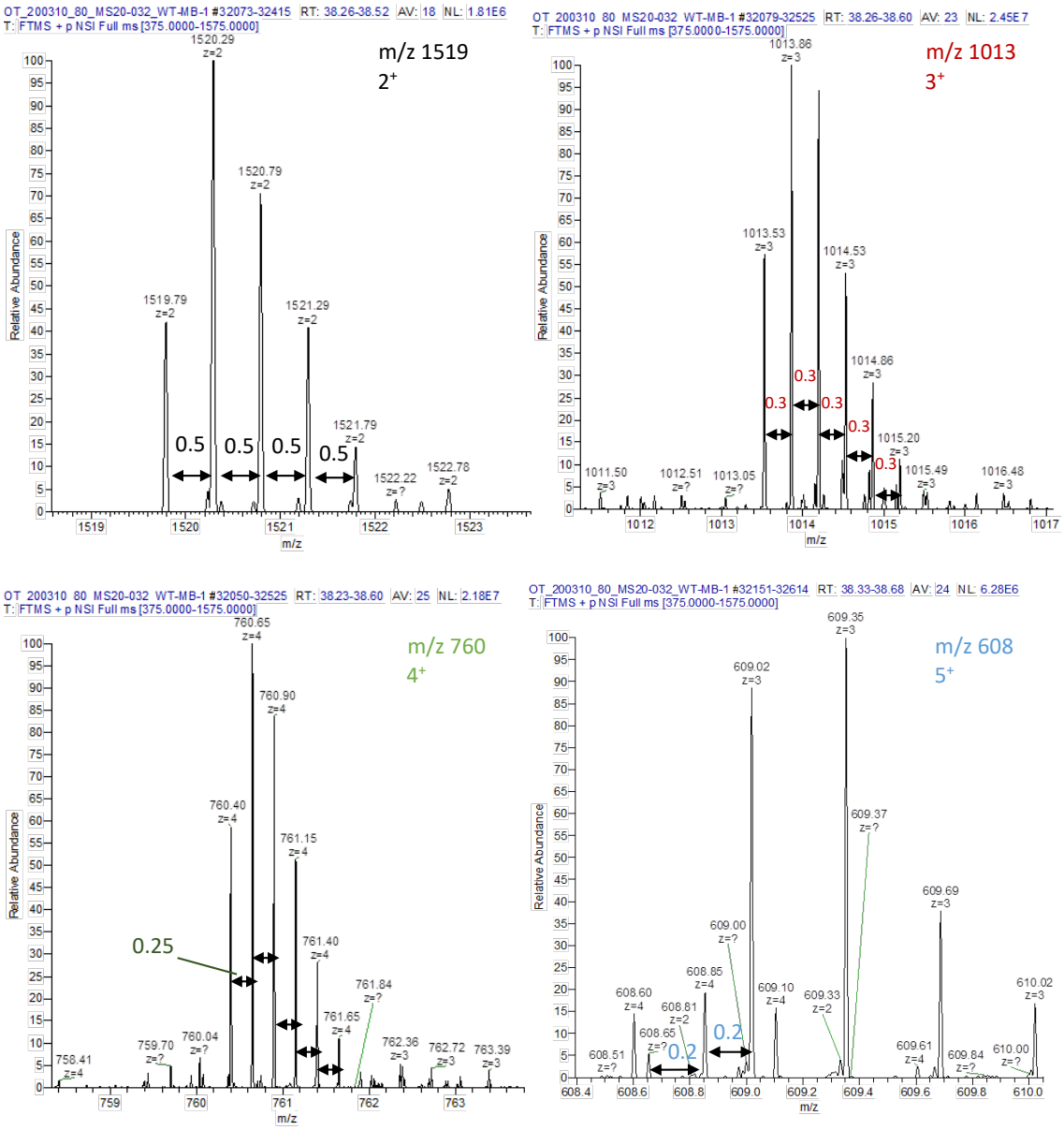

Appendix 7 | MS analysis detecting the PPTase-modified peptide of protein A4X7U8, at different charge states. Chromatograms show isolated ion spectra with the mass differences between related peaks that are indicative of the ion charge represented by an arrow.